iScience

CellPress

Article

Anticancer Molecule Discovery via C2-Substituent Promoted Oxidative Coupling of Indole and Enolate

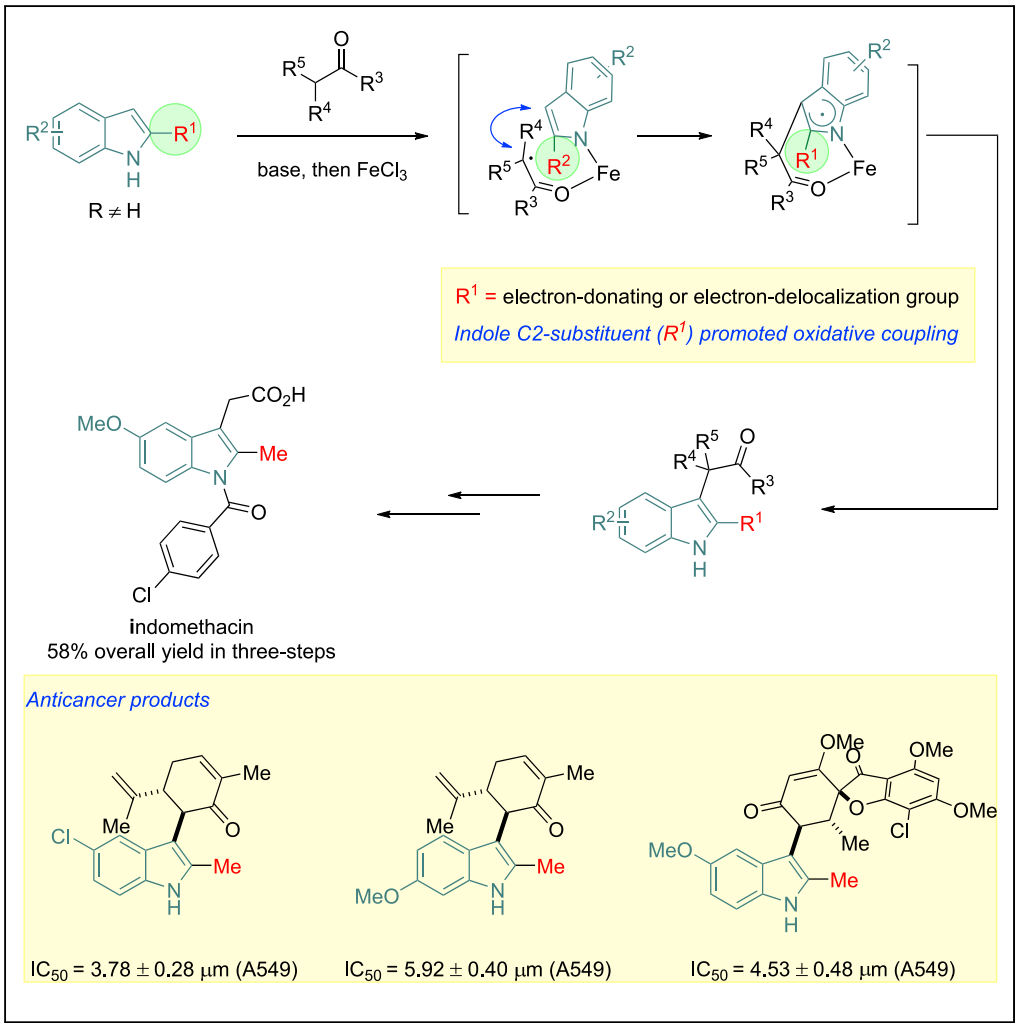

Helin Lu, Guirong Zhu, Tiange Tang, Zhuang Ma, Qin Chen, Zhilong Chen

chenq@fudan.edu.cn (Q.C.)
czldreamer@hotmail.com (Z.C.)

HIGHLIGHTS

Fe-mediated, C2-substitutent promoted oxidative coupling of indoles and enolates

Three-steps to prepare indomethacin and its analogues

Quick access to complex indoles library bearing anticancer bioactivities

Lu et al., iScience 22, 214–228
December 20, 2019
https://doi.org/10.1016/j.isci.2019.11.021

iScience

CellPress

Article

Anticancer Molecule Discovery via C2-Substituent Promoted Oxidative Coupling of Indole and Enolate

Helin Lu,[1] Guirong Zhu,[2] Tiange Tang,[1] Zhuang Ma,[1] Qin Chen,[1,*] and Zhilong Chen[1,3,*]

SUMMARY

C2, C3-disubstituted indole is one of the most frequently encountered motifs in bioactive alkaloids and medicinal chemistry. Thus, developing novel, concise, and efficient access to it is highly desired in drug discovery. Herein, we present such an approach to this scaffold by direct oxidative coupling of C2-substituted indoles and enolates. Compared with indole bearing no C2-substituent, higher yields (up to 96%) were obtained for C2-substituted indoles in most cases. Mechanistic studies showed the reaction went through a Fe-chelated radical-anion oxidative coupling procedure promoted by C2-substituent on indole by two means: (1) stabilizing C2-radical intermediate during the reaction; (2) reducing indole homocoupling. This approach serves as a synthetic useful tool to quickly build up bioactive small molecule library of C2, C3-disubstituted indoles, and several products showed promising anticancer activities. Besides, indomethacin and its analogs were conveniently prepared in three-step sequence efficiently, indicating the potential application of our approach in medicinal chemistry.

INTRODUCTION

Modern drug discovery still requires tremendous resources and efforts. The chance from target validation to drug approval still remains very low (<10%). How to quickly identify small molecules with good potency and AMDET (absorption, metabolism, distribution, excretion, and toxicity) properties is one of the major challenges for current drug hunting. Developing concise, efficient, and selective synthetic methodologies, somehow, can contribute to solve such a challenge by providing precise and useful molecule-editing tools, which enable medicinal chemists to quickly assemble drug-like small molecule libraries with broader chemical space and accelerate SAR (Structure-Activities Relationship) studies (Dugger et al., 2017; Bostrom et al., 2018; Campos et al., 2019). As embodied in many bioactive natural products, drugs/drug leads, indole is one of the most commonly used drug-like motifs in small molecule drug design (Mase, 2010; Kochanowska-Karamyan and Hamann, 2010; Taber and Tirunahari, 2011; Gribble, 2016), especially the C2, C3-disubstituted ones (e.g., reserpine, ambiguine H, indomethacin, estrogen/progestogen receptor bazedoxifene, and anticancer reagent [Burn and Rand, 1958; Stratmann et al., 1994; Aksenov et al., 2015]) (Figure 1A).

Traditional preparation of C2, C3-disubstituted indole scaffolds, such as Fischer and Larock indole synthesis (Taber and Tirunahari, 2011; Gribble, 2016; Robinson, 1963; Herraiz-Cobo et al., 2015), normally requires multiple steps from commercially available starting materials, particularly for those bearing diverse functional groups. Thus, they are less efficient in access to complex indole molecules, calling for the development of novel, concise, and efficient methodologies. A late-stage, direct, and selective functionalization of indole, on the other hand, would be an ideal strategy to construct them (Wencel-Delord and Glorius, 2013; Cermak et al., 2015). In addition, this strategy could still maintain efficiency even when introducing complex C2- and C3-substitutes (Figure 1B).

Driven by our interest in searching for novel small molecules for cancer therapy (Ke et al., 2019), we would like to develop an approach for quick access to these scaffolds by direct and selective connecting carbonyl motifs and C2-substituted indoles, considering that carbonyl moieties are among the most synthetic useful functional groups in organic synthesis. Previous approaches in connecting carbonyl compounds and C3 position of C2-substituted indole mainly rely on carbine insertion (Keller et al., 1977; Gibe and Kerr, 2002), nucleophilic addition (Tang et al., 2012; Vander Wal et al., 2013; Maksymenko et al., 2017), and Buchwald-Hartwig coupling reactions (Esteves et al., 2017). In all these methods, either carbonyl regents

[1]School of Pharmacy, Huazhong University of Science and Technology (HUST), 13 Hangkong Road, Wuhan, Hubei 430030, China

[2]Research Center for Molecular Recognition and Synthesis, Department of Chemistry, Fudan University, 220 Handan Road, Shanghai 200433, China

[3]Lead Contact

*Correspondence: chenq@fudan.edu.cn (Q.C.), czldreamer@hotmail.com (Z.C.)

https://doi.org/10.1016/j.isci.2019.11.021

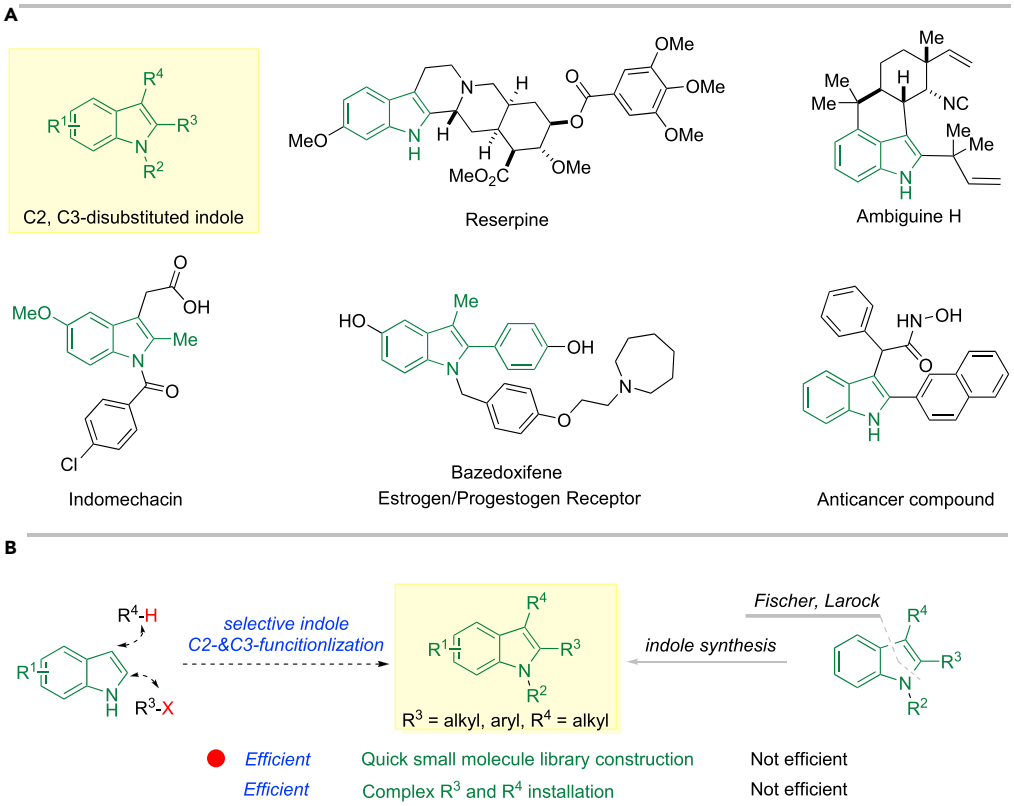

Figure 1. C2-C3-Substituted Indole Scaffolds

(A) Representative alkaloids, drugs/drug leads bearing C2-C3-substituted indole scaffolds.

(B) Strategy to prepare C2-C3-substituted indoles.

(e.g., diazo, α-bromocarbonyl, enonium species) or C3-bromoindole requires additional steps for preparation from corresponding carbonyl compounds or indoles. Therefore, direct coupling of C2-substituted indoles and carbonyl compounds, from the perspective of atom- and step-economy, is more appealing. Moreover, both carbonyl compounds and C2-substituted indoles are either commercially available or can be prepared easily. Therefore, within this approach, simply from C2-substituted indoles and carbonyl compounds, small molecular library of complex C2, C3-disubstituted indoles could be easily constructed, facilitating related medicinal chemistry research (Figure 2A).

Among many excellent coupling strategies, we would like to develop oxidative coupling of C2-substituted indoles and enolates without carbon-metal bond formation, given that aryl halide could not be well tolerated in many transition-metals-catalyzed reactions (Sun et al., 2010; Wendlandt et al., 2011; Liu et al., 2011; Yeung and Dong, 2011; Zhang et al., 2012), which will restrict the derivatization of products to certain extent. Oxidative homocoupling of enolates was discovered in 1935, but limited progress was achieved in the following 50 years (Babler and Haack, 1983; Brocksom et al., 1975; Guo et al., 2012; Ito et al., 1975, 1977; Ivanoff and Spasoff, 1935; Kauffmann et al., 1968; Ojima et al., 1992; Rathke and Lindert, 1971). Baran first reported the intermolecular cross-coupling of indoles and enolates under similar reaction conditions via a copper-chelated radical-anion coupling procedure (Baran and Richter, 2004). By switching the oxidant from Cu(II) salts to iodine, Ma discovered that similar intramolecular reaction worked smoothly as well in a non-chelated radical-radical coupling fashion (Zuo et al., 2010). Inspired by their seminal research, it is reasonable to hypothesize that the intermolecular oxidative cross-coupling of C2-substituted indoles and enolates might also work, thus affording the desired products. According to the reaction mechanism proposed by either Baran (Richter et al., 2007) or Ma (Zuo et al., 2010), certain C2-substitute (Figure 2, R^3) on indole (e.g., electron-donating group, electron-delocalization group), we believe, could (Figure 2B, **TS-II**, **TS-II-1**, **TS-III**, and **Ts-III-1**) promote the reaction by stabilizing the electrophilic indole C2-/C3-radicals intermediates albeit its harmful steric repulsion.

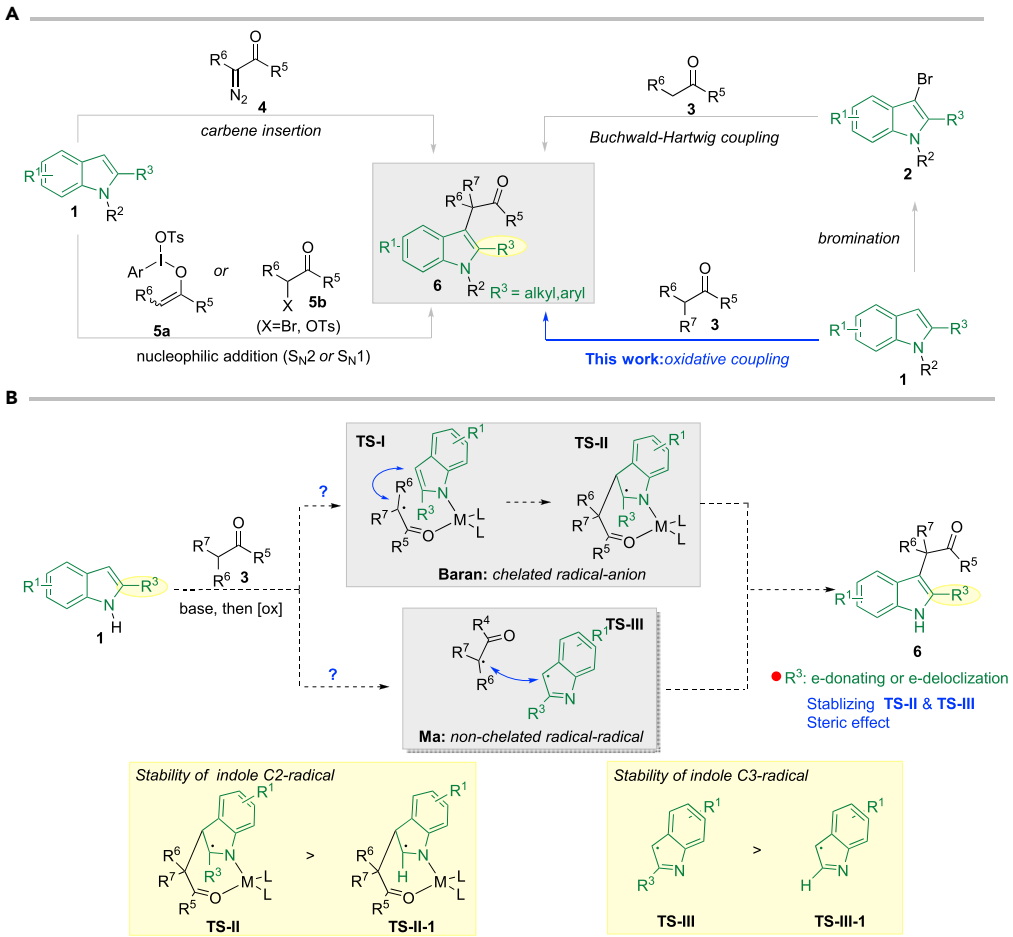

Figure 2. Reported Synthetic Approaches to C2, C3-disubstituted Indoles and Our Reaction Design

(A) Previous synthetic methods toward C2, C3-disubstituted indole from C2-substituted indole.

(B) Our reaction design via C2-substituent promoted oxidative coupling of indole and enolate.

RESULTS AND DISCUSSION

Condition Optimization for Oxidative Coupling of C2-Substituted Indole and Enolate

2-Methyl indole (**1-1**) and (*R*)-carvone (**3-1**) were selected as model substrates to investigate this reaction. Initially, we utilized Baran's condition (Richter et al., 2007) to test our hypothesis. However, the reaction failed to complete, producing low yield of the desired product **6-1** (Table 1, entry 2). Then we turned our attention to Ma's condition (Zuo et al., 2010), but disappointing result was observed (Table 1, entry 3). Other oxidants, like $Cu(OAc)_2$ and $Fe(acac)_3$, also failed to afford the product in good efficiency (Table 1, entry 7). To our delight, the yield was greatly improved in the presence of 4.0 equivalents of $FeCl_3$ (Artz and Cram, 1984) (Table 1, entry 4). Further improvement was achieved by maintaining the overall reaction at −78°C after adding $FeCl_3$ (57% versus 80%, Table 1, entry 6 and 7). Ultimately, the yield could be increased to 89%–93% by adding $FeCl_3$ in THF solution rather than as solid in open air (Table 1, entry 1). Other oxidants, like AgO, AgOAc, CAN, and $CeCl_3$, failed to give better yield. Changing the reaction solvents from THF to others, like DMF and toluene, did not enhance the efficiency either (Table 1, also see Table S2).

Mechanistic Investigations

This highly efficient transformation has intrigued our great interest, since it somehow proved our hypothesis that C2-substituent could promote the reaction. To further understand this reaction, several control and competing experiments were conducted. First, we compared Baran's and our condition for indole (**1–20**)/2-methylindole (**1-1**) in coupling with (*R*)-carvone (**3-1**), respectively, as shown in Figure 3A. Higher yield was obtained from 2-methylindole (**1-1**) under our reaction; in contrast, Baran's condition favored

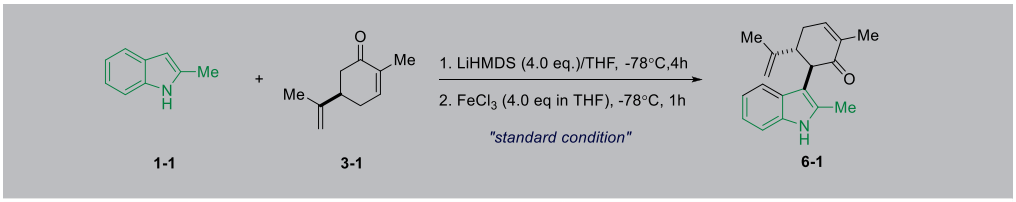

Entry[a]	Deviation from "Standard Condition"	Yield (%)/dr[a]
1	None	89–93/>20:1
2	$Cu(2\text{-ethylhexanoate})_2$ (1.5 eq.) instead of $FeCl_3$ (Baran's condition)	26–30[b]/>20:1
3	I_2 instead of $FeCl_3$ (Ma's condition)	ND
4	$FeCl_3$ was added in one portion as solid, then −78°C	80/>20:1
5	$FeCl_3$ was added in one portion as solid, then −78°C to rt, 30 min	57/>20:1
6[c]	$Fe(acac)_3$ (3.0 eq.) instead of $FeCl_3$	20/>20:1
7[c]	$Cu(OAc)_2$ (3.0 eq.) instead of $FeCl_3$	46/>20:1
8	LDA instead of LiHMDS	41/>20:1
9	Toluene instead of THF	41/>20:1
10[c]	With 1.0 equivalent of 2-methyl indole	28/>20:1

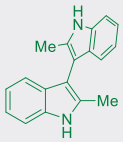

7-1

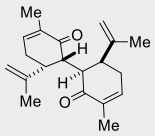

8-1

Table 1. Condition Optimization

[a]All the reactions were conducted with 1-1 (2.0 mmol, 2.0 equiv.), (*R*)-carvone (3-1, 1.0 mmol, 1.0 equivalent), LiHMDS (1.3 M in THF, 4.0 mmol, 4.0 equivalent), and $FeCl_3$ (99%, 4.0 mmol, 4.0 equivalent in THF), isolated yield, diastereomer ration (dr) was determined by ^1H NMR of isolated product 6-1.

[b]$Cu(2\text{-ethylhexanoate})_2$ (1.5 mmol, 1.5 eq.) was added at −78°C and then warmed to room temperature.

[c]The oxidants were added at −78°C and then warmed to room temperature and the reaction mixture was stirred for 2 h; ND = no desired product.

indole (**1–20**), suggesting that these two conditions can be complementary for each other depending on the indole substrates. Such evident difference between Cu(II) and Fe(III) in this reaction probably originated from their coordination ability and oxidation potential. And Fe(III) can better tolerate the steric effects from C2-substituent on indole, giving higher yield. To our surprise, in a competing experiment with (*R*)-carvone (**3-1**), 2-phenylindole (**1-16**) afforded more coupling product **6-16** than indole (**1-20**) under both conditions, although 2-phenylindole (**1-16**) is more steric hindered and less electron rich, which further supported our hypothesis about C2-substituent-promoted coupling (Figure 3B, see also Figure S6). Meanwhile, less tetramer of indole (**10**) was isolated in the background reaction under our condition, and no dimer product **7-2** was observed. Interestingly, only dimmer of C2-methyl/phenylindole (**7-1**, **7-3**) was isolated when indole **1-1** and **1-16** were subjected to the same background reactions, which can serve as a complementary approach for synthesis of 3,3′- bisindoles. Apparently, all these experiments illustrated that both C2-substitutent and our reaction condition contributed to reducing the homocoupling of indole (Figure 3C, also see Figures S7 and S8).

Both products **6** and **7**, as reported by Scott (Scott et al., 1964) and Xia (Deng et al., 2014), could be generated from the dimerization of indole C3-radicals (**III**). Therefore, compound **1-14** was utilized to probe such

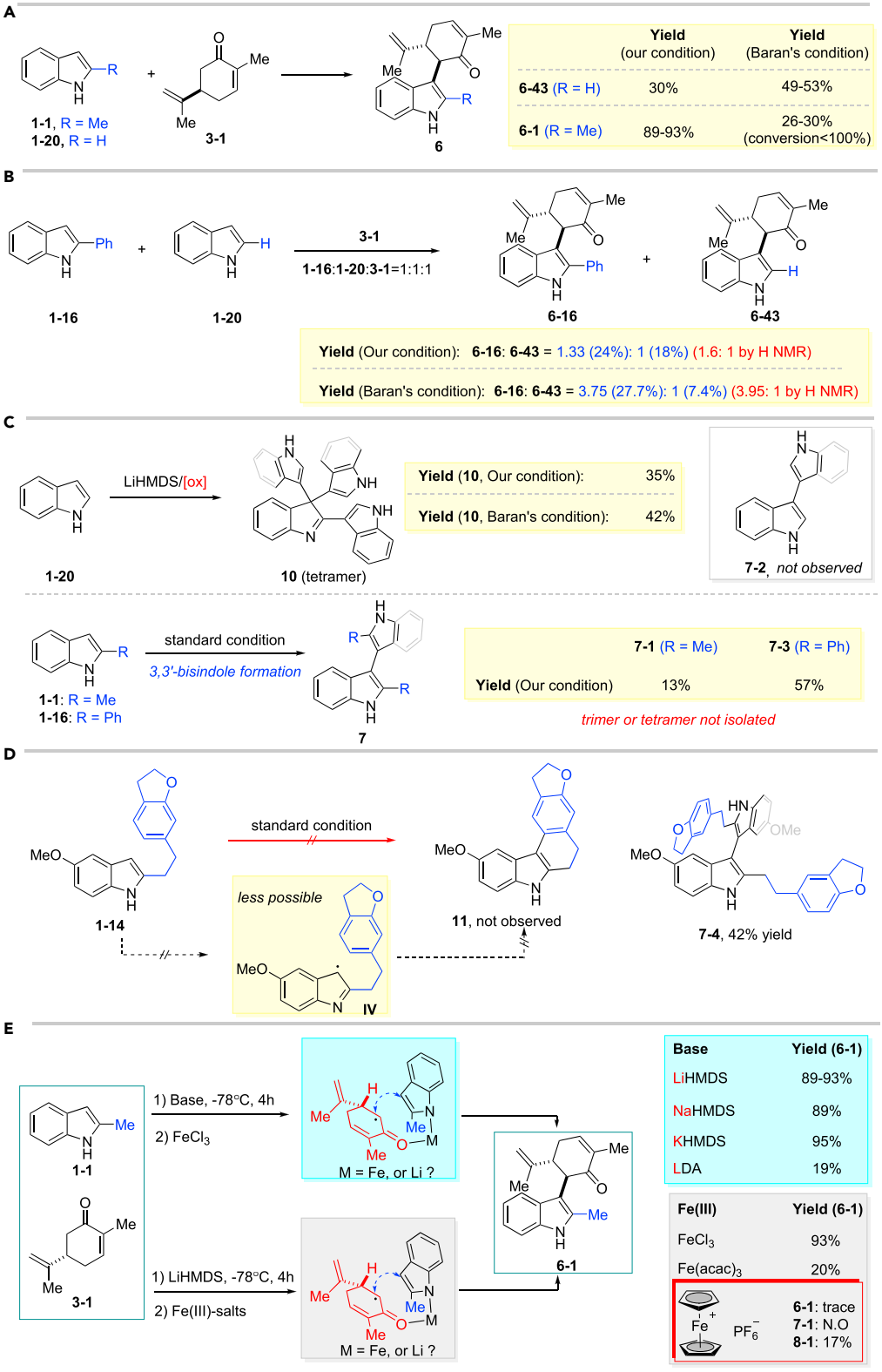

Figure 3. Mechanistic Investigation

(A) Control experiments between 2-methylindole (**1-1**) and indole (**1-10**).

(B) Competing experiments between 2-phenylindole (**1-16**) and indole (**1-20**), also see Figure S6.

Figure 3. *Continued*

(C) Background reaction from homocoupling of indole (**1-20**), 2-methylindole (**1-1**), and 2-phenylindole (**1-16**), also see Figure S7 and S8.

(D) Indole C3-radical trapping experiments, also see Figure S9.

(E) Experiments to identify the chelating effects, also see Table S3.

possibility. However, no anticipated cyclized product **13** was observed; instead, only product **7-4** was isolated, indicating that the reaction might not involve indole C3-radical in our reaction (Figure 3D, also see Figure S9).

Furthermore, to figure out whether this oxidative coupling went through Fe- or Li-chelated or non-chelated procedure (Richter et al., 2007; Casey and Flowers, 2011), different base (MHMDS, M = Li, Na, K, and LDA) and Fe(III)-oxidants were probed. All MHMDS afforded nearly the same results except evident lower yield from LDA (Jahn and Hartmann, 2001). Much inferior efficiency was observed with $Fe(acac)_3$ bearing strong ligand, and only low yield of dimmer of (*R*)-carvone (**3-1**) was isolated in the presence of non-cheating $[FeCp_2]PF_6$ along with trace amount of **6-1**. These results clearly suggested that the reaction went through a Fe-chelated radical-anion coupling procedure (Figure 3E, also see Table S3).

Proposed Reaction Mechanism

Based on information obtained from the mechanistic studies, we proposed reaction mechanism as following. Overall, the reaction went through Fe(III)-Fe(II)-mediated radical-anion coupling procedure (Neumann and Kochi, 1975; Al-Afyouni et al., 2014; Cassani et al., 2016; Mako and Byers, 2016). After deprotonation, $FeCl_3$ chelated with indole anion and enolate (**TS-IV**), followed by an internal or out-sphere single-electron-transfer (SET) process affording enolate radical intermediate **TS-V** or **TS-VII**, which was then trapped by indole to generate indole C2-radical **TS-VI** or **TS-VIII** via radical-anion coupling (path a, b). Such indole C-2 radials were then oxidized into indole, affording the desired product **6**. The C2-substituent, as shown in **TS-VI** or **TS-VIII**, can stabilize such indole C2-radical intermediates, thus enhancing the reaction efficiency. On the other hand, the indole C3-radical intermediate, either **TS-IX** or **TS-X**, was less possibly involved. Taking into account that the dimerization of (*R*)-carvone (**8-1**) still occurred even in the presence of $[FeCp_2]PF_6$ (Figure 3E), evidently the enolates can transfer into corresponding radicals via out-sphere SET process. Thus, path b is more likely. Based on all the mechanistic studies, C2-substituent of indole plays dual roles in promoting the reaction albeit the steric repulsion: (1) stabilizing the indole C2-radical intermediates; (2) reducing homocoupling of indole (Figure 4).

Evaluation of C2-Substituted Indole as Coupling Partner

Within the optimized condition at hand, the C2-substituted indole scope for this reaction was probed first as shown in Table 2. Generally, indoles bearing electron-donating groups afford the desired products in relatively higher yield compared with those bearing electron-withdrawing ones (**6-2**, **6-6** versus **6-3**, **6-4**; **6-6** versus **6-10**). More steric effects hurt the reaction. For example, dropped yield was observed from 2-ethyl-indole (**6-11**), and no desired product could be isolated using 2-*tert*-butylindole (**6-12**). C2, C4-disubstituted indole can also be tolerated in this reaction, given that its huge steric hindrance might push the carbonyl substrate away (**6-9**). Indoles bearing complex moieties on C2-position, like dihydrobenzofuran and phthalimide, also worked smoothly in this reaction (**6-14** and **6-15**). C2-(hereto)aryl indoles also worked under the standard condition (**6-16**–**6-18**). Pyridine motif can be tolerated too, given that it is a good ligand to iron leading to inhibition of the reaction (**6-19**). Notably, the difference of the yields between product **6-16** and **6-18** (electron-rich arene > electron-deficient arene) also supports our hypothesis about the electrophilic nature of indole C2-radical.

Evaluation of Carbonyl Compounds as Coupling Partner

The carbonyl substrate scope was explored as shown in Table 3. Various carbonyl compounds embodying C_α-H could be tolerated in the reaction. Diverse cyclohexanones can afford the desired products in moderate to good yields (**6-20**–**6-23**, **6-32**, **6-34**–**6-36**). Quite interestingly, simple cyclopentanone failed to afford any product under standard reaction condition (**6-31**), whereas its derivatives, *cis*-jasmon and isojasmone, gave products in moderate yield (**6-26**, **6-27**). Utilizing stronger base, LDA, instead of LiHMDS, did afford the product **6-31**. Cycloheptanone and cyclooctenone with ring-strain can also react smoothly under standard condition (**6-24**, **6-25**). The desired products were isolated in moderate to good yield from linear enone, ester, lactone, and amide (**6-28**, **6-29**, **6-38**–**6-40**). It is worth pointing out that the thioester could

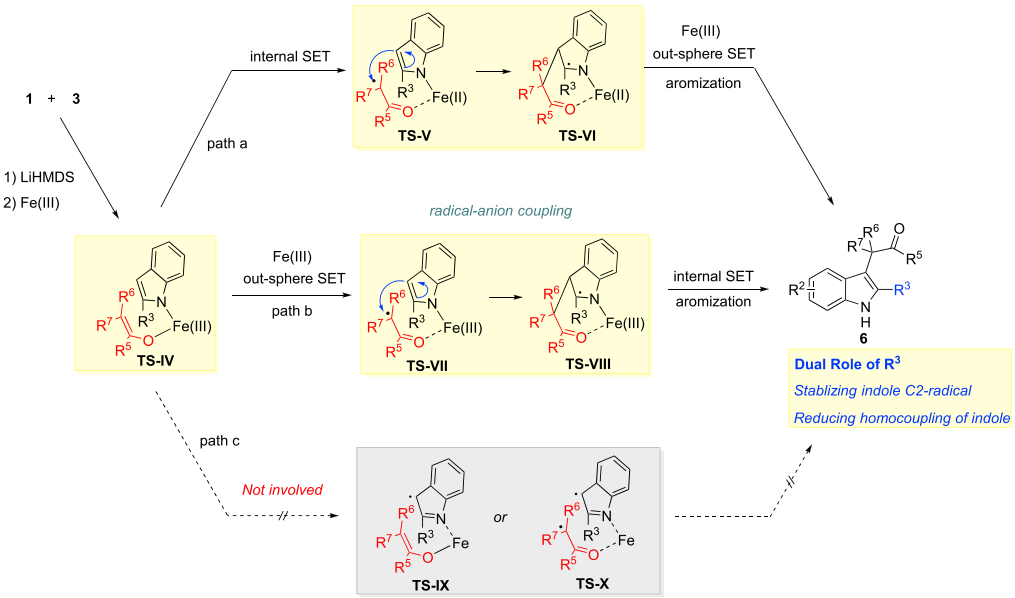

Figure 4. Proposed Reaction Mechanism

also afford the desired product in moderate yield, which was not reported in previous research about oxidative coupling of enolates (**6-39**). The methyl ketones, prone to dimerization as documented in the literature (Richter et al., 2007), also yielded the cross-coupling products (**6-41**, **6-42**).

Bisindole Products Formation

Quite interestingly, instead of the normal coupling product **6-43** and **6-44**, the highly steric hindered bisindole **9-1** and **9-2** were obtained from cyclized benzylenolate **3-23** and **3-24**, respectively. We suspected that the normal product **6-44/6-45** could easily be oxidized into enolate-radical intermediate **XII**, which was stabilized by two arenes followed by coupling with another indole in the presence of $FeCl_3$ (Wu, et al., 2015) (Figure 5).

Limitation of Substrate Scope

Although our reaction expands the landscape for oxidative coupling of indole and enolate, providing a concise access to construct diverse C2, C3-disubstituted indole scaffolds, however, limitation of substrate scope still exists as shown in Figure 6. Extremely low-yield oxidative coupling product (2% isolated yield) was isolated from C2-carboxylate indoles (**1-22** and **1-23**). For the carbonyl compounds, no desired product was obtained when chroman-2-one (**3-45**) was investigated; instead, an amide product from indole opening the lactone was isolated. Other carbonyl compounds, like those bearing highly steric hindrance (**3-46** and **3-47**), heterocycles (**3-48** and **3-49**), small rings (**3-50** and **3-51**), ynone (**3-52**), aldehyde (**3-53**), or α-ketone-ester (**3-54**), all could not afford the desired coupling products. About 8% yield of the desired oxidative coupling product was isolated when cyclopentane-1,2-dione **3-55** was utilized in this reaction, although 1,2-diketone has never been studied in oxidative coupling of enolates. The intramolecular reaction was also conducted; however, the desired ring-closing products were failed to be isolated (Figure S6, also see Figure S5).

Synthetic Application

Synthesis of Indomethacin and Its Analogue

Indomethacin is a selective COX-1 (cyclooxygenases-1) inhibitor, which has been broadly used as an anti-inflammatory drug for decades. Recent research showed that inhibition of COX is beneficial for cancer therapy by inhibiting drug resistance and immune evasion of certain cancer cells (Yu et al., 2009; Vinogradova et al., 2011; Zelenay et al., 2015; Hashemi et al., 2019). Therefore, design and synthesis of novel selective COX inhibitors based on indomethacin can potentially benefit cancer therapy. Previous research about indomethacin analogues synthesis required multiple steps (Rosenbaum et al., 2015; Arisawa et al., 2012);

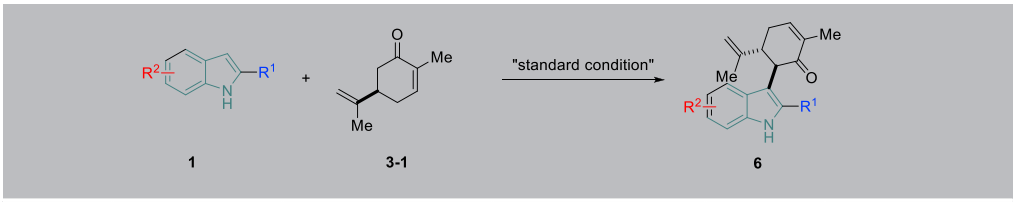

R^1	R^2	Product, Yield	R^1	R^2	Product, Yield
—Me	H	**6-1**, 93%(78%[b])	—Et	H	**6-11**,77%
	5-Me	**6-2**, 96%	—^{t}Bu	H	**6-12**, ND
	5-Cl	**6-3**, 78%	—(CH$_2$)$_4$Me	5-OMe	**6-13**, 63%
	5-F	**6-4**, 67%	—(CH$_2$)$_2$-(2,3-dihydrofuran)		**6-14**, 95%
	5-Br	**6-5**, 77%	—(CH$_2$)$_3$-(phthalimide)	H	**6-15**, 63%
	5-OMe	**6-6**, 89%	—Ph		**6-16**, 74%
	6-Me	**6-7**, 91%	—Ph-OMe		**6-17**, 69%
	6-OMe	**6-8**, 70%	—Ph-CO$_2$Me		**6-18**, 23%
	4-OMe	**6-9**, 53%	—(3-pyridyl)		**6-19**, 39%
	4-F, 5-OMe	**6-10**, 69%			

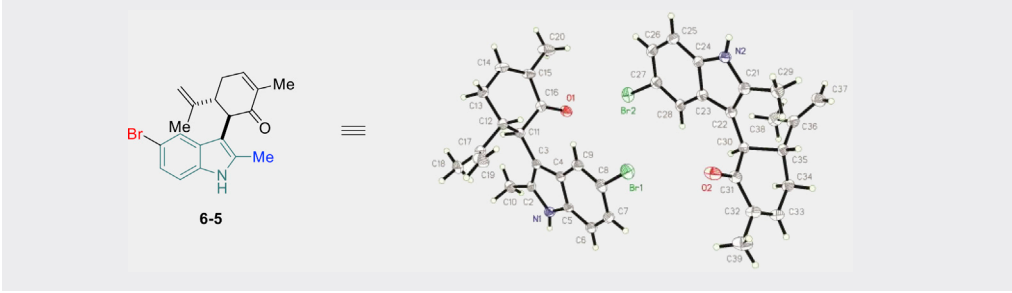

Table 2. Scope of C2-substituted Indole

[a]All the reactions were conducted under standard condition with 1.0 mmol of (*R*)-carvone (3-1) and 2.0 mmol indole unless noted, isolated yield.

[b]Gram scale; ND = no desired product.

thus, developing concise and efficient synthetic routes for synthesis of indomethacin analogues is important. Based on this reaction, both indomethacin and its analogues could be prepared in a three-step sequence. Under the standard reaction condition, 2-methyl-5-methoxy indole (**1-6**) and *tert*-butyl acetate smoothly afford the precursor of indomethacin **6-46** in moderate yield (61%). After installing the 4-chlorobenzoyl moiety on N1-position and deprotection of *tert*-butyl with trifluoroacetic acid (TFA) sequentially,

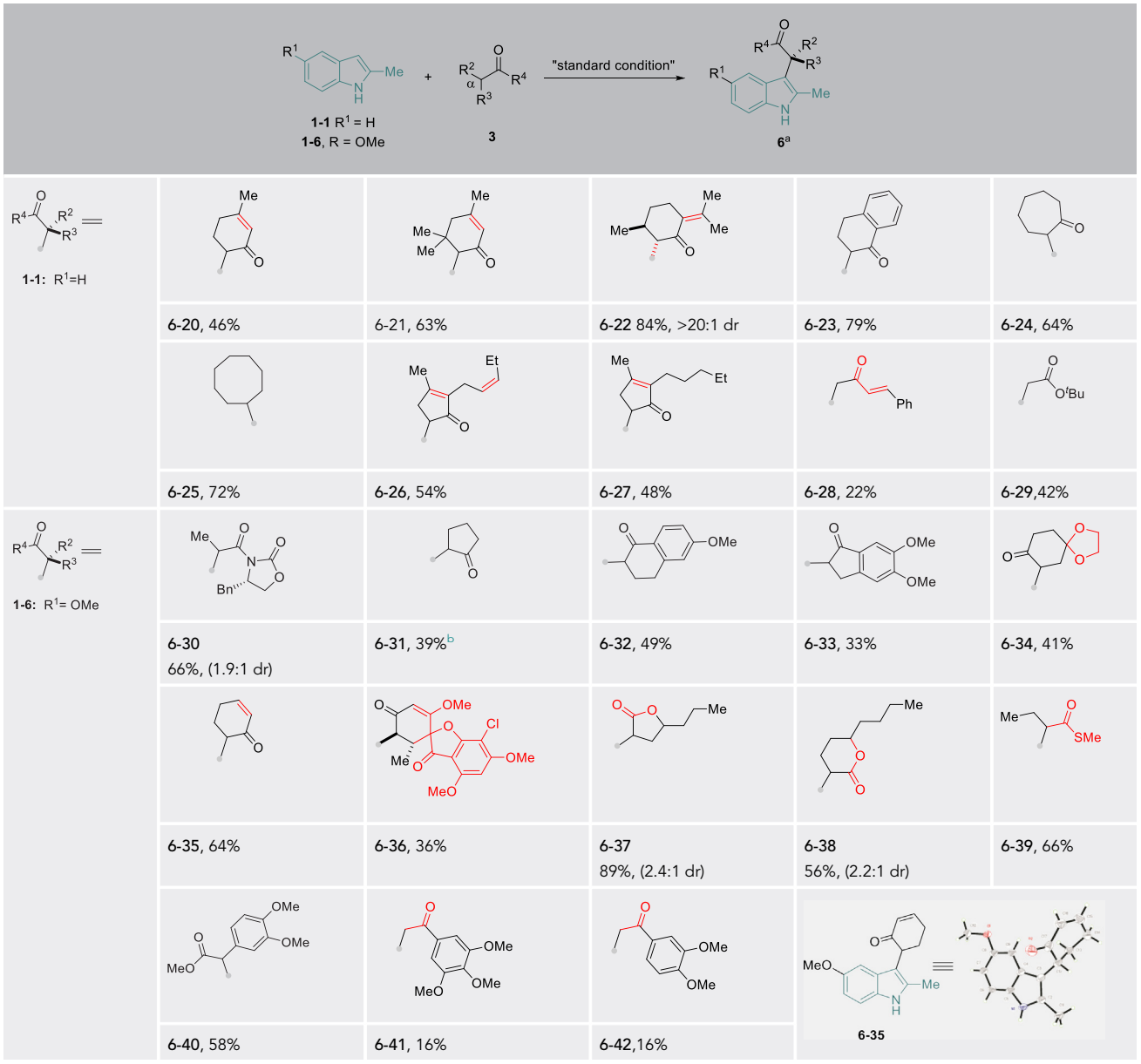

Table 3. Enolate Scope

[a]All the reactions were conducted under standard condition with 1.0 mmol of carbonyl compound and 2.0 mmol indole unless noted, isolated yield.
[b]LDA was used instead of LHMDS.

indomethacin **12-2** was obtained in excellent yield (58% total yield). The indomethacin analogue was prepared conveniently and similarly from indole: selective C2-functionation, C3-alkylation via oxidative coupling, and N1-acylation. For example, the selective C2-alkylation of indole **1-21** could be conveniently achieved to afford **1-14** under Bath's condition (Jiao and Bach, 2011). The desired product **12-4** can be obtained in good yield followed by the same procedure as synthesis of indomethacin smoothly (Figure 7A, also see Figure S4).

C3-Aryl Indole Construction

C3-aryl indole scaffolds can also be found in many bioactive small molecules (Liu et al., 2000; Güzel et al., 2009; Luz et al., 2015). We hypothesized that the oxidative aromatization of carvone moiety in product could afford such scaffold. Therefore, several transformations were utilized to transfer compound **6-1**

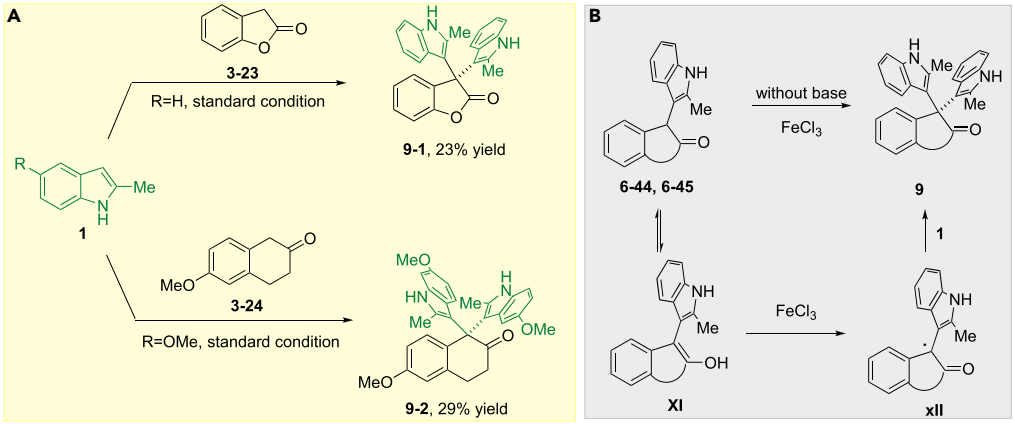

Figure 5. Bisindole Products Formation

(A) Bisindole products observed in the reaction.

(B) Proposed reaction mechanism for bisindole product formation.

into C3-aryl indoles. Many commonly used oxidants failed to afford the desired aromatization product, such as $CuBr_2$ and Iodobenzene diacetate (Hisahiro et al., 2002; Dethe et al., 2015). Low yield of compound **13-1** was obtained when DDQ (Sadak et al., 2010) was utilized in high reaction temperature. Such inert reactivity in aromatization may probably be due to highly steric hindrance of carvone motif as shown in X-ray of product **6-5**. Interestingly, when iodine was utilized as stoichiometric in DMSO, only trace amount of the desired product was obtained; however, good conversion was observed when catalytic amount of iodide in 2.0 equivalent of DMSO was used (Wang et al., 2016; Liang et al., 2016). Finally, the desired product **13-1** could be obtained in moderate yield (Figure 7B, also see Table S2).

Biological Evaluation

Anticancer Bioactivities Evaluation against A549 Cells

Given that indoles have promising anticancer potential, we selected a dozen of our reaction products for the evaluation of cytotoxicity in human lung cancer cell line A549. To our delight, all the tested products exhibited significant anticancer bioactivities at 100 μM (Figure 8A). Then the compounds with an inhibitory rate higher than 50% at 10 μM were further investigated. As shown in Figure 8B, compounds **6-3**, **6-8**, **6-36**,

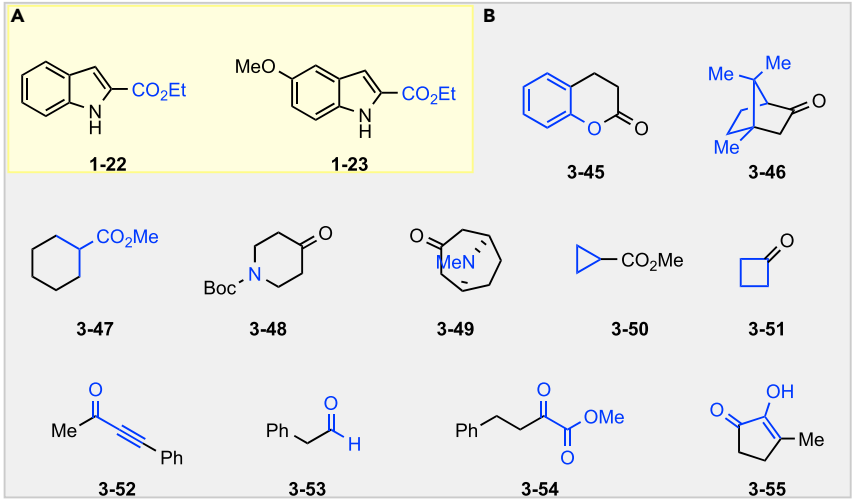

Figure 6. Failed Substrates

(A) Failed indole substrates.

(B) Failed carbonyl substrates.

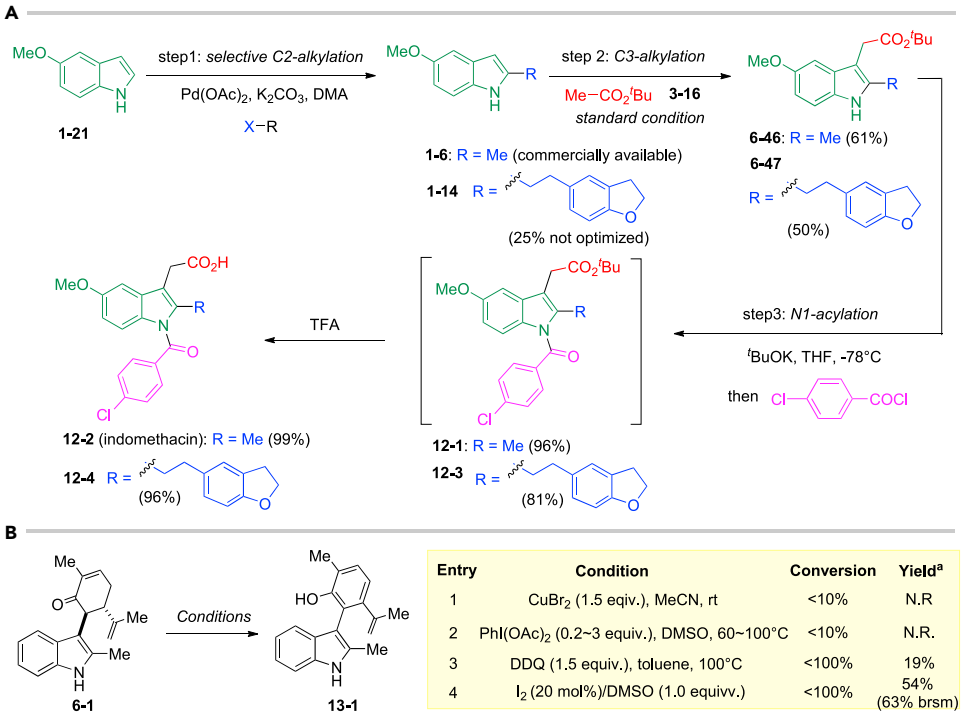

Figure 7. Synthetic Application

(A) Three steps to prepare indomethacin and its analogue, see also Figure S4.

(B) C3-aryl indole synthesis via aromatization, see also Table S1.

and **13-1** showed marked cytotoxicities with IC_{50} (concentration to inhibit cell growth by 50%) in the low micromolar range, serving as a promising starting point for novel anticancer drug discovery. Notably, compound **13-1** showed comparable IC_{50} value as those of compound **6-3** and **6-8**, indicating that such observed cytotoxicity of compound **6-3** and **6-8** might not be from being Michael acceptor in carvone.

Multidrug Resistance Evaluation

Multidrug resistance (MDR) (Szakács et al., 2006; Housman et al., 2014) is a major impediment to effective chemotherapy of cancer. The cytotoxicities of compounds **6-3**, **6-8**, **13-1**, and **6-36** were evaluated in an MDR cell line. Resistance factor (RF), the ratio of the IC_{50} against MDR cells (KB/VCR) to that against the parental cells (KB-3-1), was calculated. The RF value for vincristine (VCR) was 206, which validated the MDR phenotype of KB/VCR cells. However, compounds **6-3**, **6-8**, **13-1**, and **6-36** maintained their potency against KB/VCR cells, suggesting that they could overcome multidrug resistance (Figure 8C).

Cell Cycle Progression Investigation

To further explore the mechanism underlying the anti-proliferative activities of compounds **6-3**, **6-8**, **13-1**, and **6-36**, their effects on cell cycle progression were examined. 4′-Demethylepipodophyllotoxin (DPP), a microtubule inhibitor, induced G2/M arrest in exponentially growing A549 cells. Although compounds **6-2**, **6-8**, **13-1**, and **6-36** share some structural similarities with DPP, they did not have significant impact on cell cycle progression, suggesting they exerted their anticancer activity through a mechanism different from that of DPP. Further studies on the exact mechanism are currently ongoing in our laboratory (Figure 8D).

Anticancer Bioactivities Evaluation against H1299, HCT116, HT29, K562, MV-4-11, and HepG2 Cells

Some of the products showed promising anticancer activity against A549 cells; however, whether they were effective in other cancer cell lines remains unknown. Thus, compound **6-3**, **6-8**, **6-36**, and **13-1** were investigated in several other cancer lines, including human lung cancer (H1299), colon cancer (HCT116, HT29), leukemia (K562, MV-4-11), and liver cancer (HepG2) cells. To our delight, the primary results showed promising results. For example, compound **6-8** and **6-36** showed good to excellent inhibition rate against all

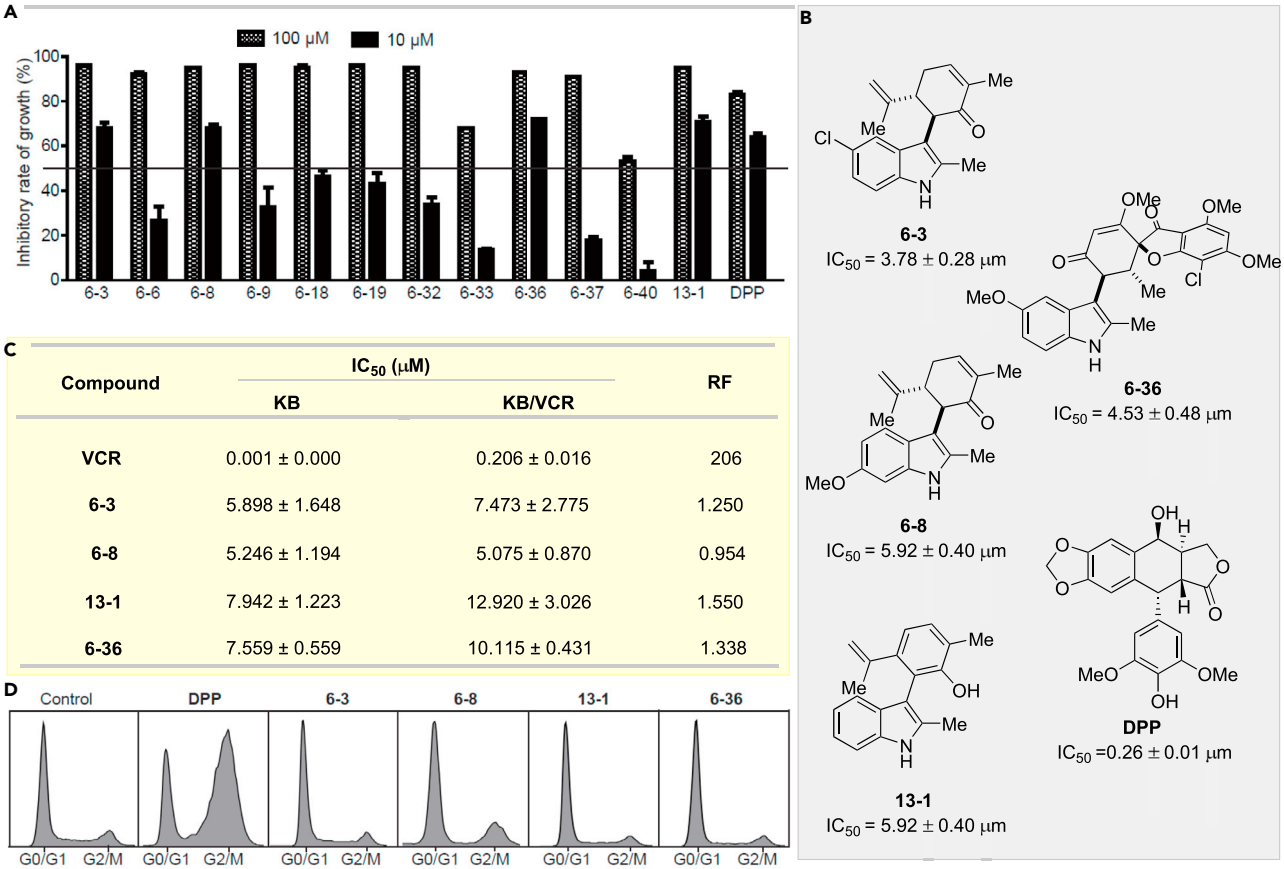

Compound	IC_{50} (μM)		RF
	KB	KB/VCR	
VCR	0.001 ± 0.000	0.206 ± 0.016	206
6-3	5.898 ± 1.648	7.473 ± 2.775	1.250
6-8	5.246 ± 1.194	5.075 ± 0.870	0.954
13-1	7.942 ± 1.223	12.920 ± 3.026	1.550
6-36	7.559 ± 0.559	10.115 ± 0.431	1.338

Compound	Inhibition Rate (%, 30 μM)					
	H1299	HCT116	HT29	K562	MV-4-11	HepG2
6-3	44.8±1.39	30.22±2.82	87.32±1.22	97.92±0.67	79.8±3.14	48.69±3.69
6-8	68.33±4.48	87.80±0.56	87.38±0.21	84.55±0.96	97.96±0.84	48.32±2.09
6-36	60.01±4.86	69.75±0.56	61.48±0.87	106.68±3.0	91.62±2.43	66.29±1.88
13-1	17.26±5.21	13.94±0.08	31.0±23.88	64.1±0.14	49.62±6.46	31.01±5.45
DPP	68.27±3.41	90.91±0.93	79.64±0.56	82.44±0.81	100.45±0.13	86.94±0.78

Figure 8. Bioactivity Evaluation

(A) Cytotoxicity evaluation of selected products against A549 cells.

(B) Structure and IC_{50} Value of selected molecules against A549 cells.

(C) Resistance factors (RFs) of the compounds in KB-3-1 and KB/VCR cells; cells were treated with different concentrations of indicated compounds for 72 h and IC_{50} values were measured by sulforhodamine B assays.

(D) The effects of the compounds on cell cycle progression; A549 cells were treated with indicated compounds (10 μM) for 24 h and cell cycle distribution was measured by flow cytometry.

(E) Cytotoxicity evaluation of selected products against H1299, HCT116, HT29, K562, MV-4-11, and HepG2 cells for selected compounds.

Also see in Supplemental Information.

these cell lines except HepG2 for compound **6-8**. And all these compounds except **13-1** exhibited good to excellent inhibition effects in leukemia cell lines K562 and M-V-411. In contrast, compound **13-1** showed only a moderate inhibition rate in K562 cell. These results showed that our products could serve a good starting point for anticancer drug discovery. Further biological study of these compounds is under way in our laboratory (Figure 8E).

Conclusion

In summary, we have developed an efficient approach to construct C2, C3-disubstituted indole by C2-substituent-promoted oxidative coupling of indole and enolate. Broad substrate scope and moderate to excellent yield were observed. The mechanism studies illustrated that the C2-substituent has dual effects to promote the reaction: stabilizing of the indole C2-radicals and decreasing the homocoupling of indole. Moreover, several products showed promising anticancer activities in several cell lines and can overcome multidrug resistance in KB/VCR cells in primary biological evaluation, which potentially serves as starting points for novel anticancer drug discovery.

METHODS

All methods can be found in the accompanying Transparent Methods supplemental file.

DATA AND CODE AVAILABILITY

The data for the X-ray crystallographic structures of **6-5**, **6-5**, and **6-35** are available free of charge from the Cambridge Crystallographic Data Center under accession numbers CCDC: 1913053, 1914654, and 1913054, respectively.

SUPPLEMENTAL INFORMATION

Supplemental Information can be found online at https://doi.org/10.1016/j.isci.2019.11.021.

ACKNOWLEDGMENTS

Financial support was provided by the National Natural Science Foundation of China (21602011, 81572695). The author would like to thank Prof. Chaomei Xiong in HUST for NMR spectra collection and Dr. Dingche Yan in Analytical and Testing Centre of HUST for assistance in HRMS and FTIR collection. The authors would like to thank Prof. Hui Qian in Fudan University for his help in biological evaluation of products.

AUTHOR CONTRIBUTIONS

Z.C. designed the whole project and chemistry experiments; Q.C. and Z.C. designed the biological evaluation experiments; H.L. conducted most of the chemistry experiments and collected the chemistry experimental data; T.T. and Z.M. conducted partial work in chemistry experiments; G.Z. conducted the biological evaluation of selected products; Z.C. wrote the manuscript of chemistry experiments; Q.C. wrote the manuscript of biological evaluation.

DECLARATION OF INTERESTS

The authors declare no competing interests.

Received: July 16, 2019
Revised: November 9, 2019
Accepted: November 12, 2019
Published: December 20, 2019

REFERENCES

Aksenov, A.V., Smirnov, A.N., Magedov, I.V., Reisenauer, M.R., Aksenov, N.A., Aksenova, I.V., Pendleton, A.L., Nguyen, G., Johnston, R.K., Rubin, M., et al. (2015). Activity of 2-aryl-2-(3-indolyl)acetohydroxamates against drug-resistant cancer cells. J. Med. Chem. *58*, 2206–2220.

Al-Afyouni, M.H., Fillman, K.L., Brennessel, W.W., and Neidig, M.L. (2014). Isolation and characterization of a tetramethyliron(III) Ferrate: an intermediate in the reduction pathway of ferric salts with MeMgBr. J. Am. Chem. Soc. *136*, 15457–15460.

Arisawa, M., Kasaya, Y., Obata, T., Sasaki, T., Nakamura, T., Araki, T., Yamamoto, K., Sasaki, A., Yamano, A., Ito, M., et al. (2012). Design and synthesis of indomethacin analogues that inhibit P-glycoprotein and/or multidrug resistant protein without cox inhibitory activity. J. Med. Chem. *55*, 8152–8163.

Artz, S.P., and Cram, D.J. (1984). Host-guest complexation. 28. Hemispherands with four self-organizing units. J. Am. Chem. Soc. *106*, 2160–2171.

Babler, J.H., and Haack, R.A. (1983). Intramolecular Oxidative Coupling of the Bis Enolate Derived from Dimethyl β, β-Dimethylglutarate: a facile stereoselective route to a versatile synthon for preparation of insecticidal pyrethroids. Synth. Commun. *13*, 905–911.

Baran, P.S., and Richter, J.M. (2004). Direct coupling of indoles with carbonyl compounds short, enatioselective, gram-scale synthetic entry into the hapalindole and fischerindole alkaloid. J. Am. Chem. Soc. *126*, 7450–7451.

Bostrom, J., Brown, D.G., Young, R.J., and Keseru, G.M. (2018). Expanding the medicinal

chemistry synthetic toolbox. Nat. Rev. Drug Discov. *17*, 709–727.

Brocksom, T.J., Petragnani, N., Rodrigues, R., and Teixeira, L.S. (1975). Ester enolates II: the preparation of di- and tetra-substituted succinate esters. Synthesis *7*, 396–397.

Burn, J.H., and Rand, M.J. (1958). .The action of sympathomimetic amines in animals treated with reserpine. J. Physiol. *144*, 314–336.

Campos, K.R., Coleman, P.J., Alvarez, J.C., Dreher, S.D., Garbaccio, R.M., Terrett, N.K., Tillyer, R.D., Truppo, M.D., and Parmee, E.R. (2019). The importance of synthetic chemistry in the pharmaceutical industry. Science *363*, 244–251.

Casey, B.M., and Flowers, R.A., II (2011). On the nature of the oxidative heterocoupling of lithium enolates. J. Am. Chem. Soc. *133*, 11492–11495.

Cassani, C., Bergonzini, G., and Wallentin, C.-J. (2016). Active species and mechanistic pathways in iron-catalyzed C–C bond-forming cross-coupling reactions. ACS Catal. *6*, 1640–1648.

Cermak, T., Dykstra, K.D., Tyagarajan, S., Vachal, P., and Krska, S.W. (2015). .The medicinal chemist's toolbox for late stage functionalization of drug-like molecules. Chem. Soc. Rev. *45*, 546–576.

Deng, X., Liang, K., Tong, X., Ding, M., Li, D., and Xia, C. (2014). Copper-catalyzed radical cyclization to access 3-hydroxypyrroloindoline: biomimetic synthesis of protubonine A. Org. Lett. *16*, 3276–3279.

Dethe, D.H., Dherange, B.D., and Boda, R. (2015). $Hg(OAc)_2$ mediated highly regio- and/or diastereoselective allylic tert-acetylation of olefins. Org. Chem. Front *2*, 159–162.

Dugger, S.A., Platt, A., and Goldstein, D.B. (2017). Drug development in the era of precision medicine. Nat. Rev. Drug Discov. *17*, 183–196.

Esteves, C.H.A., Smith, P.D., and Donohoe, T.J. (2017). Catalytic enolate arylation with 3-bromoindoles allows the formation of beta-carbolines. J. Org. Chem. *82*, 4435–4443.

Gibe, R., and Kerr, M.A. (2002). Convenient preparation of indolyl Malonates via carbenoid insertion. J. Org. Chem. *67*, 6247–6249.

Gribble, G.W. (2016). Indole Ring Synthesis: from Natural Products to Drug Discovery (John Wiley and Sons Ltd.).

Guo, F., Clift, M.D., and Thomson, R.J. (2012). Oxidative coupling of enolates, enol silanes and enamines: methods and natural product synthesis. E. J. Org. Chem. *26*, 4881–4896.

Güzel, Ö., Maresca, A., Scozzafava, A., Salman, A., Balaban, A.T., and Supuran, C.T. (2009). Discovery of low nanomolar and subnanomolar inhibitors of the mycobacterial-carbonic anhydrases Rv1284 and Rv3273. J. Med. Chem. *52*, 4063–4067.

Hashemi, G.N., Najafi, M., Salehi, E., Farhood, B., and Mortezaee, K. (2019). Cyclooxygenase-2 in cancer: a review. J. Cell. Physiol. *234*, 5683–5699.

Herraiz-Cobo, J., Albericio, F., and Álvarez, M. (2015). Advances in Heterocyclic Chemistry. Chapter One-The Larock Reaction in the Synthesis of Heterocyclic Compounds, *116* (Academic Press), pp. 1–35.

Hisahiro, H., Tomoyuki, O., Hiroki, O., Vijayendra, P.K., Takashi, H., Toshio, S., and Masayoshi, A. (2002). Total synthesis of bisabolanesesquiterpenoids, α-bisabol-1-one, curcumene, curcuphenol and elvirol: utility of catalytic enamine reaction in cyclohexenone synthesis. J. Chem. Soc. Perkin Trans. *1*, 895–900.

Housman, G., Byler, S., Heerboth, S., Lapinska, K., Longacre, M., Snyder, N., and Sarkar, S. (2014). Drug resistance in cancer: an overview. Cancers *6*, 1769–1792.

Ito, Y., Konoike, T., and Saegusa, T. (1975). Reaction of ketone enolates with copper dichloride. Synthesis of 1, 4-diketones. J. Am. Chem. Soc. *97*, 2912–2914.

Ito, Y., Konoike, T., Harada, T., and Saegusa, T. (1977). Synthesis of 1, 4-diketones by oxidative coupling of ketone enolates with copper(II) chloride. J. Am. Chem. Soc. *99*, 1487–1493.

Ivanoff, D., and Spasoff, A. (1935). Synthesis with sodium magnesylphenylacetate. IV. Addition of oxygen and bromination. Bull. Soc. Chim. Fr. *2*, 76–78.

Jahn, U., and Hartmann, P. (2001). Oxidative radical cyclizations of malonate enolates induced by the ferrocenium ion-a remarkable influence of enolate counterion and additives. J. Chem. Soc. Perkin Trans. *1*, 2277–2282.

Jiao, L., and Bach, T. (2011). Palladium-catalyzed direct 2-alkylation of indoles by norbornene-mediated regioselective cascade C–H activation. J. Am. Chem. Soc. *133*, 12990–12993.

Kauffmann, T., Beissner, G., Berg, H., Köppelmann, E., Legler, J., and Schönfelder, M. (1968). Dimerization of oxaallyl, azaallyl, oxaphosphaallyl, and oxathiaallyl groups by way of organocopper compounds. Angew. Chem. Int. Ed. *7*, 540–541.

Ke, L., Zhu, G., Qian, H., Xiang, G., Chen, Q., and Chen, Z. (2019). Catalytic selective oxidative coupling of secondary *N*-alkylaniline: an approach to azoxyarene. Org. Lett. *21*, 4008–4013.

Keller, H., Langer, E., and Lehner, H. (1977). Synthesen 2-substituierter 3-Indol-alkansäuren. Monatsh. Chem. *108*, 123–131.

Kochanowska-Karamyan, A.J., and Hamann, M.T. (2010). Marine indole alkaloids: potential new drug leads for the control of depression and anxiety. Chem. Rev. *110*, 4489–4497.

Liang, Y.-F., Song, S., Ai, L., Li, X., and Jiao, N. (2016). A highly efficient metal-free approach to meta- and multiple-substituted phenols via a simple oxidation of cyclohexenones. Green Chem. *18*, 6462–6467.

Liu, C., Zhang, H., Shi, W., and Lei, A. (2011). Bond formations between two nucleophiles: transition metal catalyzed oxidative cross-coupling reactions. Chem. Rev. *111*, 1780–1824.

Liu, K., Xu, L., Szalkowski, D., Li, Z., Ding, V., Kwei, G., Huskey, S., Moller, D.E., Heck, J.V., Zhang, B.B., and Jones, A.B. (2000). Discovery of a potent, highly selective, and orally efficacious small-molecule activator of the insulin receptor. J. Med. Chem. *43*, 3487–3494.

Luz, J.G., Carson, M.W., Condon, B., Clawson, D., Pustilnik, A., Kohlman, D.T., Barr, R.J., Bean, J.S., Dill, M.J., Sindelar, D.K., et al. (2015). Indole glucocorticoid receptor antagonists active in a model of dyslipidemia act via a unique association with an agonist binding site. J. Med. Chem. *58*, 6607–6618.

Mako, T.L., and Byers, J.A. (2016). Recent advances in iron-catalyzed cross coupling reactions and their mechanistic underpinning. Inorg. Chem. Front. *3*, 766–790.

Maksymenko, S., Parida, K.N., Pathe, G.K., More, A.A., Lipisa, Y.B., and Szpilman, A.M. (2017). Transition-metal-free intermolecular alpha-arylation of ketones via enolonium species. Org. Lett. *19*, 6312–6315.

Mase, B.U.W. (2010). Heterocyclic Scaffolds II: Reactions and Applications of Indoles (Springer).

Neumann, S.M., and Kochi, J.K. (1975). Synthesis of olefins. Cross-coupling of alkenyl halides and Grignard reagents catalyzed by iron complexes. J. Org. Chem. *40*, 599–606.

Ojima, I., Brandstadter, S.M., and Donovan, R.J. (1992). Oxidative dimerization of lithium-enolates of esters promoted by titanium tetrachloride. Chem. Lett. *21*, 1591–1594.

Rathke, M.W., and Lindert, A. (1971). Reaction of ester enolates with copper(II) salts. Synthesis of substituted succinate esters. J. Am. Chem. Soc. *93*, 4605–4606.

Richter, J.M.W., Whitefield, B.W., Maimone, T.J., Lin, D.W., Castroviejo, M.P., and Baran, P.S. (2007). Scope and mechanism of direct indole and pyrrole couplings adjacent to carbonyl compounds: total synthesis of acremoauxin A and oxazinin 3. J. Am. Chem. Soc. *129*, 12857–12869.

Robinson, B. (1963). The Fischer indole synthesis. Chem. Rev. *63*, 373–401.

Rosenbaum, C., Röhrs, S., Müller, O., and Waldmann, H. (2015). Modulation of MRP-1-mediated multidrug resistance by indomethacin analogues. J. Med. Chem. *48*, 1179–1187.

Sadak, A.E., Arshlan, T., Celebioglu, N., and Saracoglu, N. (2010). New 3-vinylation products of indole and investigation of its Diels-Alder reactivity: synthesis of unusual Morita-Baylis-Hillman-type products. Tetrahedron *66*, 3214–3221.

Scott, A.I., McCapra, F., and Hall, E.S. (1964). Chimonanthine. One-step synthesis and biosynthetic model. J. Am. Chem. Soc. *86*, 302–303.

Stratmann, K., Moore, R.E., Bonjouklian, R., Deeter, J.B., Patterson, G.M.L., Shaffer, S., Smith, C.D., and Smitka, T.A. (1994). Welwitindolinones, Unusual alkaloids from the blue-green algae *Hapalosiphon welwitschii* and *Westiella intricata*, relationship to fischerindoles and hapalinodoles. J. Am. Chem. Soc. *16*, 9935–9942.

Sun, C.-L., Li, B.-J., and Shi, Z.-J. (2010). Pd-catalyzed oxidative coupling with organometallic reagents *via* C–H activation. Chem. Commun. *46*, 677–685.

Szakács, G., Paterson, J.K., Ludwig, J.A., Booth-Genthe, C., and Gottesman, M.M. (2006). Targeting multidrug resistance in cancer. Nat. Rev. Drug Discov. *5*, 219–234.

Taber, D.F., and Tirunahari, P.K. (2011). Indole synthesis: a review and proposed classification. Tetrahedron *67*, 7195–7210.

Tang, Q., Chen, X., Tiwari, B., and Chi, Y.R. (2012). Addition of indoles to oxyallyl cations for facile Access to α-Indole carbonyl compounds. Org. Lett. *14*, 1922–1925.

Vander Wal, M.N., Dilger, A.K., and MacMillan, D.W.C. (2013). Development of a generic activation mode: nucleophilic α-substitution of ketones via oxy-allyl cations. Chem. Sci. *4*, 3075–3079.

Vinogradova, Y., Coupland, C., and Hippisley-Cox, J. (2011). Exposure to cyclooxygenase-2 inhibitors and risk of cancer: nested case-control studies. Br. J. Cancer *105*, 452–459.

Wang, S.-K., Chen, M.-T., Zhao, D.-Y., You, X., and Luo, Q.L. (2016). Iodine-catalyzed oxidative aromatization: a metal-free concise approach to *meta*-substituted phenols from cyclohex-2-eones. Adv. Syn. Cat *358*, 4093–4099.

Wencel-Delord, J., and Glorius, F. (2013). C-H bond activation enable the rapid construction and late-stage diversification of functional molecule. Nat. Chem. *5*, 369–375.

Wendlandt, A.E., Suess, A.M., and Stahl, S.S. (2011). Copper-catalyzed aerobic oxidative C-H functionalizations: Trends and mechanistic insights. Angew. Chem. Int. Ed. *50*, 11062–11087.

Wu, H.-R., Huang, H.-Y., Ren, C.-L., Liu, L., Wang, D., and Li, C.-J. (2015). Fe(III)-catalyzed cross-dehydrogenative arylation (CDA) between oxindoles and arenes under an air atmosphere. Chem. Eur. J. *21*, 16744–16748.

Yeung, C.S., and Dong, V.M. (2011). Catalytic dehydrogenative cross-coupling: forming carbon–carbon bonds by oxidizing two carbon–hydrogen bonds. Chem. Rev. *111*, 1215–1292.

Yu, L., Wu, W.K.K., Li, Z.J., Liu, Q.C., Li, H.T., Wu, Y.C., and Cho, C.H. (2009). Enhancement of doxorubicin cytotoxicity on human esophageal squamous cell carcinoma cells by indomethacin and 4-[5-(4-Chlorophenyl)-3-(trifluoromethyl)-1*H*-pyrazol-1-yl]benzenesulfonamide (SC236) via inhibiting P-glycoprotein activity. Mol. Pharmacol. *75*, 1364–1373.

Zelenay, S., van der Veen, A.G., Bottcher, J.P., Snelgrove, K.J., Rogers, N., Acton, S.E., Chakravarty, P., Girotti, M.R., Marais, R., Quezada, S.A., et al. (2015). Cyclooxygenase-dependent tumor growth through evasion of immunity. Cell. *162*, 1257–1270.

Zhang, C., Tang, C., and Jiao, N. (2012). Recent advances in copper-catalyzed dehydrogenative functionalization *via* a single electron transfer (SET) process. Chem. Soc. Rev. *41*, 3464–3484.

Zuo, Z., Xie, W., and Ma, D. (2010). Total synthesis and absolute stereochemical assignment of (–)-communesin F. J. Am. Chem. Soc. *132*, 13226–13228.

ISCI, Volume *22*

Supplemental Information

Anticancer Molecule Discovery via C2-Substituent Promoted Oxidative Coupling of Indole and Enolate

Helin Lu, Guirong Zhu, Tiange Tang, Zhuang Ma, Qin Chen, and Zhilong Chen

I. Transparent Methods

I-1. General information

Glassware and stir bars were dried in an oven at 95 °C for at least 12h and then cooled in a desiccator cabinet over Drierite prior to use. Optimization and substrate screen were performed in 25 mL Schlenk flask. All other reactions were performed in round-bottom flasks sealed with rubber septa. Plastic syringes or pipets were used to transfer liquid reagents. Reactions were stirred magnetically using Teflon-coated, magnetic stir bars. Analytical thin-layer chromatography (TLC) was performed using glass plates pre-coated with 0.25 mm of 230–400 mesh silica gel impregnated with a fluorescent indicator (254 nm and 320 nm). TLC plates were visualized by exposure to ultraviolet light and/or exposure to $KMnO_4$ stain as well as phosphomolydic acid (PMA) and cerium molybdate stain. Organic solutions were concentrated under reduced pressure using a rotary evaporator. Flash-column chromatography was performed on silica gel (60 Å, standard grade).

Materials and Instrumentation. Nuclear magnetic resonance spectra were recorded at ambient temperature (unless otherwise stated) on Bruke 400 MHz spectrometers. All values for proton chemical shifts are reported in parts per million (δ) and are referenced to the residual protium in $CDCl_3$ (δ 7.26), CD_3OD (δ 3.31) and DMSO-d_6 (δ 2.50). All values for carbon chemical shifts are reported in parts per million (δ) and are referenced to the carbon resonances in $CDCl_3$ (δ 77.16), CD_3OD (49.00) and DMSO-d_6 (39.52). NMR data are represented as follows: chemical shift, multiplicity (s = singlet, d = doublet, t = triplet, q = quartet, quin = quintet, m = multiplet, br = broad), coupling constant (Hz), and integration. Infrared spectroscopic data was recorded by Bruker VERTEX 70 and reported in wavenumbers ($cm^{-}1$). High-resolution mass spectra were obtained using a liquid chromatography-electrospray ionization and Time-of-flight mass spectrometer by Bruker SolariX 7.0T.

I-2. Starting material synthesis

I-2-1. Preparation of C2-substituted indole

General procedure A Step 1: To a 0 °C solution of 6-methyl-1*H*-indole (15.2 mmol, 2.0 g, 1.0 equivalent) in THF (40 mL) was added NaH (60%, 916 mg, 22.8 mmol, 1.5 equivalent) under N_2 protection. The mixture was stirred for 1 h before benzenesulfonyl chloride (2.4 mL, 18.8 mmol, 1.25 equivalent) was added dropwise at the same temperature. The reaction mixture was then allowed to warm to room temperature and stirred for an additional 1 h. After completion of the reaction monitored by TLC, the reaction mixture was poured into a saturated NH_4Cl solution (100 mL). The aqueous phase was separated and extracted with ethyl acetate (50 mL × 2), the combined organic layers were washed with water (50 mL × 2) and brine (50 mL), dried over Na_2SO_4, and evaporated in *vacuo*. The residue was recrystallized (petroleum ether, EtOAc) to obtain the intermediate **14-1** (3.75 g, 91% yield) as a yellow crystal.

Step 2: To a -40 °C mixture of the indole intermediate **14-1** obtained from step 1(1408 mg, 5.2 mmol, 1.0 equivalent) in THF (35 mL) was added *n*-BuLi dropwise (3.9 mL, 1.6 M, 6.24 mmol, 1.2 equivalent) under N_2 protection. The mixture was stirred for an additional 1.5 h, then MeI (0.4 mL, 6.24 mmol, 1.2 equivalent) was added at the same temperature followed by warming to room temperature for an extra 3 h. After completion of the reaction confirmed by TLC, the mixture was poured into a saturated aqueous NH_4Cl solution (85 mL) and extracted with EtOAc (85 mL). The aqueous phase was separated and the organic layers were washed with water (40 mL × 2) and brine (40 mL), dried over Na_2SO_4, and evaporated in *vacuo*. The residue **15-1** was directly used for next step without purification.

Step 3: A mixture of **15-1** (1055.5 mg, 3.7 mmol, 1.0 equivalent), TBAF (1.0M in THF, 29.6 mL, 29.6 mmol, 8.0 equivalent), and THF (30 mL) was refluxed overnight. After completion of the reaction confirmed by TLC, the residual THF was evaporated in *vacuo*, and H_2O (15 mL) was added to the residue. The mixture was extracted with EtOAc (100 mL), The aqueous phase was separated and the organic layers were washed with water (15 mL × 2) and brine (15 mL), dried over Na_2SO_4, and evaporated in *vacuo*. The crude product was purified by column chromatography (silica gel, petroleum ether, ethyl acetate) to give the product **1** as a yellow solid (Figure S1).

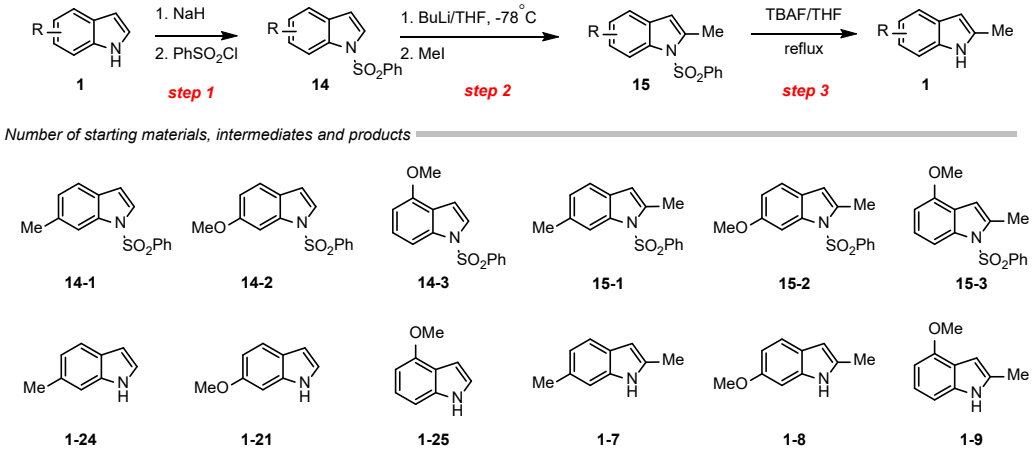

Figure S1. General procedure A for C2-substutited indole preparation, Related to Table 2

General procedure B To a 100 mL round bottom flask was successively charged with **1-21** (1471.8 mg, 10.0 mmol, 1.0 equivalent), norbornene (1881.5 mg, 20.0 mmol, 2.0 equivalent), K_2CO_3 (2.76 g, 20.0 mmol, 2.0 equivalent), $Pd(OAc)_2$ (224.9 mg, 10.0 mol %), **16-3** (2271.5 mg, 10.0 mmol, 1.0 equivalent) and DMA (50 mL, 0.5 M H_2O). The resulting solution was evacuated and backfilled with N_2 for 3 times followed by heating to 80 ℃ for 18 h. After completion of the reaction confirmed by TLC, the reaction mixture was diluted with DCM (100 mL) and filtered. The filtrate was washed with plenty of water several times to remove most of DMA. The aqueous phase was separated and the organic layers were washed with brine (30 mL x 2), dried over Na_2SO_4, and evaporated in *vacuo*. The residue was purified by flash column chromatography (silica gel, petroleum ether, EtOAc, DCM) to give the product **1-14** as a yellow solid (Figure S2).

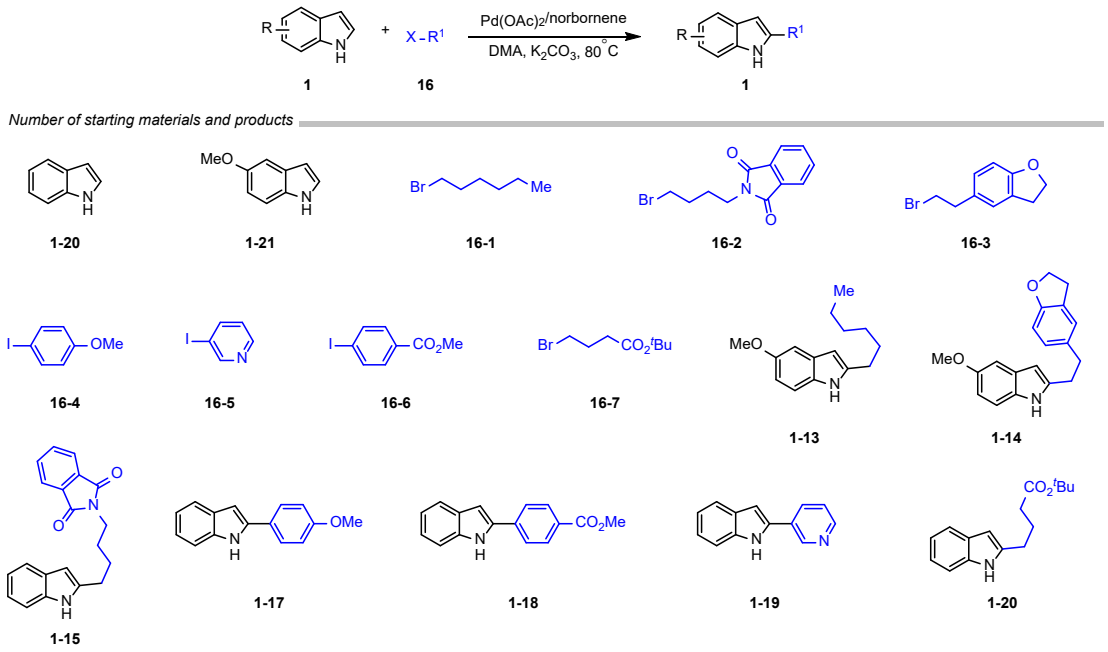

Figure S2. General procedure B for C2-substutited indole preparation, Related Table 2

I-2-2. Oxidative coupling of C2-substituted indoles and enolates

General procedure C To a 25 mL oven-dried Schlenk flask equipped with a magnetic stirring bar and a rubber stopper was charged with indole substrate **1** (2.0 mmol, 2.0 equivalent) and carbonyl compound **3** (1.0 mmol, 1.0 equivalent). The flask was evacuated and backfilled with N_2 for 3 times at least before adding THF (5 mL) by syringe. The resulting mixture was cooled to -78℃ and then LiHMDS (1.3 M in THF, 4.0 mmol, 4.0 equivalent) was added dropwise. The reaction mixture was stirred at -78 ℃ for 3h, followed by adding $FeCl_3$ (648 mg, 4.0 mmol, 4.0 equivalent, in 2 mL THF) for an additional 1 h at the same temperature, then H_2O (15 mL) and EtOAc (50 mL) was added, the aqueous phase was separated and the organic layers were washed with water (15 mL × 2) and brine (15 mL), dried over Na_2SO_4, and evaporated in *vacuo*. The crude product was purified by column chromatography (silica gel, petroleum ether, ethyl acetate) to give the desired product **6** (Figure S3).

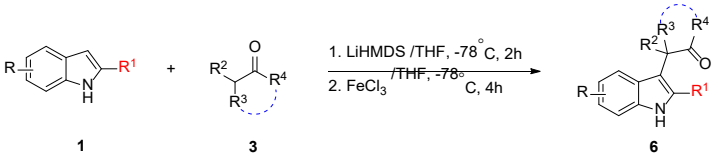

Figure S3. Oxidative coupling of C2-substituted indoles and enolates, Related to Table 1, Table 2 and Table 3

I-2-3. Center-to-axial chirality transfer reaction to synthesize C3 axially chiral indole

To the mixture of compound **6-1** (1.0 equivalent) and solvent was added oxidant. Next, the reaction was conducted according to following **Table 1** and monitored by TLC analysis, and then quenched by adding EtOAc and washed by H_2O, $Na_2S_2O_3$ (aq.), brine and dried by Na_2SO_4. The desired product **13-1** was isolated by flash chromatography (**Table S1**, entry 1: 0.3 mmol **6-1**; **13-1** was obtained as sticky oil, 16 mg, 19% yield; entry 9: **6-1** 27.9 mg, 0.1 mmol, 1.0 equivalent; **13-1** was obtained in 54% yield, 15.1 mg).

Table ST1. **Condition for aromization of compound 6-1, Related to Figure 7b**

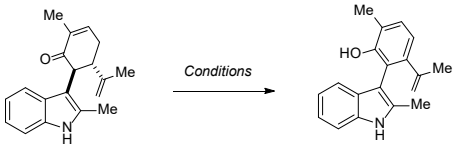

6-1 **13-1**

Entry	Condition	Conversion	Yield[a]	ee/es[b]
1	$CuBr_2$ (1.5 equiv.), MeCN, rt	<10%	N.R	--
2	AgOAc (1.5 equiv.), MeCN, rt.	<10%	N.R	--
3	NBS (1.5 equiv.), DCM, rt	100%	<5%	--
4	$IPh(OAc)_2$ (0.2~3 equiv.), DMSO, 60~100°C	<10%	N.R.	--
5	MnO_2 (3 equiv.), DMSO, 80°C	<10%	N.R.	--
6	$Hg(OAc)_2$ (2 equiv.), toluene, rt-50°C	<100%	messy	--
7	DDQ (1.5 equiv.), toluene, 100°C	<100%	19%	N.D
8	I_2 (2.0 equiv.)/ DMSO(sol)	<50%	<10%	--
9	I_2 (10 mol%)/DMSO (1.0 equiv)	<100%	54% (63% brsm)	rac/0%

I-2-4. Three-step synthesis of Indomethacin and its analogue

Step 1: Compound **6-45** (84.3 mg, 61% yield, 1 mmol scale from **1-6**) and **6-46** (102.2 mg, 50% yield, 0.5 mmol scale from **1-14**) were obtained according to **general procedure C**.

Step 2: To a 25 mL Schlenk vial equipped with a magnetic stirring bar was charged with indole substrate **6-45** (0.055 mmol, 1.0 equivalent) or **6-46** (0.158 mmol, 1.0 equivalent) The vial was evacuated and backfilled with N_2 for 3 times before adding THF (4 mL). The resulting mixture was cooled to -78℃ and *t*-BuOK (1.4 equivalent, in 2 mL THF) was added dropwise by syringe. After 1h, 4-Chlorobenzoyl chloride (1.3 equivalent, in 0.5 mL THF) was then added dropwise for overnight. After completion of the reaction confirmed by TLC, the mixture was poured into a saturated aqueous NH_4Cl solution (15 mL) and extracted with EtOAc (50 mL). The aqueous phase was separated and the organic layers were washed

with water (15 mL × 2) and brine (15 mL), dried over Na_2SO_4, and evaporated in *vacuo*. The residue was purified by flash column chromatography to give intermediate **12-1** (21.6 mg, 96% yield) or **12-3** (69.9 mg, 81% yield).

Step 3: intermediate **12-1**(0.052 mmol, 1.0 equivalent) or **12-3** (0.037 mmol, 1.0 equivalent) was dissolved in excess CF_3COOH (1.0 mL), and the resulting mixture was stirred for 2 h at room temperature. After completion of the reaction monitored by TLC, the residual CF_3COOH was evaporated in *vacuo*, and the crude compound was purified by flash column chromatography to give desired product **12-2** (18.4 mg, 99% yield) or **12-4** (17.5 mg, 96% yield) as a white solid (Figure S4).

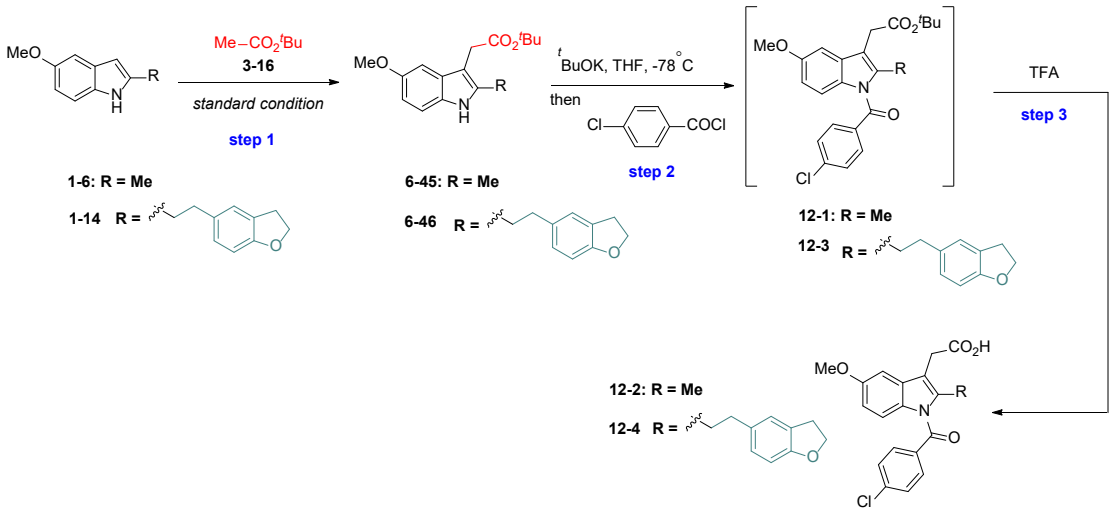

Figure S4. General procedure D for Indomethacin analogue preparation, Related to Figure 7a

I-2-5. Intramolecular Oxidative coupling of C2-substituted indoles and enolates

The intramolecular reaction was conducted similarly as General procedure C instead of utilizing 2.5 equivalent of LiHMDS and $FeCl_3$. However, the desired product from intramolecular oxidative coupling of indole and enolate, 6-49, was failed to be isolated. Instead, the homocoupling product **7-4** was isolated in 19% yield (Figure S5).

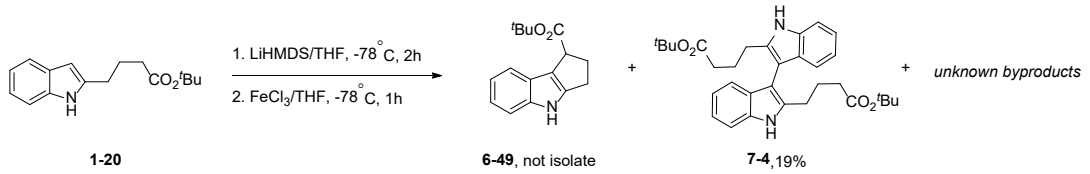

Figure S5. Fe-mediated intramolecular coupling of indole and enolate, Related Figure 6

I-3. Reaction Condition Optimization

Table ST2. Reaction Condition Optimization, Related Table 1

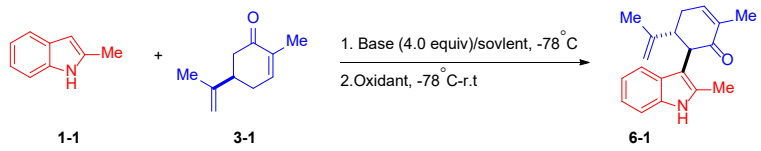

1-1 **3-1** **6-1**

Entry[a]	Base (equiv.)	Oxidant (equiv.)	Solvent	Condition	Conversion (%)	Yield (%)
1[b]	LDA (3.0)	Cu(2-ethylhexanoate)$_2$ (1.5)	THF	**A**	<100%	26-30
2[d]	LiHMDS (4.0)	$CuBr_2$ (3.0 in THF)	THF	**A**	<50%	N.R
3[e]	LiHMDS (4.0)	$CuBr_2$ (3.0)	THF	**A**	<100%	trace
4[f]	LiHMDS (4.0)	I_2 (3.0)	THF	**A**	<10%	trace
5	LiHMDS (4.0)	$Fe(acac)_3$ (3.0)	THF	**A**	<100%	20
6	LiHMDS (4.0)	$FeCl_3$ (3.0)	THF	**A**	<100%	31
7	LiHMDS (4.0)	$CuCl_2$ (3.0)	THF	**A**	<100%	30
8	LiHMDS (4.0)	$FeCl_3$ (4.0)	THF	**B**	100%	57
9	LiHMDS (2.0)	$FeCl_3$ (4.0)	THF	**B**	<100%	20
10	LiHMDS (5.0)	$FeCl_3$ (4.0)	THF	**B**	<100%	52
11	LiHMDS (4.0)	$FeCl_3$ (4.0)	DMF	**B**	<10%	trace
12	LiHMDS (4.0)	I_2 (3.0)	THF	**B**	<10%	trace
13	LDA (2.0)	$FeCl_3$ (4.0)	THF	**B**	<100%	19
14	LiHMDS (4.0)	$FeCl_3$ (4.0)	toluene	**B**	100%	41
15	*LiHMDS (4.0)*	*$FeCl_3$ (4.0)*	*THF*	***C***	*100%*	*89-93*
16	LDA (4.0)	$FeCl_3$ (4.0)	THF	**C**	100%	41

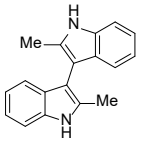

7-1

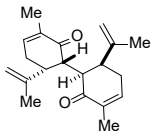

8-1

a. all the reactions were conducted with compound **1-1** (2.0 mmol, 2.0 equivalent) and (*R*)-carvone (**3-1**, 1.0 mmol, 1.0 equivalent), isolated yield; dr was determined by H-NMR of the isolated product or the yield of two isomers; b. Phil Barans best condition in oxidative coupling of indole and carvone (Richter et al., 2007); c. N.R = No Reaction; d. $CuBr_2$ cannot be able to be solved in THF, thus it was difficult to adding $CuBr_2$ in THF solution; e. dimmerization of compound **1-1** and **3-1** was observed, isolated compound **7-1** and **8-1**;f. Ma's reaction condition for intramolecular oxidative coupling of enolate and indole (Zuo et al., 2010);

Condition A: Baran's reaction condition, after adding LiHMDS or LDA at -78℃ for 0.5h followed by adding

oxidant in one portion as solid, the reaction was warmed to room temperature for 15 min.

Condition B: After adding LiHMDS or LDA at -78℃ for 3 h followed by adding oxidant in one portion as solid, the reaction was warmed to room temperature.

Condition C: After adding LiHMDS or LDA at -78℃ for 3 h followed by adding $FeCl_3$ in anhydrous THF, the reaction was stirred at -78℃ for 1h.

I-4. Mechanism study

I-4-1. Competing experiments

To the mixture of indole **1-16** (193 mg, 1.0 mmol, 1.0 equivalent), **1-20** (117 mg, 1.0 mmol, 1.0 equivalent), and (*R*)-carvone **3-1** (150 mg, 1.0 mmol, 1.0 equivalent) in THF (5 mL) at -78℃ under N_2 balloon was slowly added LiHMDS (1.3 M in THF, 4.0 mmol, 4.0 equivalent). Next, the reaction was stirred at -78℃ for 2h, followed by adding $FeCl_3$ (648 mg, 4.0 mmol, 4.0 equivalent, in 2 mL THF). After stirring for additional 5h at -78℃, the reaction was quenched by adding around 0.5 mL H_2O and diluted with around 100 mL EtOAc. The organic lawyer was then washed by H_2O, brine and dried by Na_2SO_4. The desired product **6** was isolated via flash chromatography. The distribution of product **6-16** and **6-42** was determined by both H-NMR of crude product and isolated yields (Figure S6).

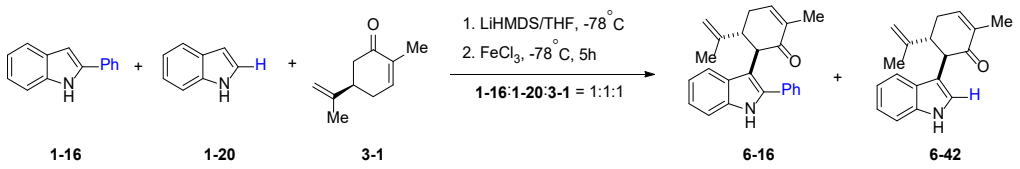

Figure S6. Competing reactions between 1-16 and 1-20 in coupling with (*R*)-carvone (3-1), Related to Figure 3b

I-4-2. Background reactions: homocoupling of C2-substituted indole

To the mixture of indole **1** (2.0 mmol, 1.0 equivalent) in THF (5 mL) at -78℃ under N_2 balloon was slowly added LiHMDS (1.3 M in THF, 4.0 mmol, 4.0 equivalent). Next, the reaction was stirred at -78℃ for 3h, followed by adding $FeCl_3$ (648 mg, 4.0 mmol, 4.0 equivalent, in 2 mL THF). After stirring for additional 5h at -78℃, the reaction was quenched by adding around 0.5 mL H_2O and diluted with around 100 mL EtOAc. The organic lawyer was then washed by H_2O, brine and dried by Na_2SO_4. The 3,3'-bisindole product **7** was isolated via flash chromatography (Figure S7).

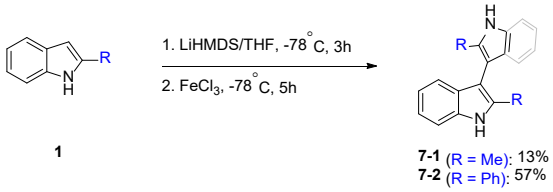

Figure S7. Homocoupling of C2-substituted indole, Related to Figure 3c

I-4-3. Comparison our and Baran's approach in background reaction of indole tetramerization

To the mixture of indole **1-20** (2.0 mmol, 1.0 equivalent) in THF (5 mL) at -78℃ under N_2 balloon was slowly added LiHMDS (1.3 M in THF, 4.0 mmol, 4.0 equivalent). Next, the reaction was stirred at -78℃ for 3h, followed by adding $FeCl_3$ (648 mg, 4.0 mmol, 4.0 equivalent, in 2 mL THF). After stirring for additional 1h at -78℃, the reaction was quenched by adding around 0.5 mL H_2O and diluted with around 100 mL EtOAc. The organic lawyer was then washed by H_2O, brine and dried by Na_2SO_4. The tetramer of indole **10** (81.2 mg, 35% yield) was isolated as yellow solid *via* flash chromatography. The control experiment of Baran's condition (3.0 equivalent of LDA, 1.5 equivalent of Cu(2-ethylhexanoate)$_2$, -78℃ to rt) was conducted according to literature, and compound **10** was obtained in 42% yield (Figure S8).

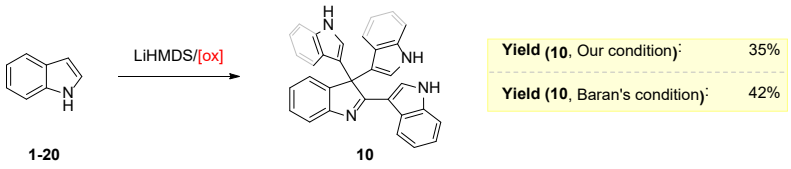

Figure S8. Background reaction of indole tetramerization, Related to Figure 3c

I-4-4. Indole C3-radical intermediate exploring reaction

To the solution of compound **1-14** (52.5 mg, 0.18 mmol, 1.0 equivalent) in THF (4 mL) was added LiHMDS (1.3 M, 0.28 mL, 0.36 mmol, 2 equivalent) and $FeCl_3$ (60 mg, 0.36 mmol, 2.0 equivalent) as **general procedure C**. After completion of the reaction, the products were isolated. And only compound **7-3** (22.2 mg, 42% yield) was isolated as brown solid (Figure S9).

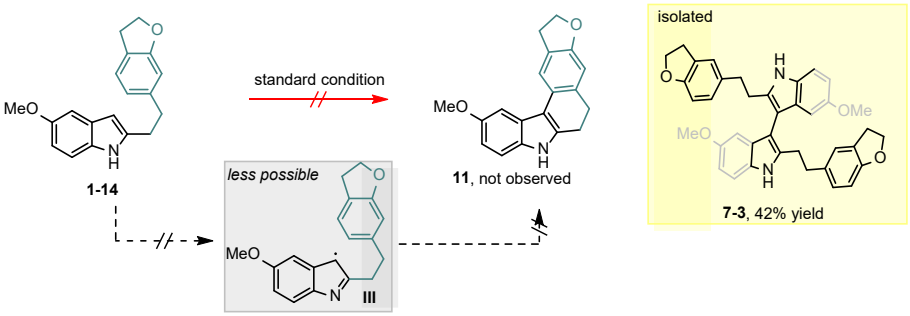

Figure S9. **Indole C3-radical trapping experiments, Related to Figure 3d**

I-4-5. Transition state investigation experiments

These experiments were conducted according to **general procedure C** by switching either the base or Fe-oxidant based as summarized in following **Table ST3** to figure the chelating metal (Fe or Li) in transition state**.** The yields of compound **6-1** in each reaction was isolated after the reaction in the same procedure as documented in **general procedure C**. For entry 6, the homocoupling of **3-1** was isolated in 17% yield (product **8-1**, with a little bit of 2-methylindole **1-1** in H-NMR spectra, as shown in following).

Table ST3. **Metal-chelating investigation, Related to Figure 3e**

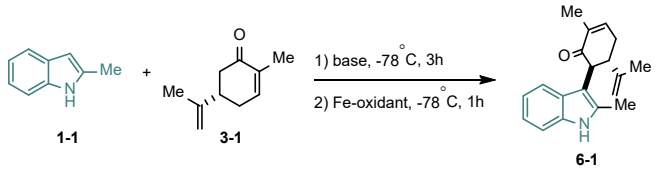

Entry[a]	base (4.0 equiv.)	oxidant (4.0 equiv.)	yield (%)
1	LiHMDS	$FeCl_3$	93% (260.1 mg)
2	NaHMDS	$FeCl_3$	89% (247.5 mg)
3	KHMDS	$FeCl_3$	95% (263.8 mg)
4	LDA	$FeCl_3$	41% (114.2 mg)
5	LiHMDS	$Fe(acac)_3$	20% (56.1 mg)
6	LiHMDS		trace

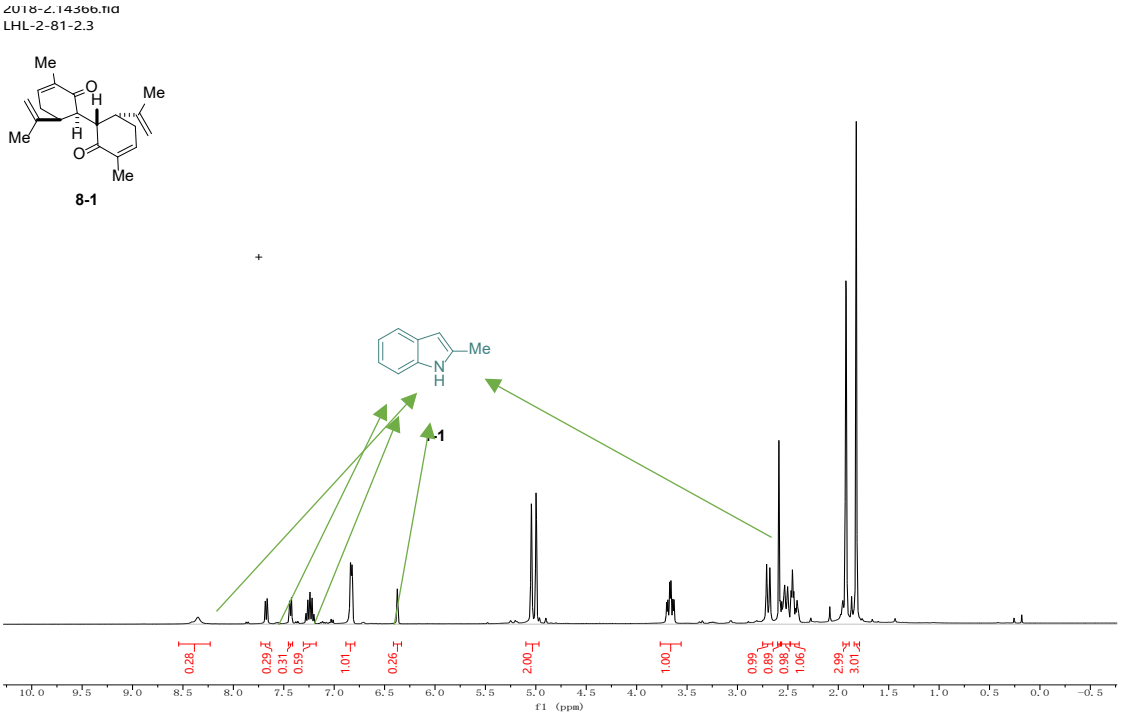

I-5. Cytotoxicity Study

Cell culture Human non-small cell lung cancer A549 and H1299 cells, Human colon cancer HCT116 and HT29, Human leukemia K562 and MV-4-11 cells, and Human liver cancer HepG2 cells were purchased from ATCC (Manassas, VA). Human cervix carcinoma KB-3-1 and KB/VCR cells were gifts from Dr. Linghua Meng (Shanghai Institute of Materia Medica, Shanghai, China). A549, H1299, K562, MV-4-11 and KB-3-1 cells were cultured in RPMI 1640 medium, containing 10% FBS, 100 U/mL penicillin and 100 μg/mL streptomycin at 37 °C in a humidified atmosphere of 5% CO_2. HCT116 and HT29 cells were cultured in McCoy' 5a, containing 10% FBS, 100 U/mL penicillin and 100 μg/mL streptomycin at 37 °C in a humidified atmosphere of 5% CO_2. HepG2 cells were cultured in DMEM, containing 10% FBS, 5 mM Hepes, 2 mM Glutamine, 100 U/mL penicillin and 100 μg/mL streptomycin and stored at 4 °C, and then cultured in 37°C in a humidified atmosphere of 5% CO_2 before being treated with tested compounds. The multidrug resistant subline KB/VCR were maintained in RPMI 1640 medium supplemented with 0.1 μg/mL vincristine.

Cytotoxicity Study of A549 cells The cells were seeded in 96-well plates at a density of 2000 cells/well. After cultured for overnight, the cells were treated with different concentrations of tested compounds for 72 h. Then the cells were fixed with 10% trichloroacetic acid followed by staining with 0.1% sulforhodamine B (SRB). After washed with 1% acetic acid to remove unbound dye, the plates were left to dry at room temperature and 100 μl TRIS base (10 mM) was added to solubilize the protein-bound SRB. The absorbance at 540 nm was measured with a microplate reader (SpectraMax M2, Molecular Devices). Inhibitory rate of growth was calculated by the following formula: inhibitory rate (%) = (A_{540} of vehicle control − A_{540} of treated cells) / (A_{540} of vehicle control − A_{540} of blank control)*100. The IC_{50} values were calculated by using GraphPad Prism 5 software. Experiments were performed in triplicate.

Cell cycle analysis Exponentially growing A549 cells were incubated with tested compounds or DMSO for 24 h. After fixed with 70% ice-cold ethanol, the cells were incubated in a DNA staining solution containing 50 μg/mL propidium iodide and 0.5 mg/mL RNase for 30 minutes. The DNA content was

measured with a FACSCalibur flow cytometer (Becton Dickinson, Mountain View, CA) and cell cycle phase distribution was analyzed by using FlowJo V10 software.

Cytotoxicity Study of H1299, HCT116, HT29, K562, MV-4-11 and HepG2 cells The cells were seeded in 96-well plates at certain density of cells/well (2000 cells/well for H1299, HCT116 and K562 cells; 3000 cells/well for HT29 cells; 5000 cells/well for HepG2 cells; 10000 cells/well for MV-4-11 cells). After cultured for overnight, the cells were treated with 20 μL of tested compounds (30 μM) for 72 h. And then 10 μL of CCK-8 solution to each well, followed by incubating the plate for 4h at 37 °C in a humidified atmosphere of 5% CO_2. The absorbance at 450 nm was measured with a microplate reader (Nivo). Inhibitory rate of growth was calculated by the following formula: inhibitory rate (%) = (A_{450} of vehicle control – A_{450} of treated cells) / (A_{450} of vehicle control – A_{450} of blank control)*100.

II. Spectra of starting material and products

14-1

6-methyl-1-(phenylsulfonyl)-1*H*-indole (14-1) (Chen et al., 2011) was synthesized according to **general procedure A** and obtained as a white solid (15.2 mmol scale, 3.75g, 91% yield).

^{1}H NMR (400 MHz, CDCl3) δ 7.87 (d, *J* = 7.9 Hz, 2H), 7.81 (s, 1H), 7.53 (t, *J* = 7.4 Hz, 1H), 7.49 (d, *J* = 3.7 Hz, 1H), 7.47 – 7.37 (m, 3H), 7.06 (d, *J* = 8.0 Hz, 1H), 6.61 (d, *J* = 3.7 Hz, 1H), 2.48 (s, 3H).

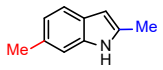

1-7

2,6-dimethyl-1*H*-indole (1-7) (Miyata et al., 2002) was synthesized according to **general procedure A** and obtained as a yellow solid (3.7 mmol scale, 406.2 mg, 76% yield).

^{1}H NMR (400 MHz, CDCl3) δ 7.70 (s, 1H), 7.39 (d, *J* = 8.0 Hz, 1H), 7.07 (s, 1H), 6.91 (d, 1H), 6.16 (s, 1H), 2.45 (s, 3H), 2.42 (s, 3H).

14-2

6-methoxy-1-(phenylsulfonyl)-1*H*-indole (14-2) (Trabbic et al., 2016) was synthesized according to **general procedure A** and obtained as a white solid (13.6 mmol scale, 3.60 g, 92% yield).

^{1}H NMR (400 MHz, CDCl3) δ 7.86 (dd, *J* = 8.4, 1.3 Hz, 2H), 7.62 – 7.50 (m, 2H), 7.49 – 7.35 (m, 4H), 6.87 (dt, *J* = 8.6, 1.5 Hz, 1H), 6.58 (dd, *J* = 3.7, 0.9 Hz, 1H), 3.88 (s, 3H).

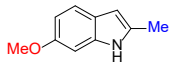

1-8

6-methoxy-2-methyl-1*H*-indole (**1-8**) (Trabbic et al., 2016) was synthesized according to **general procedure A** and obtained as a yellow solid (3 mmol scale, 459.4 mg, 95 % yield).

^{1}H NMR (400 MHz, $CDCl_3$) δ 7.73 (s, 1H), 7.37 (d, *J* = 8.6 Hz, 1H), 6.80 (d, *J* = 2.2 Hz, 1H), 6.74 (dd, *J* = 8.5, 2.2 Hz, 1H), 6.13 (s, 1H), 3.83 (s, 3H), 2.40 (s, 3H).

14-3

4-methoxy-1-(phenylsulfonyl)-1*H*-indole (**14-3**) (Stempel et al., 2018) was synthesized according to **general procedure A** and obtained as a white solid (13.6 mmol scale, 3.52 g, 90% yield).

^{1}H NMR (400 MHz, CDCl3) δ 7.87 (d, *J* = 7.7 Hz, 2H), 7.60 (d, *J* = 8.3 Hz, 1H), 7.52 (t, *J* = 7.4 Hz, 1H), 7.47 (d, *J* = 3.7 Hz, 1H), 7.43 (t, *J* = 7.6 Hz, 2H), 7.22 (d, *J* = 8.2 Hz, 1H), 6.78 (d, *J* = 3.7 Hz, 1H), 6.65 (d, *J* = 8.0 Hz, 1H), 3.89 (s, 3H).

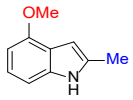

1-9

4-methoxy-2-methyl-1*H*-indole (**1-9**) (Trabbic et al., 2016) was synthesized according to **general procedure A** and obtained as a yellow solid (4 mmol scale, 481.1 mg, 75% yield).

^{1}H NMR (400 MHz, $CDCl_3$) δ 7.85 (s, 1H), 7.03 (t, *J* = 7.9 Hz, 1H), 6.93 (d, *J* = 8.1 Hz, 1H), 6.51 (d, *J* = 7.8 Hz, 1H), 6.32 (s, 1H), 3.94 (s, 3H), 2.43 (s, 3H).

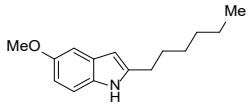

1-13

2-hexyl-5-methoxy-1*H*-indole (**1-13**) (Yamagishi et al., 2012) was synthesized according to **general procedure B** and obtained as a brown oil (20 mmol scale, 1090.9 mg, 24 % yield).

^{1}H NMR (400 MHz, $CDCl_3$) δ 7.77 (s, 1H), 7.17 (d, *J* = 8.7 Hz, 1H), 7.04 (d, *J* = 2.5 Hz, 1H), 6.79 (dd, *J* = 8.7, 2.4 Hz, 1H), 6.18 (s, 1H), 3.86 (s, 3H), 2.72 (t, *J* = 7.7 Hz, 2H), 1.71 (p, *J* = 7.5 Hz, 2H), 1.44 – 1.37 (m, 2H), 1.36 – 1.29 (m, 4H), 0.92 (t, *J* = 6.9, 5.8, 3.6 Hz, 3H).

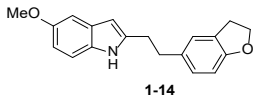

1-14

2-(2-(2,3-dihydrobenzofuran-5-yl)ethyl)-5-methoxy-1*H*-indole (**1-14**) was synthesized according to

general procedure B and obtained as a yellow solid (10 mmol scale, 732.3 mg, 28% yield).

^{1}H NMR (400 MHz, $CDCl_3$) δ 7.78 (s, 1H), 7.15 (d, *J* = 8.7 Hz, 1H), 7.06 (d, *J* = 2.5 Hz, 2H), 6.96 (dd, *J* = 8.2, 1.9 Hz, 1H), 6.82 (dt, *J* = 8.9, 2.5 Hz, 1H), 6.76 (dd, *J* = 8.1, 1.8 Hz, 1H), 6.23 (s, 1H), 4.58 (t, *J* = 8.7 Hz, 2H), 3.87 (s, 3H), 3.19 (t, *J* = 8.6 Hz, 2H), 3.05 – 2.91 (m, *J* = 4.3 Hz, 4H).

^{13}C NMR (101 MHz, $CDCl_3$) δ 158.5, 154.1, 140.2, 133.3, 131.0, 129.2, 127.8, 127.3, 125.0, 111.1, 110.9, 109.1, 102.1, 99.6, 71.3, 55.9, 35.1, 30.7, 29.8.

HRMS-API (m/z): calcd. for $C_{19}H_{18}NO_2$ [M - H^+] 292.1332, found 292.1339

FTIR (film, cm^{-1}): 3338, 1621, 1589, 1489, 1440, 1202, 1167 cm^{-1}

M.p.: 109 - 110 ℃

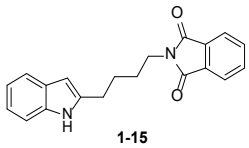

1-15

2-(4-(1*H*-indol-2-yl)butyl)isoindoline-1,3-dione (**1-15**) was synthesized according to **general procedure B** and obtained as a light yellow solid (10 mmol scale, 707.5 mg, 22% yield).

^{1}H NMR (400 MHz, $CDCl_3$) δ 8.11 (s, 1H), 7.85 (dd, *J* = 5.5, 3.1 Hz, 2H), 7.71 (dd, *J* = 5.4, 3.1 Hz, 2H), 7.50 (d, *J* = 7.7 Hz, 1H), 7.31 (d, *J* = 7.9 Hz, 1H), 7.14 – 7.01 (m, 2H), 6.23 (s, 1H), 3.75 (t, *J* = 6.6 Hz, 2H), 2.83 (t, *J* = 7.0 Hz, 2H), 1.77 (hept, *J* = 5.2, 4.8 Hz, 4H).

^{13}C NMR (101 MHz, $CDCl_3$) δ 168.7(x 2C), 139.2, 136.1, 134.1(x 2C), 132.2(x 2C), 128.9, 123.4(x 2C), 121.2, 119.9, 119.7, 110.5, 99.9, 37.4, 28.1, 27.6, 26.6.

HRMS-API (m/z): calcd. for $C_{20}H_{19}N_2O_2$ [M + H^+] 319.1441, found 319.1441

FTIR (film, cm^{-1}): 3381, 1763, 1706, 1401, 1040, 722 cm^{-1}

M.p.: 123 – 124 ℃

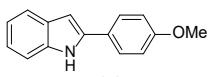

1-17

2-(4-methoxyphenyl)-1*H*-indole (**1-17**) (Yang et al., 2008) was synthesized according to **general procedure B** and obtained as a yellow solid (10 mmol scale, 1155.8 mg, 52% yield).

^{1}H NMR (400 MHz, DMSO-d_6) δ 11.41 (s, 1H), 7.83 – 7.76 (m, 2H), 7.50 (dd, 1H), 7.38 (dd, *J* = 8.0, 1.0

Hz, 1H), 7.05 (td, *J* = 7.5, 1.6 Hz, 3H), 6.98 (ddd, *J* = 8.0, 7.0, 1.1 Hz, 1H), 6.76 (dd, *J* = 2.2, 0.9 Hz, 1H), 3.81 (s, 3H).

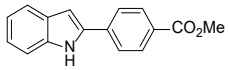

1-18

Methyl 4-(1*H*-indol-2-yl)benzoate (**1-18**) (Wetzel et al., 2016) was synthesized according to **general procedure B** and obtained as a yellow solid (10 mmol scale, 1331.4 mg, 53% yield).

^{1}H NMR (400 MHz, DMSO-d_6) δ 11.75 (s, 1H), 8.01 (q, *J* = 8.3 Hz, 4H), 7.57 (d, *J* = 7.9 Hz, 1H), 7.47 (d, *J* = 8.2 Hz, 1H), 7.17 (t, *J* = 7.6 Hz, 1H), 7.08 – 7.00 (m, 2H), 3.85 (s, 3H).

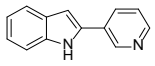

1-19

2-(pyridin-3-yl)-1*H*-indole (**1-19**) (Molander et al., 2009) was synthesized according to **general procedure B** and obtained as a yellow solid (10 mmol scale, 926.3 mg, 48% yield).

^{1}H NMR (400 MHz, $CDCl_3$ + DMSO-d_6) δ 8.98 (d, *J* = 2.3 Hz, 1H), 8.93 (s, 1H), 8.55 (dd, *J* = 4.8, 1.6 Hz, 1H), 7.96 (dt, *J* = 8.1, 2.0 Hz, 1H), 7.66 (d, *J* = 7.9 Hz, 1H), 7.42 (d, *J* = 8.1 Hz, 1H), 7.36 (dd, *J* = 8.0, 4.7 Hz, 1H), 7.22 (t, 1H), 7.15 (t, *J* = 7.4 Hz, 1H), 6.90 (d, *J* = 2.2 Hz, 1H).

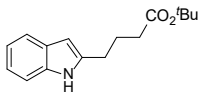

1-20

tert*-butyl** 4-(1H***-indol-2-yl)butanoate (**1-20**) was synthesized according to **general procedure B** and obtained as a white solid (5 mmol scale, 612.6 mg, 47% yield).

^{1}H NMR (400 MHz, $CDCl_3$) δ 8.16 (s, 1H), 7.54 (dd, *J* = 7.6, 1.4 Hz, 1H), 7.34 – 7.28 (m, 1H), 7.10 (dtd, *J* = 20.6, 7.1, 1.3 Hz, 2H), 6.26 (dd, *J* = 2.3, 1.0 Hz, 1H), 2.80 (t, *J* = 7.3 Hz, 2H), 2.31 (t, *J* = 7.3 Hz, 2H), 2.00 (p, *J* = 7.3 Hz, 2H), 1.47 (s, 9H).

^{13}C NMR (101 MHz, $CDCl_3$) δ 173.1, 138.8, 136.1, 128.9, 121.2, 119.9, 119.7, 110.5, 100.1, 80.6, 34.8, 28.3(x 3C), 27.4, 25.0.

HRMS-API (m/z): calcd for $C_{16}H_{22}NO_2^+$ [M + H$^+$] 260.1645, found 260.1644

FTIR (film, cm^{-1}): 3369, 1711, 1367, 1154, 779 cm^{-1}

M.p.: 92 - 93 ℃

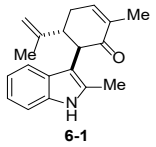

6-1

(5*R*,6*R*)-2-methyl-6-(2-methyl-1*H*-indol-3-yl)-5-(prop-1-en-2-yl)cyclohex-2-en-1-one (**6-1**) was synthesized according to **general procedure C** and obtained as a white solid (1 mmol scale, 259.1 mg, 93% yield).

^{1}H NMR (400 MHz, $CDCl_3$) δ 8.23 (s, 1H), 7.34 – 7.27 (m, 1H), 7.07 – 6.97 (m, 3H), 6.89 (d, *J* = 6.0 Hz, 1H), 4.59 (d, *J* = 1.9 Hz, 1H), 4.51 (d, *J* = 2.0 Hz, 1H), 3.80 (d, *J* = 13.0 Hz, 1H), 3.45 – 3.33 (m, 1H), 2.65 (ddt, *J* = 18.6, 11.3, 2.7 Hz, 1H), 2.45 (dt, *J* = 18.4, 5.4 Hz, 1H), 2.00 (s, 3H), 1.94 (s, 3H), 1.53 (s, 3H).

^{13}C NMR (101 MHz, $CDCl_3$) δ 200.1, 145.8, 144.4, 135.6, 135.5, 133.0, 127.9, 120.2, 118.6, 118.2, 112.3, 110.8, 108.0, 49.5, 48.5, 32.0, 19.3, 16.4, 11.9.

HRMS-ESI (m/z): calcd for $C_{19}H_{22}NO$ [M + H^+] 280.1695, found 280.1699

FTIR (film, cm^{-1}): 3329, 2916, 1670, 1459, 1431, 1366, 902, 742 cm^{-1}

M.p.: 126 – 127 ℃

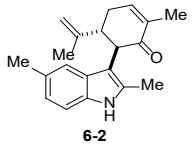

6-2

(5*R*,6*R*)-6-(2,5-dimethyl-1*H*-indol-3-yl)-2-methyl-5-(prop-1-en-2-yl)cyclohex-2-en-1-one (**6-2**) was synthesized according to **general procedure C** and obtained as a white solid (0.5 mmol scale, 140.4 mg, 96% yield).

^{1}H NMR (400 MHz, $CDCl_3$) δ 7.90 (s, 1H), 7.06 – 6.97 (m, 2H), 6.86 (td, *J* = 7.9, 1.8 Hz, 2H), 4.59 (d, *J* = 1.9 Hz, 1H), 4.52 (t, *J* = 1.7 Hz, 1H), 3.75 (d, *J* = 13.0 Hz, 1H), 3.37 (ddd, *J* = 12.9, 11.2, 4.4 Hz, 1H), 2.64 (ddt, *J* = 18.6, 11.3, 2.6 Hz, 1H), 2.46 (td, *J* = 5.1, 4.6, 2.8 Hz, 1H), 2.40 (s, 3H), 2.09 (s, 3H), 1.92 (s, 3H), 1.53 (s, 3H).

^{13}C NMR (101 MHz, $CDCl_3$) δ 199.9, 146.1, 144.1, 135.7, 133.9, 132.8, 128.3, 127.8, 122.0, 118.3, 112.3, 110.3, 108.0, 49.6, 48.5, 32.1, 21.8, 19.4, 16.5, 12.3.

HRMS-ESI (m/z): calcd for $C_{20}H_{24}NO$ [M + H^+] 294.1852, found 294.1854

FTIR (film, cm^{-1}): 3355, 2917, 1670, 1446, 1435, 1366, 1307, 1227, 899, 790 cm^{-1}

M.p.: 160 – 161 ℃

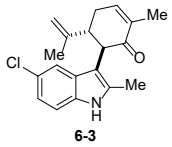

6-3

(5*R*,6*R*)-6-(5-chloro-2-methyl-1*H*-indol-3-yl)-2-methyl-5-(prop-1-en-2-yl)cyclohex-2-en-1-one (6-3) was synthesized according to **general procedure C** and obtained as a light yellow solid (1 mmol scale, 244.2 mg, 78% yield).

^{1}H NMR (400 MHz, $CDCl_3$) δ 8.05 (s, 1H), 7.19 (d, *J* = 1.9 Hz, 1H), 7.02 – 6.93 (m, 2H), 6.88 (d, *J* = 6.1 Hz, 1H), 4.56 (s, 1H), 4.50 (s, 1H), 3.70 (d, *J* = 13.2 Hz, 1H), 3.30 (ddd, *J* = 13.3, 11.3, 4.4 Hz, 1H), 2.62 (ddq, *J* = 19.1, 10.9, 2.6 Hz, 1H), 2.44 (dt, *J* = 18.6, 5.4 Hz, 1H), 2.10 (s, 3H), 1.89 (s, 3H), 1.49 (s, 3H).

^{13}C NMR (101 MHz, $CDCl_3$) δ 199.6, 145.7, 144.5, 135.7, 134.5, 134.0, 129.1, 124.6, 120.8, 118.0, 112.7, 111.6, 108.4, 49.5, 48.6, 32.2, 19.3, 16.5, 12.4.

HRMS-ESI (m/z): calcd for $C_{19}H_{21}ClNO$ [M + H^+] 314.1306, found 314.1308

FTIR (film, cm^{-1}): 3336, 2920, 1665, 1458, 1370, 1310, 889, 882, 854, 791 cm^{-1}

M.p.: 149 – 150 ℃

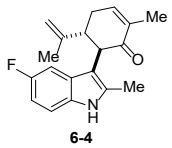

6-4

(5*R*,6*R*)-6-(5-fluoro-2-methyl-1*H*-indol-3-yl)-2-methyl-5-(prop-1-en-2-yl)cyclohex-2-en-1-one (6-4) was synthesized according to **general procedure C** and obtained as a light brown solid (0.5 mmol scale, 99.1 mg, 67% yield).

^{1}H NMR (400 MHz, $CDCl_3$) δ 8.07 (s, 1H), 6.96 (dd, *J* = 8.7, 4.5 Hz, 1H), 6.89 (dd, *J* = 10.1, 2.6 Hz, 2H), 6.74 (td, *J* = 9.1, 2.5 Hz, 1H), 4.57 (s, 1H), 4.51 (d, *J* = 2.2 Hz, 1H), 3.70 (d, *J* = 13.1 Hz, 1H), 3.36 – 3.24 (m, 1H), 2.63 (ddq, *J* = 19.1, 10.9, 2.6 Hz, 1H), 2.44 (dt, *J* = 18.5, 5.4 Hz, 1H), 2.07 (s, 3H), 1.90 (s, 3H), 1.50 (s, 3H).

^{13}C NMR (101 MHz, $CDCl_3$) δ 199.8, 157.6 (d, J_{C-F} = 232.5 Hz, 1C), 145.8, 144.5, 135.7, 134.9, 132.1, 128.3 (d, J_{C-F} = 9.8 Hz, 1C), 112.6, 111.1 (d, J_{C-F} = 9.9 Hz, 1C), 108.8 (d, J_{C-F} = 4.4 Hz, 1C), 108.5 (d, J_{C-F} = 26.0 Hz, 1C), 103.5 (d, J_{C-F} = 23.7 Hz, 1C), 49.5, 48.5, 32.1, 19.3, 16.4, 12.4.

F-NMR: -125.5

HRMS-ESI (m/z): calcd for $C_{19}H_{21}FNO$ [M + H^+] 298.1601, found 298.1603

FTIR (film, cm^{-1}): 3345, 2919, 1665, 1486, 1453, 1368, 892, 843, 793 cm^{-1}

M.p.: 63 - 64 ℃

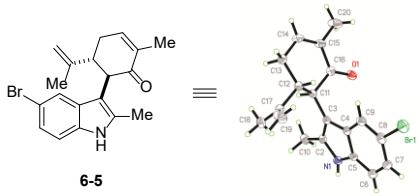

6-5

(5*R*,6*R*)-6-(5-bromo-2-methyl-1*H*-indol-3-yl)-2-methyl-5-(prop-1-en-2-yl)cyclohex-2-en-1-one (6-5) was synthesized according to **general procedure C** and obtained as a yellow solid (1 mmol scale, 275.8 mg, 77% yield).

^{1}H NMR (400 MHz, $CDCl_3$) δ 8.06 (s, 1H), 7.34 (d, *J* = 1.9 Hz, 1H), 7.09 (dd, *J* = 8.5, 1.9 Hz, 1H), 6.98 (d, *J* = 8.5 Hz, 1H), 6.89 – 6.85 (m, 1H), 4.57 (s, 1H), 4.50 (s, 1H), 3.70 (d, *J* = 13.2 Hz, 1H), 3.30 (ddd, *J* = 13.2, 11.3, 4.5 Hz, 1H), 2.63 (ddt, *J* = 18.6, 11.3, 2.6 Hz, 1H), 2.44 (dddd, *J* = 18.1, 5.9, 4.4, 1.4 Hz, 1H), 2.13 (s, 3H), 1.89 (s, 3H), 1.50 (s, 3H).

^{13}C NMR (101 MHz, $CDCl_3$) δ 199.7, 145.7, 144.5, 135.7, 134.4, 134.3, 129.7, 123.3, 120.9, 112.7, 112.3, 112.1, 108.2, 49.5, 48.6, 32.2, 19.3, 16.5, 12.3.

HRMS-ESI (m/z): calcd for $C_{19}H_{20}BrNONa$ [M + Na^+] 380.0620, found 380.0625

FTIR (film, cm^{-1}): 3336, 2888, 1670, 1473, 1364, 1310, 884, 801 cm^{-1}

M.p.: 155 – 156 ℃

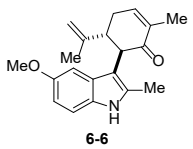

6-6

(5*R*, 6*R*)-6-(5-methoxy-2-methyl-1*H*-indol-3-yl)-2-methyl-5-(prop-1-en-2-yl)cyclohex-2-en-1-one (6-6)

was synthesized according to **general procedure C** and obtained as a yellow solid (0.5 mmol scale, 137.9 mg, 89% yield).

^{1}H NMR (400 MHz, $CDCl_3$) δ 7.83 (s, 1H), 7.03 (d, *J* = 8.6 Hz, 1H), 6.86 (d, *J* = 5.7 Hz, 1H), 6.74 – 6.67 (m, 2H), 4.59 (s, 1H), 4.52 (s, 1H), 3.80 (s, 3H), 3.73 (d, *J* = 12.9 Hz, 1H), 3.32 (td, *J* = 12.1, 4.4 Hz, 1H), 2.69 – 2.57 (m, 1H), 2.43 (dt, *J* = 18.1, 5.0 Hz, 1H), 2.14 (s, 3H), 1.89 (s, 3H), 1.52 (s, 3H).

^{13}C NMR (101 MHz, $CDCl_3$) δ 199.7, 153.6, 146.0, 144.1, 135.8, 133.7, 130.9, 128.6, 112.4, 111.1, 109.7, 108.5, 101.8, 56.1, 49.6, 48.5, 32.1, 19.4, 16.4, 12.5.

HRMS-ESI (m/z): calcd for $C_{20}H_{23}NO_2Na$ [M + Na^+] 332.1621, found 332.1623

FTIR (film, cm^{-1}): 3354, 2940, 1664, 1485, 1458, 1217, 1029, 902, 826 cm^{-1}

M.p.: 124 – 125 ℃

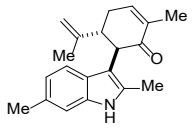

6-7

(5*R*,6*R*)-6-(2,6-dimethyl-1H-indol-3-yl)-2-methyl-5-(prop-1-en-2-yl)cyclohex-2-en-1-one (6-7) was synthesized according to **general procedure C** and obtained as a white solid (1 mmol scale, 267.2 mg, 91% yield).

^{1}H NMR (400 MHz, $CDCl_3$) δ 7.93 (s, 1H), 7.14 (d, *J* = 8.0 Hz, 1H), 6.87 (m, 2H), 6.82 (d, *J* = 8.0 Hz, 1H), 4.59 (s, 1H), 4.52 (s, 1H), 3.75 (d, *J* = 12.9 Hz, 1H), 3.35 (ddd, *J* = 13.0, 11.2, 4.4 Hz, 1H), 2.68 – 2.58 (m, 1H), 2.46 (t, *J* = 5.4 Hz, 1H), 2.40 (s, 3H), 2.11 (s, 3H), 1.90 (s, 3H), 1.53 (s, 3H).

^{13}C NMR (101 MHz, $CDCl_3$) δ 199.8, 146.1, 144.0, 136.0, 135.8, 131.9, 130.0, 125.8, 120.6, 118.2, 112.3, 110.8, 108.4, 49.6, 48.6, 32.1, 21.7, 19.5, 16.4, 12.2.

HRMS-API (m/z): calcd. for $C_{20}H_{24}NO$ [M + H+] 294.1852, found 294.1846

FTIR (film, cm^{-1}): 3367, 2920, 1674, 1466, 1367 cm^{-1}

M.p.: 161 – 162 ℃

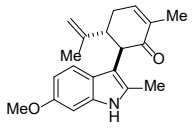

6-8

(5*R*,6*R*)-6-(6-methoxy-2-methyl-1*H*-indol-3-yl)-2-methyl-5-(prop-1-en-2-yl)cyclohex-2-en-1-one (6-8) was synthesized according to **general procedure C** and obtained as a yellow oil (1 mmol scale, 217.1 mg, 70% yield).

^{1}H NMR (400 MHz, $CDCl_3$) δ 7.90 (s, 1H), 7.11 (d, *J* = 8.5 Hz, 1H), 6.89 – 6.83 (m, 1H), 6.67 – 6.59 (m, 2H), 4.56 (s, 1H), 4.51 (s, 1H), 3.77 (s, 3H), 3.71 (d, *J* = 12.9 Hz, 1H), 3.32 (ddd, *J* = 13.0, 11.3, 4.4 Hz, 1H), 2.61 (ddt, *J* = 18.6, 11.3, 2.6 Hz, 1H), 2.47 – 2.38 (m, 1H), 2.11 (s, 3H), 1.89 (s, 3H), 1.51 (s, 3H).

^{13}C NMR (101 MHz, $CDCl_3$) δ 199.8, 155.4, 146.0, 144.0, 136.4, 135.8, 131.4, 122.4, 119.1, 112.3, 108.4, 108.4, 94.8, 55.7, 49.7, 48.7, 32.1, 19.5, 16.4, 12.3.

HRMS-ESI (m/z): calcd for $C_{20}H_{23}NO_2Na$ [M + Na^+] 332.1621, found 332.1623

FTIR (film, cm^{-1}): 3353, 2919, 1666, 1463, 1160 cm^{-1}

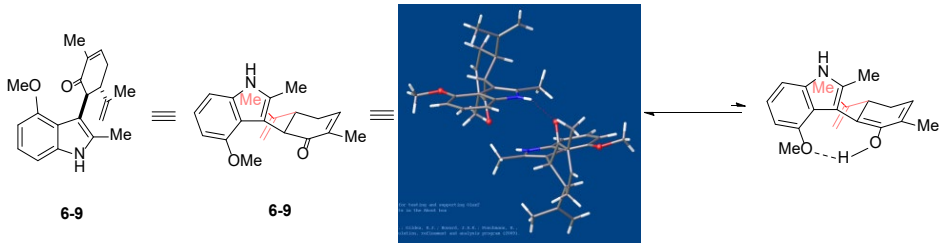

(5*R*,6*R*)-6-(4-methoxy-2-methyl-1*H*-indol-3-yl)-2-methyl-5-(prop-1-en-2-yl)cyclohex-2-en-1-one (**6-9**) was synthesized according to **general procedure C** and obtained as a gray solid (1 mmol scale, 163.0 mg, 53% yield). The H&C-NMR spectra of compound **6-9** is a little bit different compared to other products, probably due to its partial enolization to form an intramolecular H-bonding in solution.

^{1}H NMR (400 MHz, $CDCl_3$) δ 7.91 (s, 1H), 6.94 (t, *J* = 7.9 Hz, 1H), 6.79 (dd, *J* = 12.1, 7.2 Hz, 2H), 6.41 (d, *J* = 7.8 Hz, 1H), 4.53 (s, 2H), 3.75 (s, 3H), 3.47 (d, *J* = 60.0 Hz, 2H), 2.65 – 2.52 (m, 1H), 2.36 (dt, *J* = 17.8, 5.3 Hz, 1H), 2.14 (s, 3H), 1.89 (s, 3H), 1.47 (s, 3H).

^{13}C NMR (101 MHz, DMSO-d_6) δ 198.7, 152.4, 147.1, 142.6, 137.0, 134.4, 131.4, 120.4, 114.1, 108.4, 104.0, 99.2, 99.0, 54.5, 49.6, 48.7, 30.9, 20.2, 16.3, 11.5.

HRMS-API (m/z): calcd. for $C_{20}H_{24}NO_2$ [M + H^+] 310.1801, found 310.1803

FTIR (film, cm^{-1}): 3321, 2918, 1668, 1507, 1257, 1107, 732 cm^{-1}

M.p.: 136 – 137 ℃

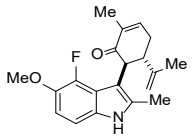

6-10

(5*R*,6*R*)-6-(4-fluoro-5-methoxy-2-methyl-1H-indol-3-yl)-2-methyl-5-(prop-1-en-2-yl)cyclohex-2-en-1-one (**6-10**) was synthesized according to **general procedure C** and obtained as a gray solid (1 mmol scale, 224.1 mg, 69% yield).

^{1}H NMR (400 MHz, $CDCl_3$) δ 7.79 (s, 1H), 6.88 – 6.75 (m, 3H), 4.57 (s, 1H), 4.53 (s, 1H), 3.86 (s, 3H), 3.72 (d, *J* = 7.7 Hz, 1H), 3.30 (td, *J* = 12.7, 2.7 Hz, 1H), 2.66 – 2.55 (m, 1H), 2.39 (dt, *J* = 18.0, 5.1 Hz, 1H), 2.21 (s, 3H), 1.86 (s, 3H), 1.58 (s, 3H).

^{13}C NMR (101 MHz, $CDCl_3$) δ C 198.8, 146.5, 144.1, 145.5 (d, $J_{C\text{-}F}$ = 240 Hz, 1C), 139.0 (d, $J_{C\text{-}F}$ = 10 Hz, 1C), 134.8 (d, $J_{C\text{-}F}$ = 10 Hz, 1C), 134.1, 133.1 (d, $J_{C\text{-}F}$ = 10 Hz, 1C), 11.8, 109.1, 106.2, 105.73, 105.70, 57.7, 49.1 (d, $J_{C\text{-}F}$ = 5 Hz, 1C), 48.9, 31.2, 19.3, 16.2, 11.7.

F-NMR: -142.2 (br), -147.5.

HRMS-API (m/z): calcd. for $C_{20}H_{23}FNO_2$ [M + H^+] 328.1707, found 328.1708

FTIR (film, cm^{-1}): 3344, 2934, 1664, 1585, 1506, 1329, 1264, 1102, 1090 cm^{-1}

M.p.: 136 – 137 ℃

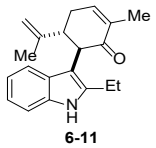

6-11

(5*R*,6*R*)-6-(2-ethyl-1*H*-indol-3-yl)-2-methyl-5-(prop-1-en-2-yl)cyclohex-2-en-1-one (**6-11**) was synthesized according to **general procedure C** and obtained as a yellow solid (1 mmol scale, 226.4 mg, 77% yield).

^{1}H NMR (400 MHz, $CDCl_3$) δ 7.96 (s, 1H), 7.27 (d, *J* = 7.6 Hz, 1H), 7.20 (d, *J* = 7.9 Hz, 1H), 7.05 (t, *J* = 7.5 Hz, 1H), 6.98 (t, *J* = 7.4 Hz, 1H), 6.86 (d, *J* = 6.0 Hz, 1H), 4.58 (s, 1H), 4.54 (s, 1H), 3.77 (d, *J* = 12.9 Hz, 1H), 3.38 (td, *J* = 12.1, 4.4 Hz, 1H), 2.68-2.56 (m, 3H), 2.44 (dt, *J* = 18.2, 5.1 Hz, 1H), 1.89 (s, 3H), 1.52 (s, 3H), 1.23 (t, *J* = 7.6 Hz, 3H).

^{13}C NMR (101 MHz, $CDCl_3$) δ 199.5, 146.0, 143.8, 138.1, 135.7, 135.6, 127.7, 120.6, 119.0, 118.8, 112.4, 110.6, 108.0, 49.7, 48.5, 31.9, 19.7, 19.6, 16.3, 13.7.

HRMS-ESI (m/z): calcd for $C_{20}H_{24}NO$ [M + H^+] 294.1852, found 294.1854

FTIR (film, cm^{-1}): 3361, 1669, 1462, 741 cm^{-1}

M.p.: 133 – 134 ℃

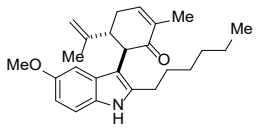

6-13

(5*R*,6*R*)-6-(2-hexyl-5-methoxy-1*H*-indol-3-yl)-2-methyl-5-(prop-1-en-2-yl)cyclohex-2-en-1-one (**6-13**) was synthesized according to **general procedure C** and obtained as a yellow solid (1 mmol scale, 239.3 mg, 63% yield).

^{1}H NMR (400 MHz, $CDCl_3$) δ 7.88 (s, 1H), 7.05 (d, *J* = 8.6 Hz, 1H), 6.86 (dt, *J* = 5.9, 2.0 Hz, 1H), 6.78 – 6.65 (m, 2H), 4.68 – 4.51 (m, 2H), 3.80 (s, 3H), 3.72 (d, *J* = 12.8 Hz, 1H), 3.35 (ddd, *J* = 12.7, 11.2, 4.4 Hz, 1H), 2.70 – 2.48 (m, 3H), 2.47 – 2.36 (m, 1H), 1.89 (dt, *J* = 2.6, 1.3 Hz, 3H), 1.63 – 1.55 (m, 2H), 1.53 (s, 3H), 1.40 – 1.19 (m, 6H), 0.89 (t, *J* = 6.6 Hz, 3H).

^{13}C NMR (101 MHz, $CDCl_3$) δ 199.5, 153.5, 146.1, 143.9, 138.3, 135.8, 130.9, 128.2, 112.4, 111.1, 109.7, 108.2, 102.1, 56.1, 49.7, 48.4, 31.9, 31.7, 29.4(x 2C), 26.8, 22.6, 19.8, 16.4, 14.1.

HRMS-ESI (m/z): calcd. for $C_{25}H_{34}NO_2$ [M + H^+] 380.2584, found 380.2587

FTIR (film, cm^{-1}): 3357, 2925, 1661, 1487, 1214, 900, 821, 789 cm^{-1}

M.p.: 133 – 134 ℃

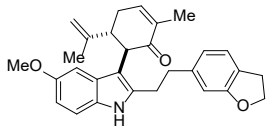

6-14

(5*R*,6*R*)-6-(2-(2-(2,3-dihydrobenzofuran-6-yl)ethyl)-5-methoxy-1*H*-indol-3-yl)-2-methyl-5-(prop-1-en-2-yl)cyclohex-2-en-1-one (**6-14**) was synthesized according to **general procedure C** and obtained as a white solid (0.5 mmol scale, 208.8 mg, 95% yield).

^{1}H NMR (400 MHz, $CDCl_3$) δ 7.77 (s, 1H), 7.02 (d, *J* = 8.7 Hz, 1H), 6.98 (d, *J* = 1.8 Hz, 1H), 6.88 (ddd, *J* = 9.2, 6.7, 2.0 Hz, 2H), 6.76 (d, *J* = 2.4 Hz, 1H), 6.74 – 6.68 (m, 2H), 4.63 (d, *J* = 1.8 Hz, 1H), 4.59 – 4.52 (m, 3H), 3.80 (s, 3H), 3.75 (d, *J* = 12.8 Hz, 1H), 3.36 (dd, *J* = 4.5, 1.6 Hz, 1H), 3.16 (t, *J* = 8.7 Hz, 2H),

2.86 – 2.72 (m, 4H), 2.69 – 2.57 (m, 1H), 2.54 – 2.38 (m, 1H), 1.90 (dt, *J* = 2.5, 1.3 Hz, 3H), 1.54 (s, 3H).

^{13}C NMR (101 MHz, $CDCl_3$) δ 199.4, 158.7, 153.7, 146.2, 143.9, 137.5, 135.8, 133.4, 130.9, 128.2, 127.9, 127.4, 125.2, 112.5, 111.2, 110.0, 109.2, 108.6, 102.2, 71.3, 56.1, 49.8, 48.5, 35.2, 32.0, 29.9, 29.2, 19.9, 16.5.

HRMS-ESI (m/z): calcd for $C_{29}H_{32}NO_3$ [M + H^+] 442.2376, found 442.2380

FTIR (film, cm^{-1}): 3342, 2919, 1664, 1490, 1240, 1215 cm^{-1}

M.p.: 152 – 153 ℃

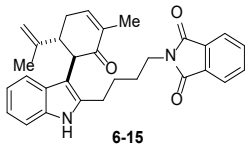

6-15

2-(4-(3-((1*R*,6*R*)-3-methyl-2-oxo-6-(prop-1-en-2-yl)cyclohex-3-en-1-yl)-1*H*-indol-2-yl)butyl)isoindoline-1,3-dione (**6-15**) was synthesized according to **general procedure C** and obtained as a white solid (0.5 mmol scale, 145.5 mg, 63% yield).

^{1}H NMR (400 MHz, $CDCl_3$) δ 8.42 (s, 1H), 7.86 (dd, *J* = 5.4, 3.0 Hz, 2H), 7.71 (dd, *J* = 5.4, 3.0 Hz, 2H), 7.30 (d, *J* = 7.8 Hz, 1H), 7.25 (d, *J* = 7.9 Hz, 1H), 7.11 – 7.04 (m, 1H), 6.99 (t, *J* = 7.4 Hz, 1H), 6.94 – 6.85 (m, 1H), 4.60 (s, 1H), 4.53 (t, *J* = 1.7 Hz, 1H), 3.89 – 3.65 (m, 3H), 3.42 (td, *J* = 12.0, 4.4 Hz, 1H), 2.80 – 2.56 (m, 3H), 2.52 – 2.41 (m, 1H), 1.94 – 1.85 (m, 3H), 1.75 (q, *J* = 6.7 Hz, 2H), 1.65 (qd, *J* = 7.8, 5.3 Hz, 2H), 1.52 (s, 3H).

^{13}C NMR (101 MHz, $CDCl_3$) δ 199.4, 168.6(x 2C), 146.1, 143.9, 136.5, 135.7, 135.6, 134.0(x 2C), 132.0(x 2C), 127.5, 123.2(x 2C), 120.6, 118.9, 118.8, 112.4, 110.7, 108.6, 49.7, 48.4, 37.2, 31.9, 28.1, 26.6, 25.7, 19.8, 16.4.

HRMS-ESI (m/z): calcd for $C_{30}H_{31}N_2O_3^+$ [M + H^+] 467.2329, found 467.2332

FTIR (film, cm^{-1}): 3383, 2943, 2922, 1768, 1706, 1671, 1463, 1438, 1397, 1371, 1036, 893, 722 cm^{-1}

M.p.: 118 – 119 ℃

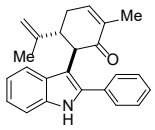

6-16

(5*R*,6*R*)-2-methyl-6-(2-phenyl-1H-indol-3-yl)-5-(prop-1-en-2-yl)cyclohex-2-en-1-one (**6-16**) was synthesized according to **general procedure C** and obtained as a white solid (1 mmol scale, 254.0 mg, 74% yield).

^{1}H NMR (400 MHz, $CDCl_3$) δ 8.0 (s, 1H), 7.5 – 7.4 (m, 6H), 7.3 (d, *J* = 8.0 Hz, 1H), 7.1 (t, *J* = 7.5 Hz, 1H), 7.0 (t, *J* = 7.5 Hz, 1H), 6.9 (d, *J* = 6.2 Hz, 1H), 4.3 (t, *J* = 1.8 Hz, 1H), 4.2 (s, 1H), 3.9 (d, *J* = 13.1 Hz, 1H), 3.5 – 3.4 (m, 1H), 2.5 (ddt, *J* = 18.7, 11.4, 2.7 Hz, 1H), 2.3 (dt, *J* = 18.4, 5.6 Hz, 1H), 2.0 – 1.9 (m, 3H), 1.2 (s, 3H).

^{13}C NMR (101 MHz, $CDCl_3$) δ 200.3, 145.2, 144.5, 137.3, 136.3, 135.6, 133.4, 128.9(x 2C), 128.8(x 2C), 128.1, 122.0, 120.1, 119.6, 112.8, 111.3, 110.3, 77.2, 49.7, 48.6, 31.9, 18.2, 16.5.

HRMS-ESI (m/z): calcd for $C_{24}H_{24}NO$ [M + H^+] 342.1852, found 342.1855

FTIR (film, cm^{-1}): 3338, 3056, 2916, 1651, 1448, 1370, 1242, 763, 741, 699 cm^{-1}

M.p.: 153 – 154 ℃

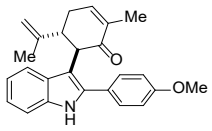

6-17

(5*R*,6*R*)-6-(2-(4-methoxyphenyl)-1H-indol-3-yl)-2-methyl-5-(prop-1-en-2-yl)cyclohex-2-en-1-one (**6-17**) was synthesized according to **general procedure C** and obtained as a white solid (1 mmol scale, 256.4 mg, 69% yield).

^{1}H NMR (400 MHz, $CDCl_3$) δ 8.00 (s, 1H), 7.40–7.32 (m, 3H), 7.27–7.23 (m, 1H), 7.09 (t, *J* = 7.5 Hz, 1H), 7.01 (t, *J* = 7.5 Hz, 1H), 6.95–6.90 (m, 2H), 6.84 (d, *J* = 6.1 Hz, 1H), 4.30 (d, *J* = 1.8 Hz, 1H), 4.24 (s, 1H), 3.88 (d, *J* = 13.2 Hz, 1H), 3.83 (s, 3H), 3.48–3.38 (m, 1H), 2.50–2.37 (m, 1H), 2.36–2.25 (m, 1H), 1.91 (s, 3H), 1.18 (s, 3H).

^{13}C NMR (101 MHz, $CDCl_3$) δ 200.4, 159.5, 145.3, 144.4, 137.2, 136.2, 135.7, 130.1 (x 2C), 127.8, 125.9, 121.7, 119.8, 119.5, 114.3 (x 2C), 112.7, 111.1, 109.7, 55.4, 49.8, 48.5, 31.9, 18.3, 16.5.

HRMS-ESI (m/z): calcd for $C_{25}H_{26}NO_2^+$ [M + H^+] 372.1958, found 372.1961

FTIR (film, cm^{-1}): 3347, 2920, 1660, 1506, 1458, 1248, 834, 743 cm^{-1}

M.p.: 140 – 141 ℃

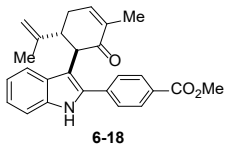

6-18

ethyl 4-(3-((1R,6R)-3-methyl-2-oxo-6-(prop-1-en-2-yl)cyclohex-3-en-1-yl)-1H-indol-2-yl)benzoate (**6-18**) was synthesized according to **general procedure C** and obtained as a white solid (0.5 mmol scale, 46.5 mg, 23% yield).

^{1}H NMR (400 MHz, $CDCl_3$) δ 8.43 (s, 1H), 8.14 – 7.88 (m, 2H), 7.52 – 7.42 (m, 2H), 7.38 (d, *J* = 7.9 Hz, 1H), 7.16 (d, *J* = 8.2 Hz, 1H), 7.08 (t, *J* = 7.6 Hz, 1H), 7.02 (t, *J* = 7.4 Hz, 1H), 6.87 (d, *J* = 6.0 Hz, 1H), 4.26 (s, 1H), 4.18 (s, 1H), 3.95 (s, 1H), 3.93 (s, 3H), 3.43 (td, *J* = 12.3, 4.6 Hz, 1H), 2.44 (dd, *J* = 18.2, 11.6 Hz, 1H), 2.32 (dt, *J* = 18.3, 5.4 Hz, 1H), 1.94 (s, 3H), 1.10 (s, 3H).

^{13}C NMR (101 MHz, $CDCl_3$) δ 200.2, 167.0, 145.0, 144.8, 138.0, 136.7, 136.0, 135.6, 130.1 (x 2C), 129.2, 128.4 (x 2C), 127.5, 122.5, 120.1, 119.8, 112.9, 111.5, 111.5, 52.3, 49.8, 48.5, 31.9, 18.2, 16.4.

HRMS-API (m/z): calcd. for $C_{26}H_{26}NO_3$ [M + H^+] 400.1907, found 400.1908

FTIR (film, cm^{-1}): 3352, 2950, 1725, 1656, 1610, 1435, 1276, 1102, 741 cm^{-1}

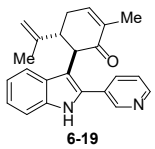

6-19

(5*R*,6*R*)-2-methyl-5-(prop-1-en-2-yl)-6-(2-(pyridin-3-yl)-1H-indol-3-yl)cyclohex-2-en-1-one (**6-19**) was synthesized according to **general procedure C** and obtained as a yellow solid (1 mmol scale, 131.9 mg, 39% yield).

^{1}H NMR (600 MHz, $CDCl_3$) δ 8.94 (s, 1H), 8.67 (s, 1H), 8.52 (d, *J* = 6.1 Hz, 1H), 7.70 (d, *J* = 7.9 Hz, 1H), 7.38 (d, *J* = 7.9 Hz, 1H), 7.29 – 7.25 (m, 1H), 7.17 (d, *J* = 8.1 Hz, 1H), 7.08 (t, *J* = 8.0 Hz, 1H), 7.02 (t, *J* = 7.5 Hz, 1H), 6.86 (d, *J* = 5.8 Hz, 1H), 4.30 (s, 1H), 4.20 (s, 1H), 3.83 (d, *J* = 13.1 Hz, 1H), 3.42 (td, *J* = 12.4, 4.5 Hz, 1H), 2.47 – 2.40 (m, 1H), 2.32 (dt, *J* = 18.5, 5.0 Hz, 1H), 1.90 (s, 3H), 1.13 (s, 3H).

^{13}C NMR (101 MHz, $CDCl_3$) δ 200.1, 149.2, 148.6, 144.9, 144.7, 136.8, 136.1, 135.5, 133.5, 129.6, 127.3, 123.6, 122.3, 119.9, 119.6, 112.8, 111.6, 111.3, 49.7, 48.3, 31.8, 18.5, 16.3.

HRMS-API (m/z): calcd. for $C_{23}H_{23}N_2O$ [M + H^+] 343.1804, found 343.1806

FTIR (film, cm^{-1}): 3333, 2922, 1666, 1455, 743 cm^{-1}

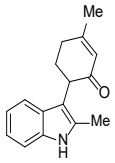

6-20

3-methyl-6-(2-methyl-1*H*-indol-3-yl)cyclohex-2-en-1-one (**6-20**) was synthesized according to **general procedure C** and obtained as a yellow solid (1 mmol scale, 102.9 mg, 46% yield).

^{1}H NMR (400 MHz, $CDCl_3$) δ 7.88 (s, 1H), 7.24 (d, *J* = 9.0 Hz, 2H), 7.07 (ddd, *J* = 8.1, 7.1, 1.3 Hz, 1H), 7.00 (ddd, *J* = 8.1, 7.1, 1.2 Hz, 1H), 6.11 (s, 1H), 3.70 (dd, *J* = 12.9, 5.1 Hz, 1H), 2.49 – 2.33 (m, 3H), 2.29 (s, 3H), 2.17 – 2.10 (m, 1H), 2.05 (t, *J* = 1.2 Hz, 3H).

^{13}C NMR (101 MHz, $CDCl_3$) δ 199.6, 162.5, 135.6, 132.2, 127.5, 127.3, 120.8, 119.1, 118.7, 110.7, 110.2, 44.2, 31.7, 30.5, 24.5, 12.1.

HRMS-ESI (m/z): calcd for $C_{16}H_{18}NO$ [M + H^+] 240.1382, found 240.1384

FTIR (film, cm^{-1}): 3311, 2910, 1647, 1462, 1214, 743 cm^{-1}

M.p.: 165 – 167 ℃

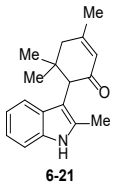

6-21

3,5,5-trimethyl-6-(2-methyl-1*H*-indol-3-yl)cyclohex-2-en-1-one (**6-21**) was synthesized according to **general procedure C** and obtained as oil (1 mmol scale, 168.5 mg, 63% yield).

^{1}H NMR (400 MHz, $CDCl_3$) δ 8.07 (s, 1H), 7.16 (t, *J* = 6.9 Hz, 2H), 7.00 (dt, *J* = 29.8, 7.6 Hz, 2H), 6.14 (d, *J* = 29.7 Hz, 1H), 3.54 (s, 1H), 2.55 (dd, *J* = 35.3, 17.9 Hz, 1H), 2.26 (d, *J* = 17.8 Hz, 1H), 2.19 (d, *J* = 5.7 Hz, 3H), 2.04 (d, *J* = 8.2 Hz, 3H), 1.00 (d, *J* = 2.5 Hz, 6H).

^{13}C NMR (101 MHz, $CDCl_3$) δ 199.4, 159.9, 135.7, 134.5, 127.8, 126.7, 121.5, 120.5, 118.9, 110.4, 107.0, 55.2, 47.1, 40.2, 29.8, 24.8, 24.4, 12.4.

HRMS-API (m/z): calcd. for $C_{18}H_{22}NO$ [M + H^+] 268.1695, found 268.1697

FTIR (film, cm^{-1}): 3311, 2946, 1650, 1461, 1310, 1292, 1222, 731, 727 cm^{-1}

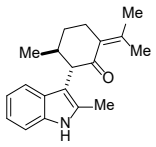

6-22

(2*S*,3*S*)-3-methyl-2-(2-methyl-1*H*-indol-3-yl)-6-(propan-2-ylidene)cyclohexan-1-one (**6-22**) was synthesized according to **general procedure C** and obtained as a yellow solid (1 mmol scale, 236.5 mg, 84% yield).

^{1}H NMR (400 MHz, $CDCl_3$) δ 7.92 (s, 1H), 7.28 – 7.24 (m, 1H), 7.21 – 7.16 (m, 1H), 7.06 (ddd, *J* = 8.1, 7.0, 1.3 Hz, 1H), 6.99 (ddd, *J* = 8.1, 7.0, 1.1 Hz, 1H), 3.28 (d, *J* = 11.5 Hz, 1H), 2.91 – 2.81 (m, 1H), 2.63 – 2.51 (m, 1H), 2.39 – 2.32 (m, 1H), 2.30 (s, 3H), 2.03 (ddt, *J* = 13.3, 5.1, 3.0 Hz, 1H), 1.96 – 1.91 (m, 3H), 1.87 (d, *J* = 1.3 Hz, 3H), 1.55 (tdd, *J* = 13.1, 11.7, 4.7 Hz, 1H), 0.85 (d, *J* = 6.4 Hz, 3H).

^{13}C NMR (101 MHz, $CDCl_3$) δ 204.6, 142.6, 135.6, 132.8, 132.7, 127.6, 120.7, 119.0, 118.9, 110.5, 110.2, 56.7, 37.1, 32.9, 29.1, 23.1, 22.3, 21.3, 12.3.

HRMS-API (m/z): calcd. for $C_{19}H_{24}NO$ [M + H^+] 282.1852, found 282.1854

FTIR (film, cm^{-1}): 3392, 2919, 1670, 1461, 1305, 1287, 744 cm^{-1}

M.p.: 117 – 119 ℃

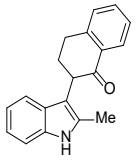

6-23

2-(2-methyl-1H-indol-3-yl)-3,4-dihydronaphthalen-1(2H)-one (6-23) (Maksymenko et al., 2017) was synthesized according to **general procedure C** and obtained as a yellow solid (1 mmol scale, 199.5 mg, 79% yield).

^{1}H NMR (400 MHz, DMSO-d_6) δ 10.78 (s, 1H), 7.95 (dd, *J* = 7.8, 1.5 Hz, 1H), 7.60 (td, *J* = 7.5, 1.5 Hz, 1H), 7.47 – 7.37 (m, 2H), 7.25 (dt, *J* = 8.2, 0.9 Hz, 1H), 7.07 (d, *J* = 7.9 Hz, 1H), 6.95 (ddd, *J* = 8.2, 7.0, 1.2 Hz, 1H), 6.81 (ddd, *J* = 8.0, 7.0, 1.1 Hz, 1H), 4.10 (dd, *J* = 13.0, 4.7 Hz, 1H), 3.24 (td, *J* = 12.4, 6.2 Hz, 1H), 3.01 (dt, *J* = 16.3, 3.7 Hz, 1H), 2.43 (td, *J* = 12.8, 4.0 Hz, 1H), 2.28 (s, 3H), 2.22 – 2.14 (m, 1H).

^{13}C NMR (101 MHz, DMSO-d_6) δ 197.9, 144.7, 135.3, 133.3, 132.7, 132.4, 129.0, 127.2, 126.8, 126.6, 119.7, 118.1, 118.0, 110.5, 109.9, 45.4, 30.9, 29.1, 11.7.

HRMS-ESI (m/z): calcd for $C_{19}H_{18}NO$ [M + H^+] 276.1382, found 276.1384

FTIR (film, cm^{-1}): 3225, 1670, 1596, 1455, 1308, 1224, 742 cm^{-1}

M.p.: 124 – 125 ℃

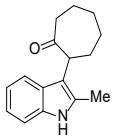

6-24

2-(2-methyl-1*H*-indol-3-yl)cycloheptan-1-one (6-24) was synthesized according to **general procedure C** and obtained as a light brown solid (1 mmol scale, 153.8 mg, 64% yield).

^{1}H NMR (400 MHz, $CDCl_3$) δ 8.01 (s, 1H), 7.53 – 7.47 (m, 1H), 7.21 – 7.14 (m, 1H), 7.07 (tt, *J* = 7.9, 5.9 Hz, 2H), 3.91 (dd, *J* = 11.4, 3.1 Hz, 1H), 2.89 (ddd, *J* = 14.5, 11.9, 2.6 Hz, 1H), 2.74 – 2.65 (m, 1H), 2.44 – 2.29 (m, 1H), 2.28 (d, 3H), 2.07 (ddt, *J* = 17.0, 13.0, 6.8 Hz, 4H), 1.72 (qt, *J* = 13.6, 2.5 Hz, 1H), 1.56 (pd, *J* = 12.7, 10.6, 4.4 Hz, 2H).

^{13}C NMR (101 MHz, $CDCl_3$) δ 214.7, 135.4, 131.7, 127.6, 120.9, 119.2, 118.9, 111.6, 110.6, 50.9, 44.1, 31.9, 30.6, 30.1, 25.3, 12.6.

HRMS-ESI (m/z): calcd for $C_{16}H_{19}NONa$ [M + Na^+] 264.1358, found 264.1360

FTIR (film, cm^{-1}): 3364, 2932, 1690, 1461, 743 cm^{-1}

M.p.: 76 – 77 ℃

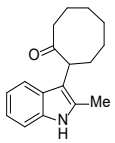

6-25

2-(2-methyl-1*H*-indol-3-yl)cycloheptan-1-one (6-25) was synthesized according to **general procedure C** and obtained as a light brown oil (1 mmol scale, 184.2 mg, 72% yield).

^{1}H NMR (400 MHz, $CDCl_3$) δ 8.21 (s, 1H), 7.98 (dd, *J* = 6.2, 3.0 Hz, 1H), 7.35 (dd, *J* = 6.1, 2.9 Hz, 1H), 7.24 (dt, *J* = 6.0, 2.8 Hz, 2H), 4.12 (d, *J* = 12.6 Hz, 1H), 3.10 – 2.89 (m, 2H), 2.59 (d, *J* = 2.2 Hz, 3H), 2.49 – 2.40 (m, 1H), 2.17 (s, 1H), 2.10 (dt, *J* = 10.3, 5.6 Hz, 2H), 2.03 – 1.90 (m, 2H), 1.84 – 1.55 (m, 4H).

^{13}C NMR (101 MHz, $CDCl_3$) δ 216.3, 135.2, 132.8, 127.6, 120.3, 119.3, 118.9, 110.5, 108.3, 50.6, 40.2,

39.7, 29.9, 27.6, 26.4, 24.7, 12.6.

HRMS-API (m/z): calcd. for $C_{17}H_{22}NO$ [M + H^+] 256.1695, found 256.1697

FTIR (film, cm^{-1}): 3357, 2926, 2854, 1689, 1459, 740 cm^{-1}

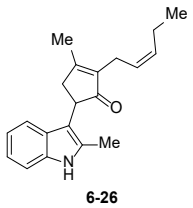

6-26

3-methyl-5-(2-methyl-1H-indol-3-yl)-2-pentylcyclopent-2-en-1-one (6-26) was synthesized according to **general procedure C** and obtained as a brown solid (1 mmol scale, 157.4 mg, 54% yield).

^{1}H NMR (400 MHz, $CDCl_3$) δ 7.97 (s, 1H), 7.21 (d, *J* = 8.0 Hz, 1H), 7.08 – 6.99 (m, 2H), 6.93 (t, *J* = 7.4 Hz, 1H), 5.48 – 5.31 (m, 2H), 3.71 (dd, *J* = 7.4, 3.0 Hz, 1H), 3.03 (dd, *J* = 45.9, 7.2 Hz, 3H), 2.72 (d, *J* = 18.5 Hz, 1H), 2.28 – 2.09 (m, 8H), 1.01 (t, *J* = 7.5 Hz, 3H).

^{13}C NMR (101 MHz, $CDCl_3$) δ 209.8, 169.5, 139.2, 135.7, 132.8, 132.7, 127.1, 125.2, 121.0, 119.2, 117.9, 110.7, 109.6, 42.8, 40.6, 21.7, 20.8, 17.4, 14.3, 11.7.

HRMS-ESI (m/z): calcd for $C_{20}H_{24}NO$ [M + H^+] 294.1852, found 294.1854

FTIR (film, cm^{-1}): 3314, 1687, 1639, 1620, 1461, 737 cm^{-1}

M.p.: 106 – 107 ℃

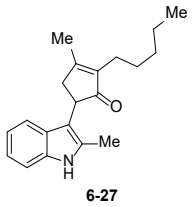

6-27

(*Z*)-3-methyl-5-(2-methyl-1*H*-indol-3-yl)-2-(pent-2-en-1-yl)cyclopent-2-en-1-one (6-27) was synthesized according to **general procedure C** and obtained as a brown solid (1 mmol scale, 142.1 mg, 48% yield).

^{1}H NMR (400 MHz, $CDCl_3$) δ 8.54 (s, 1H), 7.17 – 7.10 (m, 1H), 7.07 – 7.00 (m, 2H), 6.99 – 6.91 (m, 1H), 3.69 (dd, *J* = 7.3, 3.0 Hz, 1H), 2.98 (dd, *J* = 18.6, 7.3 Hz, 1H), 2.79 – 2.68 (m, 1H), 2.37 (dt, *J* = 8.1, 3.8 Hz, 2H), 2.17 (s, 3H), 1.86 (s, 3H), 1.61 – 1.49 (m, 2H), 1.38 (h, *J* = 3.9 Hz, 4H), 0.94 (t, *J* = 6.8 Hz, 3H).

^{13}C NMR (101 MHz, $CDCl_3$) δ 210.9, 169.6, 140.4, 135.7, 133.3, 127.0, 120.6, 118.8, 117.5, 110.8, 108.9, 42.8, 40.4, 31.9, 28.2, 23.4, 22.6, 17.2, 14.1, 11.1.

HRMS-API (m/z): calcd. for $C_{20}H_{26}NO$ [M + H^+] 296.2008, found 296.2011

FTIR (film, cm^{-1}): 3330, 2927, 1688, 1638, 1462, 735 cm^{-1}

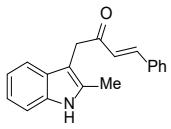

6-28

(*E*)-1-(2-methyl-1*H*-indol-3-yl)-4-phenylbut-3-en-2-one (6-28) was synthesized according to **general procedure C** and obtained as a light brown solid (1 mmol scale, 60.7 mg, 22% yield).

^{1}H NMR (400 MHz, $CDCl_3$) δ 8.01 (s, 1H), 7.63 (d, *J* = 16.0 Hz, 1H), 7.54 – 7.48 (m, 1H), 7.44 – 7.39 (m, 2H), 7.30 (d, *J* = 7.1 Hz, 3H), 7.22 (t, *J* = 4.4 Hz, 1H), 7.14 – 7.06 (m, 2H), 6.78 (d, *J* = 16.0 Hz, 1H), 3.92 (s, 2H), 2.34 (s, 3H).

^{13}C NMR (101 MHz, $CDCl_3$) δ 197.8, 142.8, 135.4, 134.5, 133.1, 130.4, 129.8, 128.9 (x 2C), 128.4 (x 2C), 124.6, 121.3, 119.7, 117.9, 110.5, 104.3, 38.2, 11.9.

HRMS-API (m/z): calcd. for $C_{19}H_{18}NO$ [M + H^+] 276.1382, found 276.1384

FTIR (film, cm^{-1}): 3346, 1651, 1175, 747 cm^{-1}

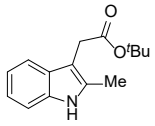

6-29

***Tert*-butyl 2-(2-methyl-1*H*-indol-3-yl)acetate (6-29)** was synthesized according to **general procedure C** and obtained as a yellow solid (1 mmol scale, 102.1 mg, 42% yield).

^{1}H NMR (600 MHz, $CDCl_3$) δ 8.00 (s, 1H), 7.58 (dd, *J* = 5.8, 3.2 Hz, 1H), 7.17 – 7.11 (m, 3H), 3.64 (s, 2H), 2.27 (s, 3H), 1.48 (s, 9H).

^{13}C NMR (101 MHz, $CDCl_3$) δ 171.7, 135.3, 132.8, 128.6, 121.0, 119.3, 118.2, 110.4, 105.0, 80.7, 31.8, 28.2(x 3C), 11.6.

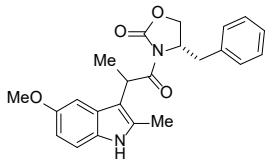

6-30 (1.9:1 dr)

(4*S*)-4-benzyl-3-(2-(5-methoxy-2-methyl-1*H*-indol-3-yl)propanoyl)oxazolidin-2-one (**6-30**) was synthesized according to **general procedure C** and obtained as a yellow solid (1 mmol scale, 258.6 mg, 66% yield).

^{1}H NMR (400 MHz, $CDCl_3$, data for major diastereomer given) δ 8.01 (s, 1H), 7.46 – 7.13 (m, 6H), 6.97 (dd, *J* = 7.3, 2.1 Hz, 1H), 6.83 (ddd, *J* = 8.8, 5.0, 2.4 Hz, 1H), 5.30 (dq, *J* = 9.6, 7.0 Hz, 1H), 4.86 (tt, *J* = 8.8, 3.7 Hz, 1H), 4.20 (t, *J* = 8.7 Hz, 1H), 4.10 – 4.01 (m, 1H), 3.95 (s, 1H), 3.90 (s, 2H), 3.19 (dd, *J* = 13.5, 3.4 Hz, 1H), 2.55 (s, 3H), 2.48 – 2.43 (m, 1H), 1.67 (dd, *J* = 7.1, 5.7 Hz, 3H).

^{13}C NMR (101 MHz, $CDCl_3$) major δ = 174.9, 153.8, 153.1, 135.1, 134.3, 130.3, 129.3 (x 2C), 128.7 (x 2C), 127.5, 127.1, 111.1, 110.8, 109.0, 101.2, 65.9, 55.8, 55.0, 37.8, 35.9, 17.2, 12.3; minor δ = 174.9, 153.8, 153.0, 135.5, 134.2, 130.4, 129.5 (x 2C), 128.9 (x 2C), 127.5, 127.3, 111.0, 110.4, 109.2, 101.5, 65.8, 56.1, 56.0, 37.8, 35.5, 17.4, 12.1.

HRMS-ESI (m/z): calcd for $C_{23}H_{25}N_2O_4$ [M + H^+] 393.1809, found 393.1811

FTIR (film, cm^{-1}): 3395, 2931, 1778, 1697, 1485, 1452, 1389, 1356, 1215 cm^{-1}

M.p.: 73 – 75 ℃

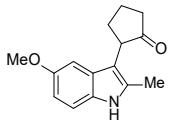

6-31

2-(5-methoxy-2-methyl-1*H*-indol-3-yl)cyclopentan-1-one (6-31) was synthesized according to **general procedure C** and obtained as a yellow solid by using LDA instead of LiHMDS (1 mmol scale, 95.1 mg, 39% yield).

^{1}H NMR (400 MHz, $CDCl_3$) δ 7.90 (s, 1H), 7.09 (d, *J* = 8.7 Hz, 1H), 6.74 (dd, *J* = 8.7, 2.4 Hz, 1H), 6.69 (d, *J* = 2.4 Hz, 1H), 3.81 (s, 3H), 3.54 – 3.42 (m, 1H), 2.58 (ddd, *J* = 18.8, 8.7, 2.1 Hz, 1H), 2.51 – 2.33 (m, 2H), 2.28 – 2.10 (m, 5H), 2.08 – 1.91 (m, 1H).

^{13}C NMR (101 MHz, $CDCl_3$) δ 220.0, 153.8, 133.7, 130.9, 127.8, 111.3, 110.1, 108.3, 101.4, 56.2, 47.5, 38.7, 31.1, 21.4, 12.1.

HRMS-API (m/z): calcd. for $C_{15}H_{18}NO_2$ [M + H^+] 244.1332, found 244.1333

FTIR (film, cm^{-1}): 3394, 2940, 1731, 1484, 1214 cm^{-1}

M.p.: 101 – 103 ℃

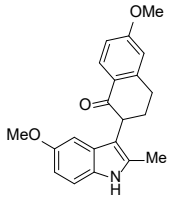

6-32

6-methoxy-2-(5-methoxy-2-methyl-1H-indol-3-yl)-3,4-dihydronaphthalen-1(2*H*)-one (6-32) was synthesized according to **general procedure C** and obtained as a light green solid (1 mmol scale, 164.3 mg, 49% yield).

^{1}H NMR (400 MHz, $CDCl_3$) δ 8.29 – 8.09 (m, 2H), 7.01 – 6.95 (m, 1H), 6.90 (dd, *J* = 8.7, 2.5 Hz, 1H), 6.79 (d, *J* = 2.5 Hz, 1H), 6.76 – 6.63 (m, 2H), 3.93 (d, *J* = 4.8 Hz, 1H), 3.89 (s, 3H), 3.73 (s, 3H), 3.16 (ddd, *J* = 16.4, 12.0, 4.4 Hz, 1H), 3.01 (dt, *J* = 16.5, 4.0 Hz, 1H), 2.54 (qd, *J* = 12.6, 4.1 Hz, 1H), 2.27 (dq, *J* = 13.2, 4.4 Hz, 1H), 2.07 (s, 3H).

^{13}C NMR (101 MHz, $CDCl_3$) δ 197.7, 163.6, 153.5, 147.1, 133.4, 130.8, 130.3, 127.9, 126.9, 113.3, 112.6, 111.3, 110.1, 109.9, 101.3, 55.9, 55.5, 46.0, 31.0, 30.2, 12.0.

HRMS-ESI (m/z): calcd for $C_{21}H_{22}NO_3$ [M + H^+] 336.1594, found 336.1597

FTIR (film, cm^{-1}): 3291, 1656, 1594, 1484, 1284, 1251, 1212 cm^{-1}

M.p.: 144 – 145 ℃

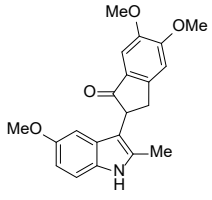

6-33

5,6-dimethoxy-2-(5-methoxy-2-methyl-1*H*-indol-3-yl)-2,3-dihydro-1*H*-inden-1-one (**6-33**) was synthesized according to **general procedure C** and obtained as a light brown solid (1 mmol scale, 122.4 mg, 33% yield).

^{1}H NMR (400 MHz, DMSO-d_6) 10.66 (s, 1H), 7.16 (dd, *J* = 16.7, 9.2 Hz, 3H), 6.61 (dd, *J* = 8.7, 2.4 Hz,

1H), 6.25 (d, *J* = 2.4 Hz, 1H), 4.06 (dd, *J* = 8.1, 3.9 Hz, 1H), 3.91 (s, 3H), 3.84 (s, 3H), 3.62 – 3.52 (m, 1H), 3.51 (s, 3H), 3.07 (dd, *J* = 17.4, 3.8 Hz, 1H), 2.27 (s, 3H).

^{13}C NMR (101 MHz, DMSO-d_6) 205.4, 155.4, 152.7, 149.3, 148.8, 133.7, 130.5, 128.9, 127.3, 111.1, 109.0, 108.8, 108.1, 104.0, 100.5, 56.0, 55.6, 55.1, 44.3, 34.2, 11.6.

HRMS-API (m/z): calcd. for $C_{21}H_{22}NO_4$ [M + H$^+$] 352.1543, found 352.1543

FTIR (film, cm^{-1}): 3375, 2922, 1699, 1588, 1501, 1487, 1310, 1264, 1220, 1112, 1033, 801 cm^{-1}

M.p.: 201 – 202 ℃

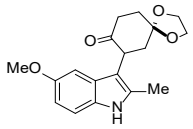

6-34

7-(5-methoxy-2-methyl-1*H*-indol-3-yl)-1,4-dioxaspiro[4.5]decan-8-one (**6-34**) was synthesized according to **general procedure C** and obtained as a yellow solid (1 mmol scale, 128.4 mg, 41% yield).

^{1}H NMR (400 MHz, $CDCl_3$) δ 7.99 (s, 1H), 7.02 (d, *J* = 8.6 Hz, 1H), 6.77 – 6.67 (m, 2H), 4.13 – 4.06 (m, 2H), 4.00 (dt, *J* = 5.7, 1.5 Hz, 2H), 3.81 (s, 3H), 2.94 – 2.80 (m, 1H), 2.62 – 2.46 (m, 2H), 2.22 – 2.14 (m, 5H), 2.08 – 1.93 (m, 2H).

^{13}C NMR (101 MHz, $CDCl_3$) δ 208.9, 153.7, 133.2, 130.7, 128.0, 111.2, 110.2, 107.8, 107.5, 101.5, 64.8, 64.7, 56.2, 44.6, 40.9, 38.4, 34.4, 12.4.

HRMS-ESI (m/z): calcd for $C_{18}H_{22}NO_4$ [M + H$^+$] 316.1543, found 316.1545

FTIR (film, cm^{-1}): 3349, 2888, 1712, 1487, 1454, 1216, 1122, 1029 cm^{-1}

M.p.: 150 – 151 ℃

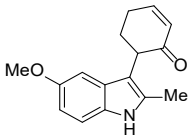

6-35

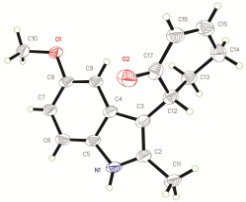

6-(5-methoxy-2-methyl-1*H*-indol-3-yl)cyclohex-2-en-1-one (**6-35**) was synthesized according to **general procedure C** and obtained as a yellow solid (1 mmol scale, 162.4 mg, 64% yield).

^{1}H NMR (400 MHz, DMSO-d_6) δ 10.62 (s, 1H), 7.16 (dd, *J* = 15.2, 8.1 Hz, 2H), 6.71 – 6.60 (m, 2H), 6.14

– 6.07 (m, 1H), 3.85 (dd, *J* = 13.5, 4.8 Hz, 1H), 3.69 (s, 3H), 2.59 (dddt, *J* = 18.4, 13.7, 4.5, 2.3 Hz, 1H), 2.48 – 2.38 (m, 1H), 2.35 – 2.27 (m, 1H), 2.23 (s, 3H), 2.03 (ddt, *J* = 13.9, 6.5, 2.6 Hz, 1H).

^{13}C NMR (101 MHz, DMSO-d_6) δ 198.9, 152.7, 151.1, 133.1, 130.4, 129.5, 127.8, 110.9, 109.4, 109.1, 100.9, 55.4, 44.4, 30.3, 26.0, 11.9.

HRMS-ESI (m/z): calcd for $C_{16}H18NO_2$ [M + H^+] 256.1332, found 256.1334

FTIR (film, cm^{-1}): 3281, 2931, 1656, 1481, 1215, 1032, 797 cm^{-1}

M.p.: 144 – 145 ℃

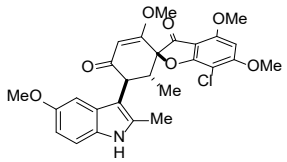

6-36

(5'*S*,6'*R*)-7-chloro-2',4,6-trimethoxy-5'-(5-methoxy-2-methyl-1H-indol-3-yl)-6'-methyl-3H-spiro[benzofuran-2,1'-cyclohexan]-2'-ene-3,4'-dione (6-36) was synthesized according to **general procedure C** and obtained as a light brown solid (1 mmol scale, 183.8 mg, 36% yield).

^{1}H NMR (400 MHz, DMSO-d_6, data for major diastereomer given) δ 10.70 (s, 1H), 7.16 (d, *J* = 8.6 Hz, 1H), 6.66 (d, *J* = 2.4 Hz, 1H), 6.57 (s, 1H), 6.52 (s, 1H), 5.84 (s, 1H), 4.17 (d, *J* = 12.5 Hz, 1H), 4.04 (s, 3H), 3.97 (s, 3H), 3.71 (d, *J* = 11.5 Hz, 6H), 3.18 (dd, *J* = 12.7, 6.7 Hz, 1H), 2.26 (s, 3H), 0.57 (d, *J* = 6.7 Hz, 3H).

^{13}C NMR (101 MHz, DMSO-d_6) δ 195.7, 191.6, 169.5, 168.6, 164.7, 157.7, 152.8, 135.4, 130.8, 126.5, 111.2, 109.2, 106.2, 104.9, 104.3, 101.3, 95.4, 91.3, 90.6, 57.6, 57.1, 56.6, 55.5, 45.0, 20.7, 12.5, 11.4.

HRMS-ESI (m/z): calcd for $C_{27}H_{27}ClNO_7$ [M + H^+] 512.1470, found 512.1474

FTIR (film, cm^{-1}): 3411, 2941, 1699, 1665, 1617, 1590, 1484, 1466, 1354, 1215 cm^{-1}

M.p.: 240 – 242 ℃

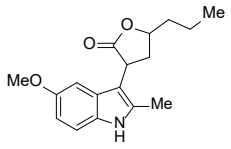

6-37

3-(5-methoxy-2-methyl-1*H*-indol-3-yl)-5-propyldihydrofuran-2(3*H*)-one (6-37) was synthesized

according to **general procedure C** and obtained as a brown solid (1 mmol scale, 255.3 mg, 89% yield, dr = 2.4:1).

^{1}H NMR (400 MHz, $CDCl_3$) **6-37-1 (anti)***:* δ 8.06 (s, 1H), 7.09 (d, *J* = 8.6 Hz, 1H), 6.81 – 6.72 (m, 2H), 4.56 (ddd, *J* = 12.7, 10.9, 5.9 Hz, 1H), 4.01 (dd, *J* = 12.6, 9.0 Hz, 1H), 3.82 (s, 3H), 2.59 (ddd, *J* = 13.2, 9.0, 5.6 Hz, 1H), 2.20 – 2.13 (m, 1H), 2.12 (d, *J* = 1.2 Hz, 3H), 1.94 – 1.85 (m, 1H), 1.78 – 1.69 (m, 1H), 1.61 – 1.45 (m, 2H), 1.01 (t, *J* = 7.3 Hz, 3H); **6-37-2 (syn)**: δ 8.16 (s, 1H), 7.06 (d, *J* = 8.7 Hz, 1H), 6.80 (s, 1H), 6.75 (dd, *J* = 8.7, 2.2 Hz, 1H), 4.76 (tt, *J* = 8.2, 4.5 Hz, 1H), 4.02 (t, *J* = 9.5 Hz, 1H), 3.82 (s, 3H), 2.53 (dt, *J* = 13.2, 8.5 Hz, 1H), 2.33 – 2.24 (m, 1H), 2.08 (s, 3H), 1.93 – 1.76 (m, 1H), 1.72 – 1.42 (m, 3H), 1.01 (t, *J* = 7.2 Hz, 3H).

^{13}C NMR (101 MHz, $CDCl_3$) δ **6-37-1 (anti)***:* 178.8, 154.0, 133.8, 130.7, 127.0, 111.5, 110.5, 106.7, 100.3, 79.1, 56.1, 37.8, 36.5, 35.2, 18.7, 13.9, 11.6.; **6-37-2 (syn)**: 178.2, 154.0, 134.0, 130.8, 127.1, 111.6, 110.7, 106.3, 100.5, 79.0, 56.1, 38.8, 37.8, 36.5, 18.6, 14.0, 11.7.

HRMS-API (m/z): calcd. for $C_{17}H_{22}NO_3$ [M + H^+] 288.1594, found 288.1595

FTIR (film, cm^{-1}): 3306, 2932, 1754, 1488, 1183 cm^{-1}

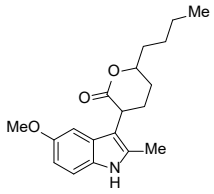

6-38 (two diastereomers)

6-butyl-3-(5-methoxy-2-methyl-1*H*-indol-3-yl)tetrahydro-2*H*-pyran-2-one (6-38) was synthesized according to **general procedure C** and obtained as a yellow oil (1 mmol scale, 175.1 mg, 56% yield, dr = 2.2:1).

^{1}H NMR (400 MHz, $CDCl_3$, data for major diastereomer given) δ 8.25 (s, 1H), 6.96 (dd, *J* = 8.7, 4.7 Hz, 1H), 6.77 (d, *J* = 2.4 Hz, 1H), 6.72 (d, *J* = 2.2 Hz, 1H), 4.61 – 4.46 (m, 1H), 3.82 (s, 3H), 3.76 (s, 1H), 2.16 – 2.00 (m, 3H), 1.94 (s, 3H), 1.87 – 1.62 (m, 3H), 1.56 (ddt, *J* = 12.1, 7.2, 3.8 Hz, 1H), 1.50 – 1.34 (m, 3H), 0.96 (t, *J* = 7.2, 1.9 Hz, 3H).

^{13}C NMR (101 MHz, $CDCl_3$) major δ = 173.2, 153.6, 133.4, 130.7, 126.8, 111.5, 109.8, 109.2, 100.6, 82.5, 56.0, 38.8, 36.0, 29.2, 28.0, 27.0, 22.5, 13.9, 11.3; minor δ = 174.2, 153.6, 133.2, 130.6, 127.3, 111.5, 110.2, 108.1, 100.6, 79.3, 55.9, 36.4, 35.2, 27.3, 27.0, 25.2, 22.5, 13.9, 11.6.

HRMS-API (m/z): calcd. for $C_{19}H_{26}NO_3$ [M + H^+] 316.1907, found 316.1905

FTIR (film, cm^{-1}): 3346, 2952, 2934, 2870, 1715, 1485, 1217, 1178, 1098, 1033, 954, 797 cm^{-1}

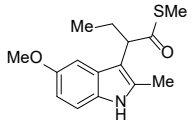

6-39

S-methyl 2-(5-methoxy-2-methyl-1*H*-indol-3-yl)butanethioate (**6-39**) was synthesized according to **general procedure C** and obtained as a light green oil (1 mmol scale, 183.3 mg, 66% yield).

^{1}H NMR (400 MHz, $CDCl_3$) δ 8.01 (s, 1H), 7.17 – 7.09 (m, 2H), 6.80 (dd, *J* = 8.7, 2.4 Hz, 1H), 3.87 (s, 3H), 3.84 (dd, *J* = 9.0, 6.4 Hz, 1H), 2.40 (s, 3H), 2.39 – 2.32 (m, 1H), 2.23 (s, 3H), 2.04 (ddt, *J* = 14.6, 8.9, 7.3 Hz, 1H), 0.91 (t, *J* = 7.4 Hz, 3H).

^{13}C NMR (101 MHz, $CDCl_3$) δ 201.6, 153.9, 134.1, 130.5, 127.9, 111.2, 110.7, 108.2, 101.7, 55.9, 53.3, 23.8, 12.3, 12.2, 11.8.

HRMS-ESI (m/z): calcd for $C_{15}H_{20}NO_2S$ [M + H^+] 278.1209, found 278.1211

FTIR (film, cm^{-1}): 3399, 2929, 1685, 1484, 1453, 1217, 1031, 996, 798 cm^{-1}

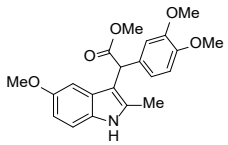

6-40

Methyl 2-(3,4-dimethoxyphenyl)-2-(5-methoxy-2-methyl-1*H*-indol-3-yl)acetate (**6-40**) was synthesized according to **general procedure C** and obtained as a brown solid (1 mmol scale, 213.3 mg, 58% yield).

^{1}H NMR (400 MHz, $CDCl_3$) δ 8.11 (s, 1H), 7.08 (d, *J* = 8.8 Hz, 1H), 6.97 (d, *J* = 2.5 Hz, 1H), 6.88 (d, *J* = 2.0 Hz, 1H), 6.83 (dd, *J* = 8.3, 2.0 Hz, 1H), 6.81 – 6.72 (m, 2H), 5.20 (s, 1H), 3.83 (s, 3H), 3.77 (d, *J* = 8.5 Hz, 6H), 3.72 (d, *J* = 2.5 Hz, 3H), 2.27 (s, 3H).

^{13}C NMR (101 MHz, $CDCl_3$) δ 173.9, 153.9, 148.7, 147.9, 133.8, 131.1, 130.3, 128.1, 120.5, 111.9, 111.1, 111.0, 110.8, 108.1, 101.5, 55.8, 54.4, 52.4, 52.1, 47.6, 12.1.

HRMS-API (m/z): calcd. for $C_{21}H_{22}NO_5$ [M - H^+] 368.1492, found 368.1502

FTIR (film, cm^{-1}): 3380, 2935, 1730, 1515, 1250, 1199, 1174, 1136, 1024 cm^{-1}

M.p.: 122 – 123 ℃

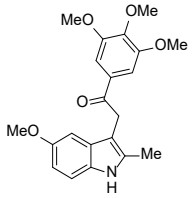

6-41

2-(5-methoxy-2-methyl-1*H*-indol-3-yl)-1-(3,4,5-trimethoxyphenyl)ethan-1-one (**6-41**) was synthesized according to **general procedure C** and obtained as a brown solid (1 mmol scale, 58.4 mg, 16% yield).

^{1}H NMR (400 MHz, $CDCl_3$) δ 7.95 (s, 1H), 7.30 (s, 2H), 7.10 (d, *J* = 8.7 Hz, 1H), 7.00 (d, *J* = 2.4 Hz, 1H), 6.75 (dd, *J* = 8.7, 2.4 Hz, 1H), 4.24 (s, 2H), 3.88 (s, 3H), 3.82 (s, 3H), 3.80 (s, 6H), 2.30 (s, 3H).

^{13}C NMR (101 MHz, $CDCl_3$) δ 196.8, 154.2, 153.0(x 2C), 142.3, 133.8, 131.9, 130.5, 128.9, 111.3, 110.7, 106.1(x 2C), 104.7, 100.5, 60.9, 56.3(x 2C), 56.0, 35.5, 12.1.

HRMS-ESI (m/z): calcd for $C_{21}H_{24}NO_5$ [M + H^+] 370.1648, found 370.1652

FTIR (film, cm^{-1}): 3424, 2940, 1673, 1587, 1483, 1456, 1413, 1332, 1212, 1153, 1127, 1030, 999 cm^{-1}

M.p.: 132 – 133 ℃

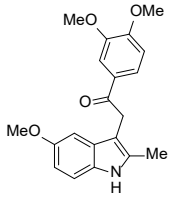

6-42

1-(3,4-dimethoxyphenyl)-2-(5-methoxy-2-methyl-1*H*-indol-3-yl)ethan-1-one (**6-42**) was synthesized according to **general procedure C** and obtained as a brown solid (1 mmol scale, 54.4 mg, 16% yield).

^{1}H NMR (400 MHz, $CDCl_3$) δ 7.92 (s, 1H), 7.73 (dt, *J* = 8.4, 1.6 Hz, 1H), 7.56 (t, *J* = 1.6 Hz, 1H), 7.08 (d, *J* = 8.7 Hz, 1H), 6.97 (d, *J* = 2.4 Hz, 1H), 6.85 (dd, *J* = 8.4, 1.2 Hz, 1H), 6.74 (dt, *J* = 8.7, 1.8 Hz, 1H), 4.24 (s, 2H), 3.91 (s, 3H), 3.83 (dd, *J* = 6.7, 1.2 Hz, 6H), 2.30 (s, 3H).

^{13}C NMR (101 MHz, $CDCl_3$) δ 196.7, 154.2, 153.2, 149.0, 133.6, 130.5, 130.1, 129.1, 123.1, 111.2, 110.8, 110.8, 110.1, 105.0, 100.6, 56.1, 56.0, 56.0, 35.0, 12.2.

HRMS-ESI (m/z): calcd for $C_{20}H_{22}NO_4$ [M + H^+] 340.1543, found 340.1546

FTIR (film, cm^{-1}): 3360, 1680, 1595, 1587, 1513, 1487, 1419, 1262, 1152, 1019 cm^{-1}

M.p.: 152- 153 ℃

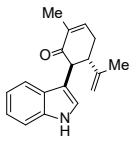

6-43

(5R,6R)-6-(1H-indol-3-yl)-2-methyl-5-(prop-1-en-2-yl)cyclohex-2-en-1-one (**6-43**) (Baran et al., 2004) was synthesized according to **general procedure C** and obtained as a white solid (1 mmol scale, 78.7 mg, 30% yield).

^{1}H NMR (400 MHz, $CDCl_3$) δ 8.30 (s, 1H), 7.46 (d, *J* = 7.8 Hz, 1H), 7.19 (d, *J* = 7.9 Hz, 1H), 7.14 (t, *J* = 7.4 Hz, 1H), 7.08 (t, *J* = 7.3 Hz, 1H), 6.84 (s, 1H), 6.52 (d, *J* = 2.0 Hz, 1H), 4.65 (d, *J* = 15.7 Hz, 2H), 3.92 (d, *J* = 10.8 Hz, 1H), 3.27 (td, *J* = 9.7, 5.1 Hz, 1H), 2.64 – 2.41 (m, 2H), 1.93 (s, 3H), 1.62 (s, 3H).

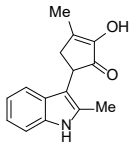

6-48

2-hydroxy-5-methyl-3-(2-methyl-1H-indol-3-yl)cyclopent-2-en-1-one (6-48) was synthesized according to **general procedure C** and obtained as a light brown solid (1 mmol scale, 21.0 mg, 9% yield).

^{1}H NMR (400 MHz, DMSO-d_6) δ 10.80 (s, 1H), 8.98 (s, 1H), 7.23 (dd, *J* = 7.7, 1.4 Hz, 1H), 7.02 – 6.92 (m, 2H), 6.86 – 6.80 (m, 1H), 3.74 (dd, *J* = 7.0, 2.4 Hz, 1H), 2.94 – 2.79 (m, 1H), 2.46 (d, *J* = 17.7 Hz, 1H), 2.29 (s, 3H), 1.99 (s, 3H).

^{13}C NMR (101 MHz, DMSO-d_6) δ 203.2, 149.2, 142.5, 135.2, 132.8, 126.8, 120.0, 118.2, 117.2, 110.6, 108.7, 40.0, 35.8, 14.2, 11.4.

HRMS-API (m/z): calcd. for $C_{15}H_{16}NO_2$ [M + H^+] 242.1175, found 242.1177

FTIR (film, cm^{-1}): 3423, 3360, 1693, 1642, 1462, 1402, 1203, 1096, 745 cm^{-1}

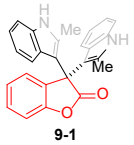

9-1

3,3-bis(2-methyl-1*H*-indol-3-yl)benzofuran-2(3*H*)-one (**9-1**) was synthesized according to **general procedure C** and obtained as a yellow solid (1 mmol scale, 87.8 mg, 23% yield).

^{1}H NMR (400 MHz, DMSO-d_6) δ 11.08 (d, *J* = 12.0 Hz, 2H), 7.46 – 7.35 (m, 2H), 7.28 (t, *J* = 7.5 Hz, 3H), 7.15 (td, *J* = 7.2, 1.5 Hz, 1H), 6.97 – 6.90 (m, 2H), 6.75 – 6.64 (m, 3H), 6.53 (d, *J* = 8.1 Hz, 1H), 2.01 (s, 3H), 1.94 (s, 3H).

^{13}C NMR (101 MHz, DMSO-d_6) δ 176.8, 151.8, 135.0, 135.0, 134.0, 132.8, 132.8, 129.2, 126.8, 126.6, 126.1, 124.4, 120.3, 120.3, 118.8, 118.7, 118.6, 118.5, 110.9, 110.8 (x 2C), 108.6, 107.7, 50.5, 13.0, 12.9.

HRMS-ESI (m/z): calcd for $C_{26}H_{20}N_2O_2Na$ [M + Na^+] 415.1416, found 415.1420

FTIR (film, cm^{-1}): 3245, 3222, 2921, 1801, 1460, 1050, 1008, 755, 739 cm^{-1}

M.p.: 128 – 130 ℃

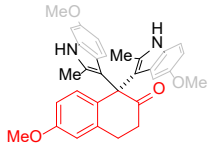

9-2

6-methoxy-1-(5-methoxy-2-methyl-1*H*-indol-3-yl)-1-(6-methoxy-2-methyl-1*H*-indol-3-yl)-3,4-dihydronaphthalen-2(1*H*)-one (**9-2**) was synthesized according to **general procedure C** and obtained as a light brown solid (1 mmol scale, 141.4 mg, 29% yield).

^{1}H NMR (400 MHz, DMSO-d_6) δ 10.92 (s, 1H), 10.89 (s, 1H), 7.24 (d, *J* = 8.3 Hz, 1H), 7.16 (dd, *J* = 10.5, 8.7 Hz, 2H), 6.88 (dd, *J* = 8.3, 2.7 Hz, 1H), 6.55 (ddd, *J* = 18.7, 8.7, 2.4 Hz, 2H), 6.35 (d, *J* = 2.7 Hz, 1H), 5.44 (d, 1H), 5.31 (d, 1H), 3.53 (s, 3H), 3.33 (s, 3H), 3.22 (s, 3H), 2.79 (t, *J* = 6.7 Hz, 2H), 2.73 – 2.53 (m, 2H), 1.80 (s, 3H), 1.71 (s, 3H).

^{13}C NMR (101 MHz, DMSO-d_6) δ 202.7, 158.0, 152.4, 152.4, 142.1, 136.1, 135.3, 130.6, 130.2, 130.2, 129.2, 128.9, 128.6, 116.5, 111.3, 110.8, 110.7, 109.3, 108.9, 107.9, 106.5, 102.0, 101.5, 58.6, 54.9, 54.7, 54.4, 36.2, 26.8, 13.9, 13.2.

HRMS-API (m/z): calcd. for $C_{21}H_{22}NO_5$ [M - H^+] 493.2121, found 493.2130

FTIR (film, cm^{-1}): 3402, 2926, 1707, 1579, 1485, 1445, 1212, 1026, 796 cm^{-1}

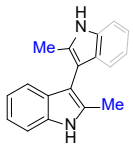

7-1

2,2'-dimethyl-1*H*,1'*H*-3,3'-biindole (7-1) (Greci et al., 2003) was synthesized according to **general procedure C** without adding carbonyl substrates and obtained as a light brown solid (2 mmol scale, 32.8 mg, 13% yield).

^{1}H NMR (400 MHz, DMSO-d_6) δ 11.01 (s, 2H), 7.33 (d, *J* = 8.0 Hz, 2H), 7.12 (d, *J* = 7.8 Hz, 2H), 7.02 (t, *J* = 7.5 Hz, 2H), 6.90 (t, *J* = 7.4 Hz, 2H), 2.27 (s, 6H).

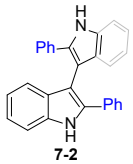

7-2

2,2'-diphenyl-1*H*,1'*H*-3,3'-biindole (7-2) (Niu et al., 2010) was synthesized according to **general procedure C** was obtained as a light brown solid (2 mmol scale, 217.6 mg, 57% yield).

^{1}H NMR (400 MHz, DMSO-d_6) δ 11.63 (s, 2H), 7.61 (d, *J* = 7.6 Hz, 4H), 7.54 (d, *J* = 8.1 Hz, 2H), 7.21 (t, *J* = 7.6 Hz, 4H), 7.15-7.10 (m, 4H), 7.02 (d, *J* = 7.9 Hz, 2H), 6.87 (t, *J* = 7.4 Hz, 2H).

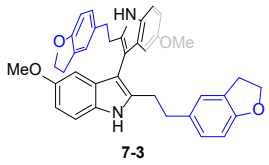

7-3

2,2'-bis(2-(2,3-dihydrobenzofuran-5-yl)ethyl)-5,5'-dimethoxy-1*H*,1'*H*-3,3'-biindole (**7-3**) was synthesized according to **general procedure C** and obtained as a brown solid (0.18 mmol scale, 22.2 mg, 41% yield).

^{1}H NMR (400 MHz, $CDCl_3$) δ 7.82 (s, 2H), 7.21 (d, *J* = 8.7 Hz, 2H), 6.89 (s, 2H), 6.82 (d, *J* = 8.3 Hz, 4H), 6.77 (s, 2H), 6.65 (d, *J* = 8.1 Hz, 2H), 4.52 (t, *J* = 8.7 Hz, 4H), 3.72 (s, 6H), 3.08 (t, *J* = 8.4 Hz, 4H), 2.93 (d, *J* = 7.3 Hz, 4H), 2.83 (d, *J* = 7.3 Hz, 4H).

^{13}C NMR (101 MHz, $CDCl_3$) δ 158.6(x 2C), 154.2(x 2C), 137.8(x 2C), 133.2(x 2C), 130.6(x 2C), 130.0(x 2C), 127.9(x 2C), 127.3(x 2C), 125.0(x 2C), 111.3(x 2C), 111.1(x 2C), 109.1(x 2C), 106.5(x 2C), 101.6(x

2C), 71.3(x 2C), 56.0(x 2C), 35.2(x 2C), 29.8(x 2C), 29.1(x 2C).

HRMS-API (m/z): calcd. for $C_{38}H_{35}N_2O_4$ [M - H^+] 583.2591, found 583.2595

FTIR (film, cm^{-1}): 3400, 2927, 1488, 1449, 1216, 981, 800 cm^{-1}

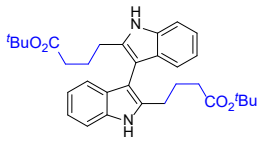

7-4

di-*tert*-butyl 4,4'-(1*H*,1'*H*-[3,3'-biindole]-2,2'-diyl)dibutyrate (7-4) was synthesized according to **general procedure C** and obtained as yellow oil (0.5 mmol scale, 24.0 mg, 19% yield) by utilizing LiHMDS (1.25 mmol, 2.5 equivalent) and $FeCl_3$ (201 mg, 1.25 mmol, 2.5 equivalent).

^{1}H NMR (400 MHz, $CDCl_3$) δ 8.51 (s, 2H), 7.39 (dt, *J* = 8.0, 0.9 Hz, 2H), 7.31 – 7.27 (m, 2H), 7.17 (ddd, *J* = 8.1, 7.0, 1.2 Hz, 2H), 7.04 (ddd, *J* = 8.0, 7.1, 1.0 Hz, 2H), 2.72 (t, *J* = 7.4 Hz, 4H), 2.19 (t, *J* = 7.2 Hz, 4H), 1.88 (p, *J* = 7.3 Hz, 4H), 1.40 (s, 18H).

^{13}C NMR (101 MHz, $CDCl_3$) δ 173.3(x 2C), 136.6(x 2C), 135.7(x 2C), 129.6(x 2C), 121.2(x 2C), 119.6(x 2C), 119.4(x 2C), 110.5(x 2C), 106.5(x 2C), 80.6(x 2C), 34.8(x 2C), 28.1(x 6C), 25.8(x 2C), 25.1(x 2C).

HRMS-API (m/z): calcd. for $C_{32}H_{41}N_2O_4^+$ [M + H^+] 517.3061, found 517.3059

FTIR (film, cm^{-1}): 3394, 2975, 2931, 1724, 1704, 1153, 741 cm^{-1}

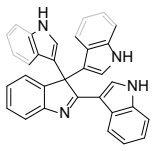

10-1

3'-(1*H*-indol-3-yl)-1*H*, 1"*H*, 3'*H*-3, 2': 3', 3"-terindole (**10-1**) (Richter et al., 2007) was isolated as a light brown solid (2 mmol scale, 81.2 mg, 35% yield).

^{1}H NMR (400 MHz, DMSO-d_6) δ 11.46 (d, *J* = 3.0 Hz, 1H), 11.06 (d, *J* = 2.6 Hz, 2H), 8.98 – 8.76 (m, 1H), 7.80 (d, *J* = 7.6 Hz, 1H), 7.67 (d, *J* = 3.0 Hz, 1H), 7.58 (d, *J* = 7.4 Hz, 1H), 7.43 (dd, *J* = 10.9, 7.9 Hz, 3H), 7.38 – 7.21 (m, 5H), 7.13 – 6.98 (m, 5H), 6.84 (t, *J* = 7.5 Hz, 2H).

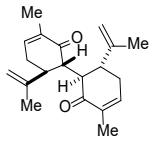

8-1

(1R,1'*S*,6*S*,6'*R*)-3,3'-dimethyl-6,6'-di(prop-1-en-2-yl)-[1,1'-bi(cyclohexane)]-3,3'-diene-2,2'-dione (**8-1**) (Bailey et al., 2018) was isolated as byproduct during the condition optimization, yield not determined.

^{1}H NMR (400 MHz, $CDCl_3$) δ 6.64 – 6.59 (m, 2H), 4.79 (dt, *J* = 19.7, 2.2 Hz, 4H), 3.43 (td, *J* = 12.2, 4.2 Hz, 2H), 2.46 (dd, *J* = 12.6, 3.0 Hz, 2H), 2.38 – 2.14 (m, 4H), 1.69 (d, *J* = 2.8 Hz, 6H), 1.59 (d, *J* = 3.1 Hz, 6H).

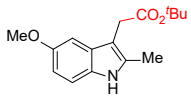

6-46

***tert*-butyl 2-(5-methoxy-2-methyl-1*H*-indol-3-yl)acetate (6-46)** was obtained as a light brown solid (0.5 mmol scale, 84.3 mg, 61% yield) according to **general procedure C**.

^{1}H NMR (400 MHz, $CDCl_3$) δ 7.85 (s, 1H), 7.08 (d, *J* = 8.7 Hz, 1H), 7.01 (d, *J* = 2.5 Hz, 1H), 6.76 (dd, *J* = 8.7, 2.4 Hz, 1H), 3.86 (s, 3H), 3.56 (s, 2H), 2.32 (s, 3H), 1.44 (s, 9H).

^{13}C NMR (101 MHz, $CDCl_3$) δ 171.7, 154.0, 133.6, 130.4, 129.1, 111.0, 110.9, 105.1, 100.6, 80.6, 56.0, 32.0, 28.2(x 3C), 11.8.

HRMS-API (m/z): calcd. for $C_{16}H_{22}NO_3$ [M + H$^+$] 276.1594, found 276.1595

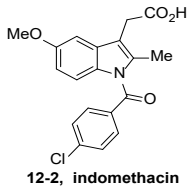

12-2, indomethacin

2-(1-(4-chlorobenzoyl)-5-methoxy-2-methyl-1*H*-indol-3-yl)acetic acid (**12-2, Indomethacin**) (Kasaya et al., 2009) was synthesized according to **general procedure D** and obtained as a white solid (0.052 mmol scale, 18.4 mg, 99% yield).

^{1}H NMR (400 MHz, $CDCl_3$) δ 7.70 – 7.61 (m, 2H), 7.47 (d, *J* = 8.4 Hz, 2H), 6.95 (d, *J* = 2.5 Hz, 1H), 6.85 (d, *J* = 9.0 Hz, 1H), 6.67 (dd, *J* = 9.0, 2.5 Hz, 1H), 3.83 (s, 3H), 3.69 (s, 2H), 2.39 (s, 3H).

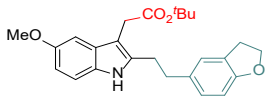

6-47

tert-butyl 2-(2-(2-(2,3-dihydrobenzofuran-5-yl)ethyl)-5-methoxy-1*H*-indol-3-yl)acetate (6-47) was synthesized according to **general procedure D** and obtained as a yellow solid (0.5 mmol scale, 102.2 mg, 50% yield)

^{1}H NMR (400 MHz, $CDCl_3$) δ 7.76 (s, 1H), 7.12 – 7.03 (m, 2H), 6.97 (d, *J* = 1.8 Hz, 1H), 6.88 (dd, *J* = 8.1, 1.9 Hz, 1H), 6.77 (dd, *J* = 8.7, 2.5 Hz, 1H), 6.71 (d, *J* = 8.1 Hz, 1H), 4.56 (t, *J* = 8.7 Hz, 2H), 3.87 (s, 3H), 3.54 (s, 2H), 3.15 (t, *J* = 8.6 Hz, 2H), 2.97 (t, *J* = 7.1 Hz, 2H), 2.87 (t, *J* = 7.4 Hz, 2H), 1.45 (s, 9H).

^{13}C NMR (101 MHz, $CDCl_3$) δ 171.6, 158.6, 154.0, 137.3, 133.3, 130.3, 128.9, 127.9, 127.2, 125.1, 111.1, 109.1, 105.0, 100.7, 80.6, 71.3, 55.9, 35.6, 32.0, 29.8, 28.9, 28.2, 28.2 (x 3C).

HRMS-API (m/z): calcd. for $C_{25}H_{30}NO_4$ [M + H^+] 408.2169, found 408.2169

FTIR (film, cm^{-1}): 3379, 2965, 1718, 1485, 1215, 1150, 829 cm^{-1}

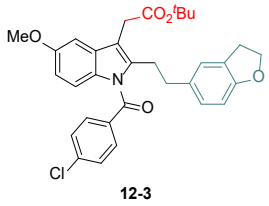

12-3

tert-butyl 2-(1-(4-chlorobenzoyl)-2-(2-(2,3-dihydrobenzofuran-5-yl)ethyl)-5-methoxy-1*H*-indol-3-yl)acetate (12-3) was synthesized according to **general procedure D** and obtained as a yellow oil (0.158 mmol scale, 69.9 mg, 81% yield)

^{1}H NMR (400 MHz, $CDCl_3$) δ 7.63 – 7.54 (m, 2H), 7.51 – 7.41 (m, 2H), 7.00 (dd, *J* = 4.5, 2.1 Hz, 2H), 6.86 (dd, *J* = 8.0, 1.9 Hz, 1H), 6.67 – 6.58 (m, 2H), 6.55 (d, *J* = 9.0 Hz, 1H), 4.48 (t, *J* = 8.7 Hz, 2H), 3.83 (s, 3H), 3.54 (s, 2H), 3.23 (dd, *J* = 9.4, 6.3 Hz, 2H), 3.06 (t, *J* = 8.7 Hz, 2H), 2.84 (dd, *J* = 9.1, 6.5 Hz, 2H), 1.47 (s, 9H).

^{13}C NMR (101 MHz, $CDCl_3$) δ 170.3, 168.4, 158.5, 155.9, 140.0, 139.5, 133.7, 133.1, 131.4 (x 2C), 131.0, 130.7, 129.1 (x 2C), 128.1, 127.2, 125.1, 114.9, 113.6, 111.8, 109.0, 101.6, 81.2, 71.2, 55.7, 35.9, 31.8, 29.8, 28.6, 28.2 (x 3C).

HRMS-ESI (m/z): calcd. for $C_{32}H_{33}ClNO_5$ [M + H^+] 546.2041, found 546.2033

FTIR (film, cm^{-1}): 2975, 2930, 1730, 1683, 1590, 1491, 1478 cm^{-1}

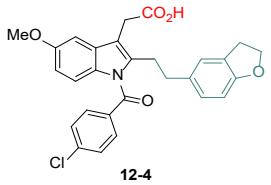

12-4

2-(1-(4-chlorobenzoyl)-2-(2-(2,3-dihydrobenzofuran-5-yl)ethyl)-5-methoxy-1*H*-indol-3-yl)acetic acid (12-4) was synthesized according to **general procedure D** and obtained as a white solid (0.037 mmol scale, 17.5 mg, 96% yield)

^{1}H NMR (400 MHz, $CDCl_3$) δ 7.60 (d, *J* = 8.2 Hz, 2H), 7.45 (d, *J* = 8.2 Hz, 2H), 6.95 (d, *J* = 3.0 Hz, 2H), 6.80 (d, *J* = 8.0 Hz, 1H), 6.61 (td, *J* = 6.9, 3.1 Hz, 2H), 6.53 (d, *J* = 9.0 Hz, 1H), 4.47 (t, *J* = 8.6 Hz, 2H), 3.80 (s, 3H), 3.61 (s, 2H), 3.23 (t, *J* = 7.7 Hz, 2H), 3.04 (t, *J* = 8.6 Hz, 2H), 2.81 (t, *J* = 7.7 Hz, 2H).

^{13}C NMR (101 MHz, $CDCl_3$) δ 176.7, 168.5, 158.6, 156.0, 140.4, 139.7, 133.6, 132.9, 131.5(x 2C), 131.0, 130.4, 129.2(x 2C), 128.1, 127.3, 125.1, 115.0, 112.3, 111.9, 109.1, 101.6, 71.2, 55.8, 35.7, 30.1, 29.8, 28.7.

HRMS-API (m/z): calcd. for $C_{32}H_{33}ClNO_5$ [M + H^+] 546.2041, found 546.2033

FTIR (film, cm^{-1}): 3079, 2946, 1698, 1679, 1491, 1476, 1218 cm^{-1}

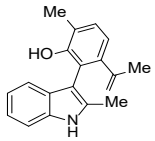

13-1

6-methyl-2-(2-methyl-1H-indol-3-yl)-3-(prop-1-en-2-yl)phenol (**13-1**) was obtained as sticky oil (0.1 mmol scale, 14.7 mg, 54% yield, 63% brsm, 3% ee) according to Table **ST1**. The enatioselectivitity was determined by Chiral HPLC analysis on CHIRALPAK® AD-H column, temperature 35℃, flow n-Hexaen/^{i}PrOH=90:10(v/v), 1mL/1min, detected by UV254 nm, t_{R1} = 5.45 min, t_{R2} = 15.7 min.

^{1}H NMR (400 MHz, $CDCl_3$) δ 8.16 (s, 1H), 7.34 (d, *J* = 8.0 Hz, 1H), 7.28 – 7.22 (m, 1H), 7.20 – 7.11 (m, 2H), 7.07 (t, *J* = 7.4 Hz, 1H), 6.84 (d, *J* = 7.7 Hz, 1H), 5.28 (s, 1H), 4.82 (d, *J* = 1.4 Hz, 2H), 2.30 (s, 3H), 2.23 (s, 3H), 1.53 (s, 3H).

^{13}C NMR (101 MHz, $CDCl_3$) δ 152.7, 146.6, 144.2, 135.7, 134.6, 130.2, 128.4, 122.6, 122.0, 120.3, 119.9,

119.4, 117.2, 114.3, 110.5, 106.6, 23.1, 16.3, 12.6.

HRMS-API (m/z): calcd. for $C_{19}H_{18}NO$ [M - H^+] 276.1382, found 276.1393

FTIR (film, cm^{-1}): 3468, 3399, 2918, 1458, 1307, 1249, 1222, 1196, 1070, 1013, 894, 818, 744 cm^{-1}

Reference

Bailey, S. J., Sapkota, R. R., Golliher, A. E., Dungan, B., Talipov, M., Holguin, F. O. and Maio, W. A. (2018). Lewis-Acid-Mediated Union of Epoxy-Carvone Diastereomers with Anisole Derivatives: Mechanistic Insight and Application to the Synthesis of Non-natural CBD Analogues. Org. Lett. *20*, 4618-4621.

Baran, P. S. and Richter, J. M. (2004). Direct Coupling of Indoles with Carbonyl Compounds: Short, Enantioselective, Gram-Scale Synthetic Entry into the Hapalindole and Fischerindole Alkaloid Families. J. Am. Chem. Soc. *126*, 7450- (2004).

Chen, J., Li, C.-M., Wang, J., Ahn, S., Wang, Z., Lu, Y., Dalton, J. T., Miller, D. D. and Li, W. (2011). Synthesis and antiproliferative activity of novel 2-aryl-4-benzoyl-imidazole derivatives targeting tubulin polymerization. Biorg. Med. Chem. *19*, 4782-4795.

Greci, L., Castagna, R., Carloni, P., Stipa, P., Rizzoli, C., Righi, L. and Sgarabotto, P. (2003). Nitrenium ions. Reactions of N,N-dimethyl-p-benzoyloxyaniline-iminium chloride with indoles and indolizines. X-ray structure of unexpected [2-chloro-4-(4-dimethylaminophenyl-ONN-azoxy)phenyl]dimethylamine (azoxy derivative). Org. Biomol. Chem. *1*, 3768-3771

Kasaya, Y., Hoshi, K., Terada, Y., Nishida, A., Shuto, S. and Arisawa, M. (2009). Aromatic Enamide/Ene Metathesis toward Substituted Indoles and Its Application to the Synthesis of Indomethacins. Eur. J. Org. Chem. 4606-4613.

Maksymenko, S., Parida, K. N., Pathe, G. K., More, A. A., Lipisa, Y. B. and Szpilman, A. M. (2017). Transition-Metal-Free Intermolecular α-Arylation of Ketones via Enolonium Species. Org. Lett. *19*, 6312-6315.

Miyata, O.; Takeda, N. and Naito, T. (2002) Synthesis of 2, 4-disubstituted indoles via thermal cyclization of N-trifluoroacetyl enehydrazines. Heterocycles. *57*, 1101-1107.

Molander, G. A. Canturk, B. and Kennedy, L. E. (2009). Scope of the Suzuki−Miyaura Cross-Coupling Reactions of Potassium Heteroaryltrifluoroborates. J. Org. Chem. *74*, 973-980.

Niu, T. and Zhang, Y. (2010). Iron-catalyzed oxidative homo-coupling of indoles via C–H cleavage. Tetrahedron Lett. *51*, 6847-6851.

Richter, J. M. W., B. W., Maimone, T. J., Lin, D. W., Castroviejo, M. P. and Baran, P. S (2007). Scope and mechanism of direct indole and pyrrole couplings adjacent to carbonyl compounds: total synthesis of acremoauxin A and oxazinin 3. J. Am. Chem. Soc. *129*, 12857-12869.

Stempel, E.; Kaml, R. F.-X.; Budisa, N. and Kalesse, M. (2018) Painting argyrins blue: Negishi cross-coupling for synthesis of deep-blue tryptophan analogue β-(1-azulenyl)-l alanine and its incorporation into argyrin C. Biorg. Med. Chem. *26*, 5259-5269.

Trabbic, C. J., George, S. M., Alexander, E. M., Du, S.; Offenbacher, J. M., Crissman, E. J., Overmeyer, J. H & Maltese, W. A and Erhardt, P. W. (2016). Synthesis and biological evaluation of isomeric methoxy substitutions on anti-cancer indolyl-pyridinyl-propenones: Effects on potency and mode of activity. Eur. J. Med. Chem.*122*, 79-91.

Yamagishi, M., Nishigai, K., Ishii, A., Hata, T. and Urabe, H. (2012). Facile Preparation of Indoles and 1,2-Benzothiazine 1,1-Dioxides: Nucleophilic Addition of Sulfonamides to Bromoacetylenes and Subsequent Palladium-Catalyzed Cyclization. Angew. Chem. Int. Ed. *51*, 6471-6474.

Yang, S.-D., Sun, C.-L., Fang, Z., Li, B.-J., Li, Y.-Z. and Shi, Z.-J. (2008). Palladium-Catalyzed Direct Arylation of (Hetero)Arenes with Aryl Boronic Acids. Angew. Chem. Int. Ed. *47*, 1473-1476.

Wetzel, A., Pratsch, G., Kolb, R. and Heinrich, M. R. (2016). Radical Arylation of Phenols, Phenyl Ethers, and Furans. Chem. Eur. J. *16*, 2547-2556.

Zuo, Z., Xie, W. and Ma, D. (2010) Total Synthesis and Absolute Stereochemical Assignment of (−)-Communesin F. J. Am. Chem. Soc*. 132*, 13226-13228.

III. Spectrum

2018-1.3250.fid
LHL-1-53-1

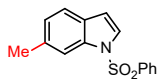

14-1

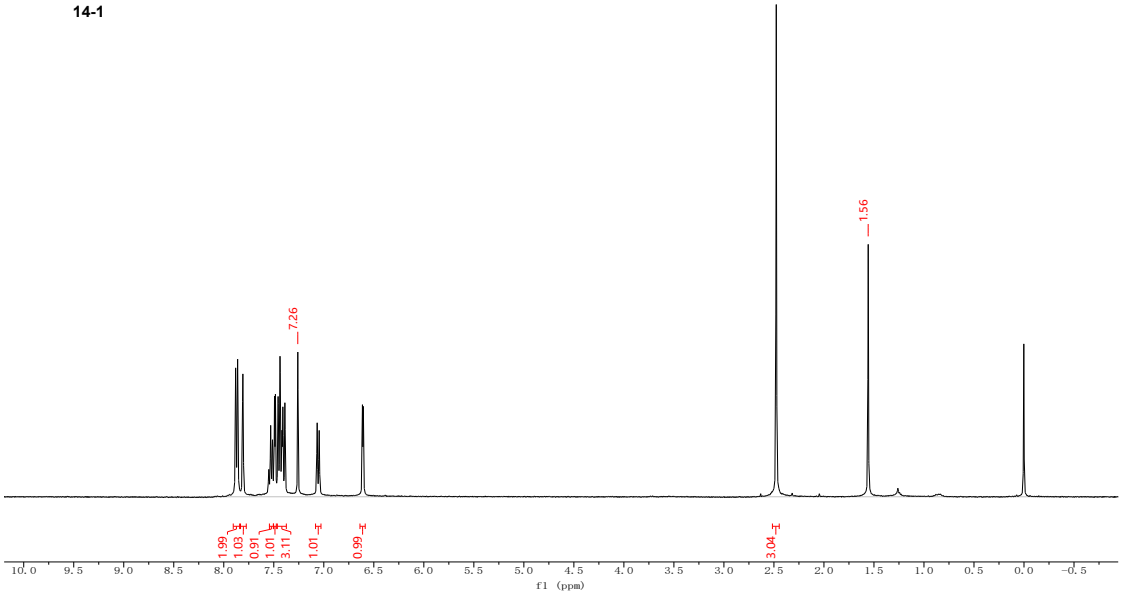

2018-1.3417.fid
LHL1-54-1

14-2

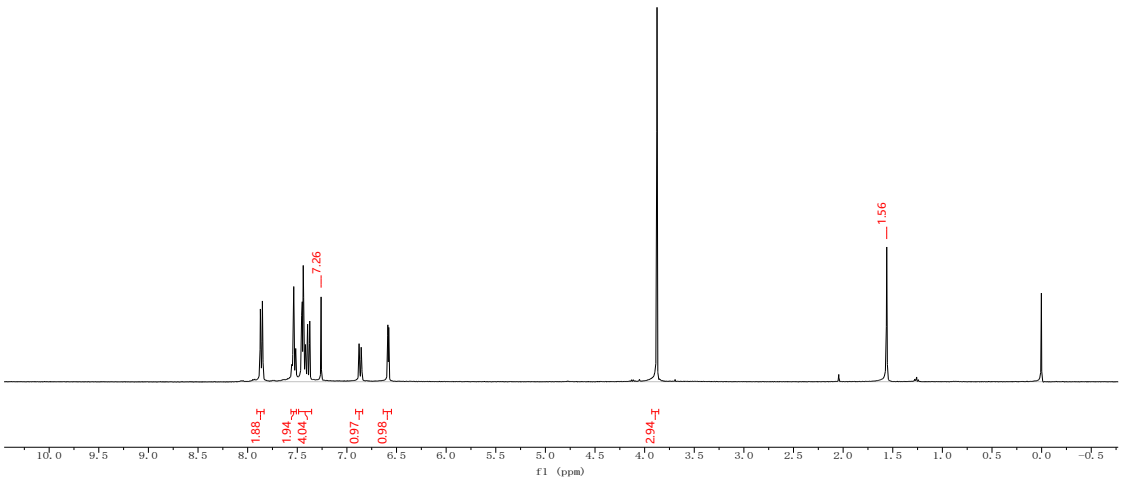

2018-1.3249.fid
LHL-1-52-2

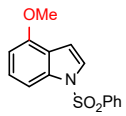

14-3

2018-2.7772.fid
LHL2-31-1

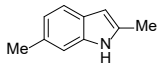

1-7

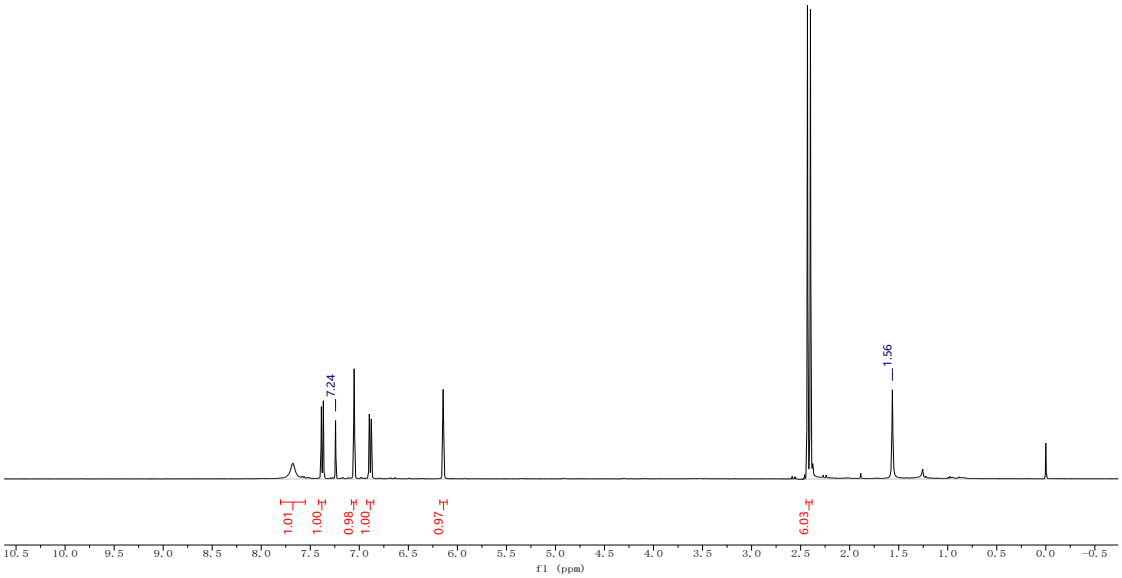

2018-2.7770.fid
LHL2-31-2

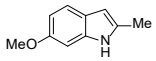

1-8

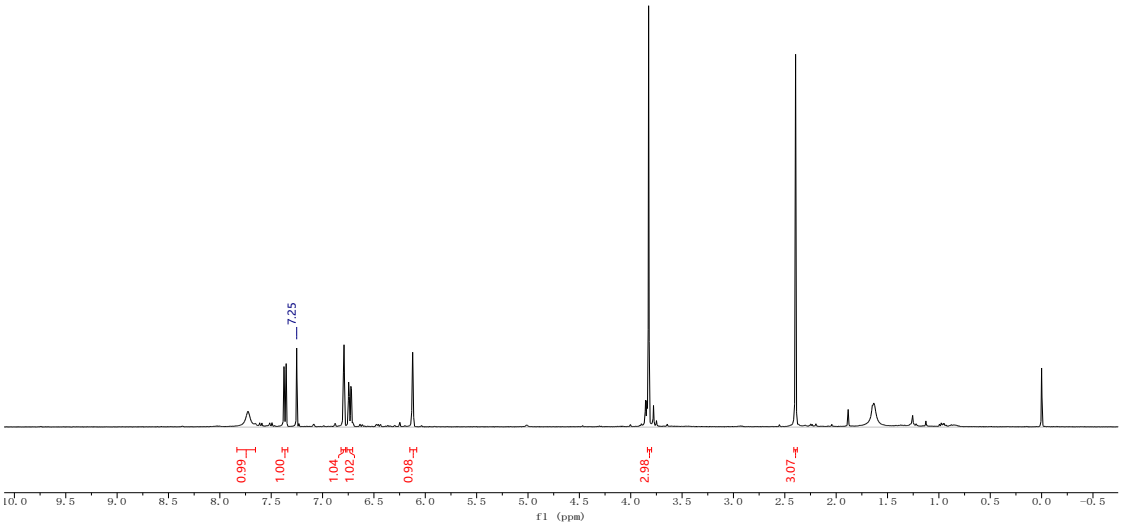

2018-2.9375.fid
LHL-2-38-1

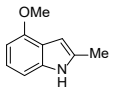

1-9

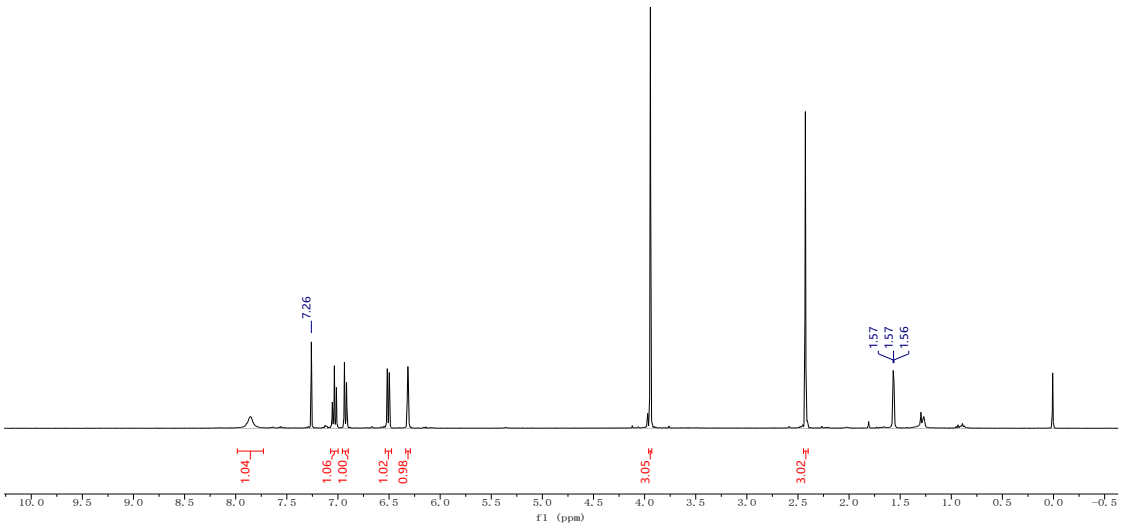

2018-2.11985.fid
LHL-2-43-1

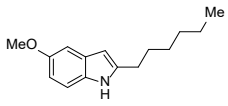

1-13

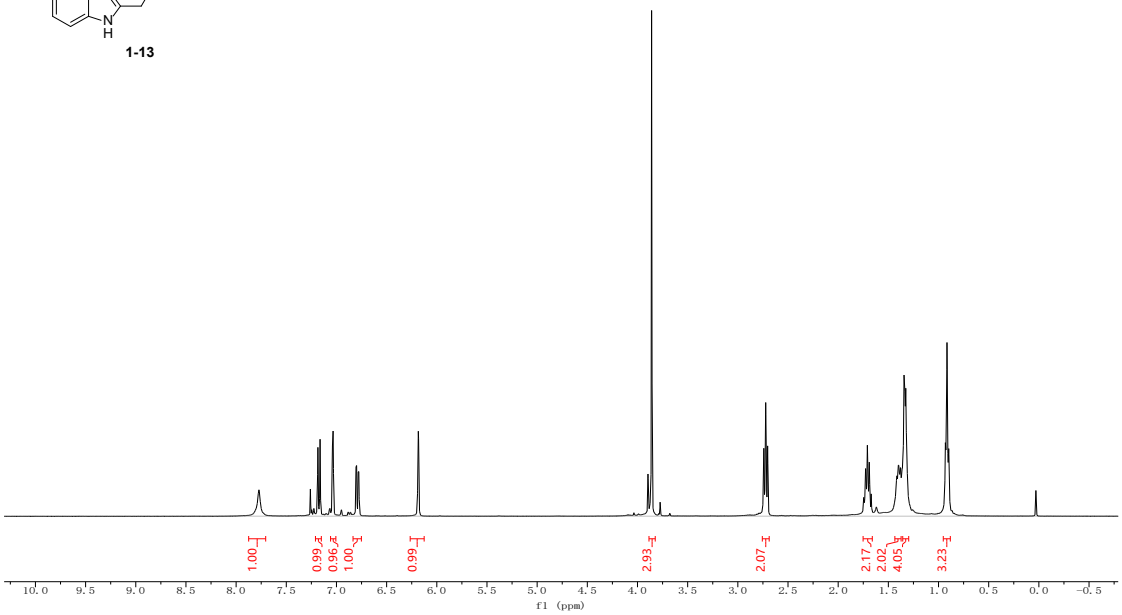

2018-2.11634.fid
LHL-2-60-2

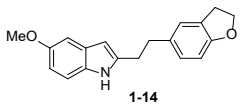

1-14

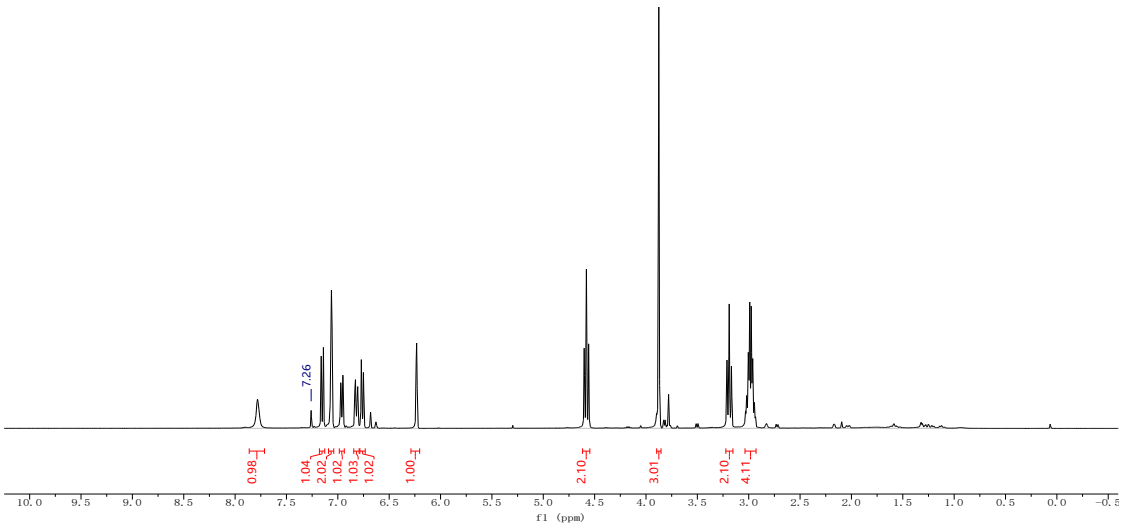

2018-2.12022.fid
LHL-2-60-2

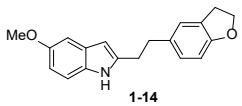

1-14

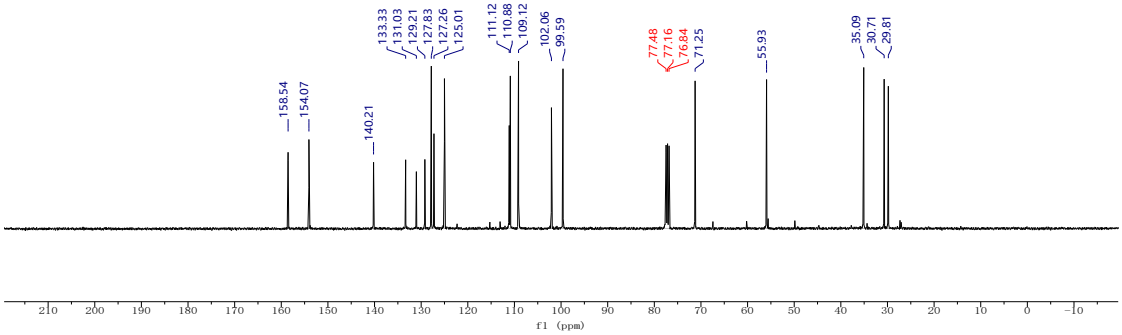

2018-2.7768.fid
LHL1-51-2

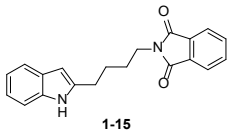

1-15

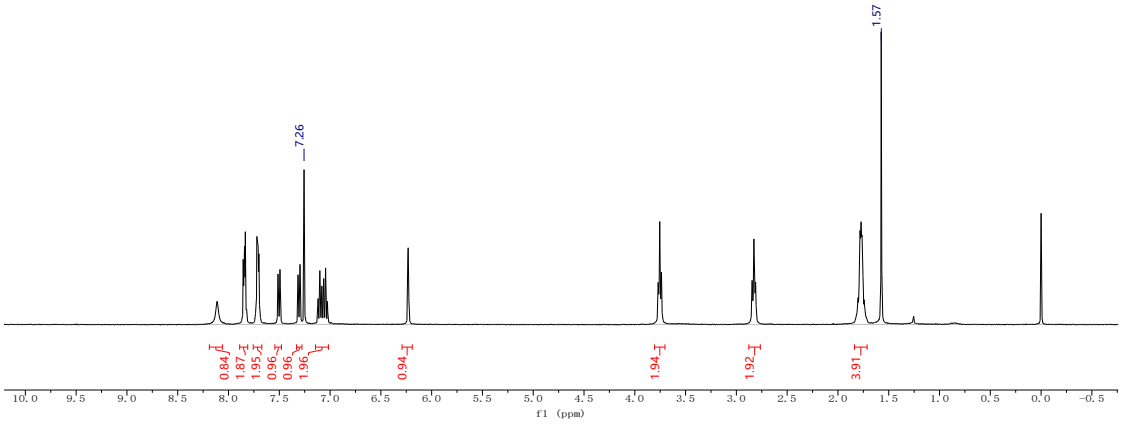

2018-2.8623.fid
LHL-1-51-2

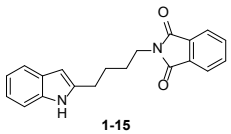

1-15

2018-1.3036.fid
LHL1-49-1.2

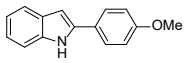

1-17

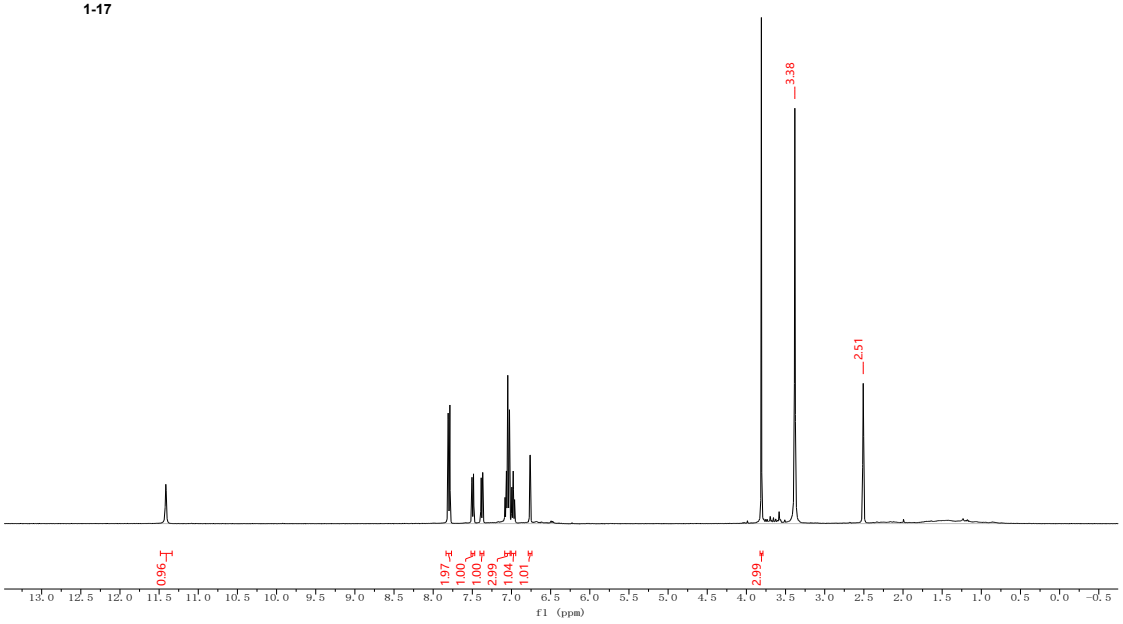

2019-1.1324.fid
LHL-3-12-1.2

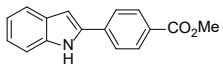

1-18

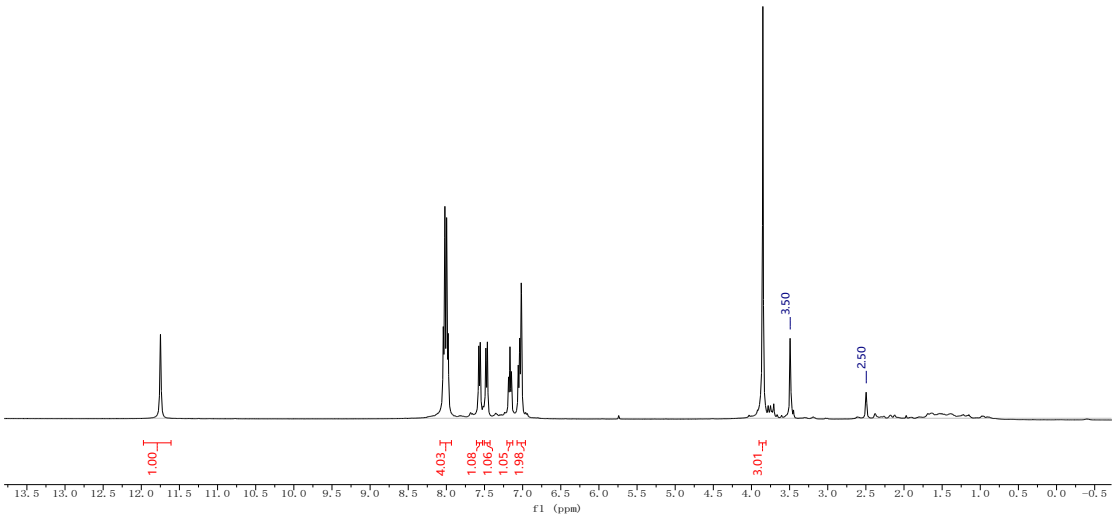

2018-1.2630.fid
LHL1-48-2

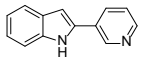

1-19

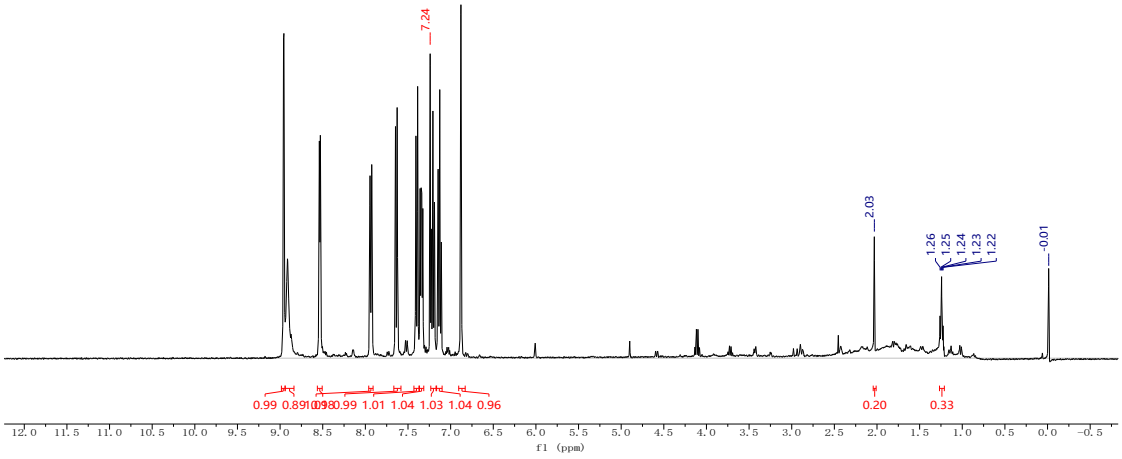

2019-1.15013.fid
LHL 4-29-1

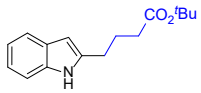

1-20

2019-1.15522.fid
LHL 4-29-1

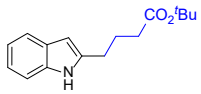

1-20

2018-2.10404.fid
LHL -2-44-1

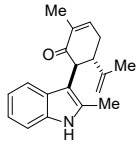

6-1

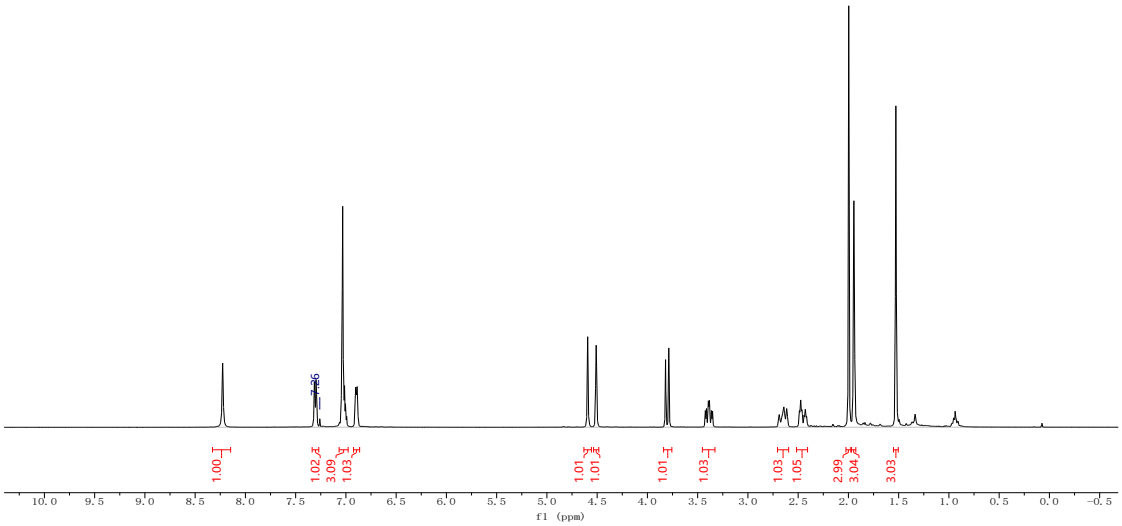

2018-2.10849.fid
LHL-2-44-1

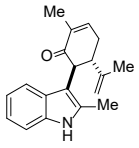

6-1

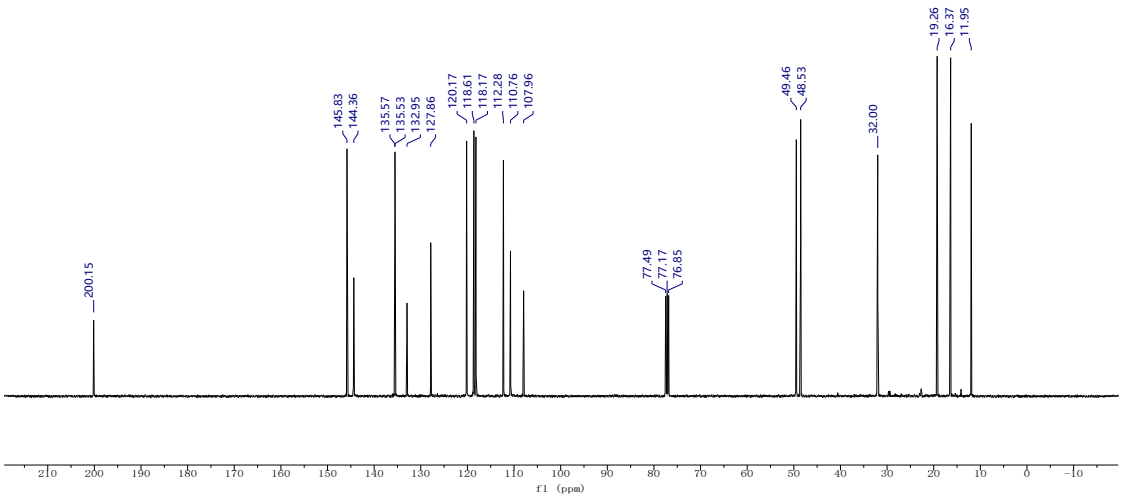

2017-3.17979.fid
LHL1-30-2

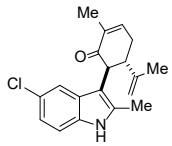

6-2

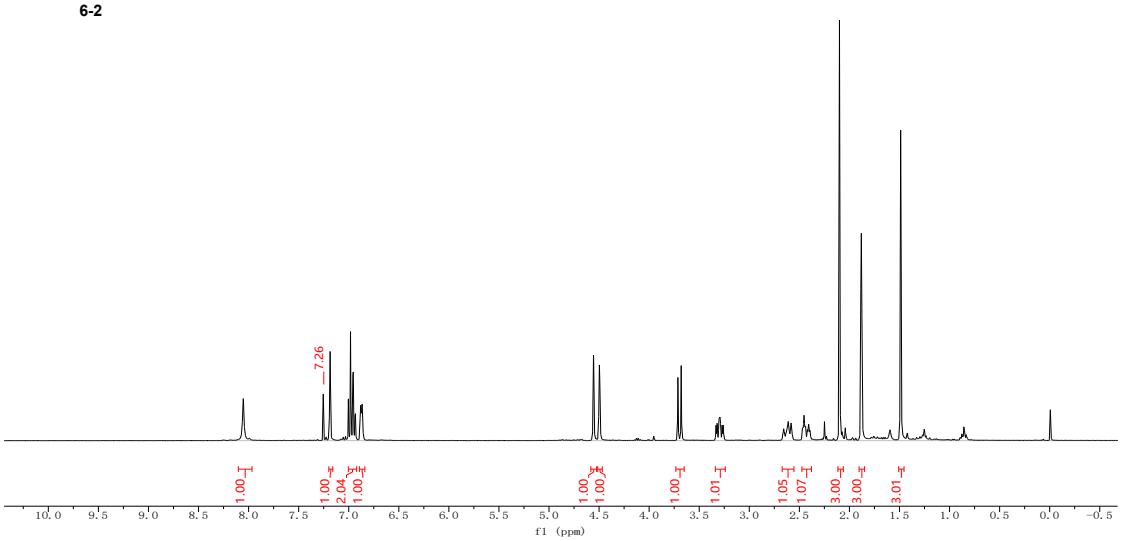

2017-3.18392.fid
LHL1-30-2

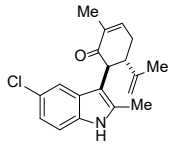

6-2

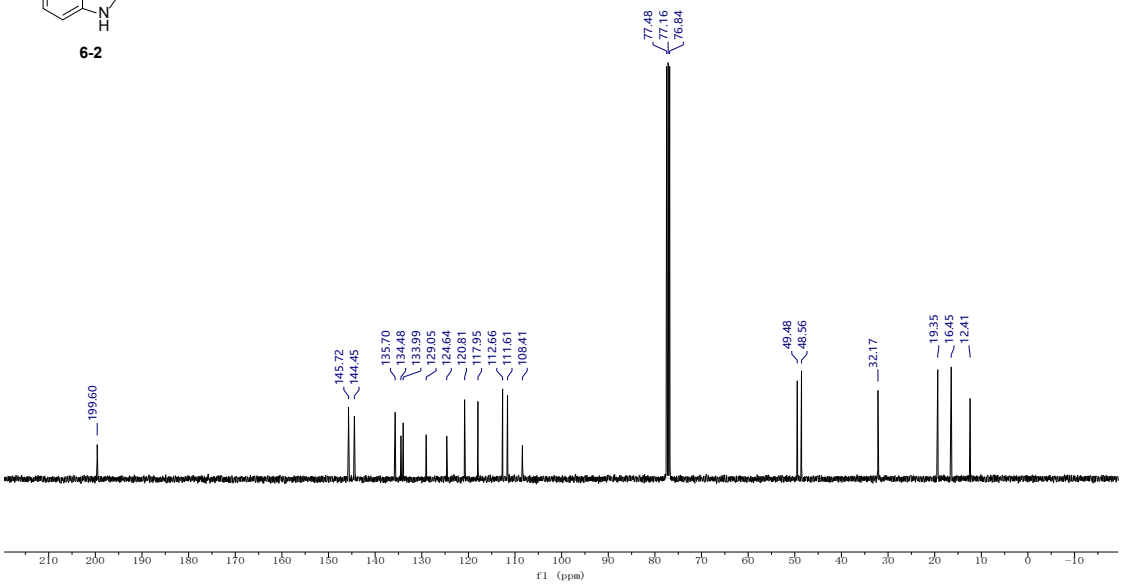

2018-1.3031.fid
LHL1-39-2

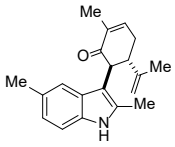

6-3

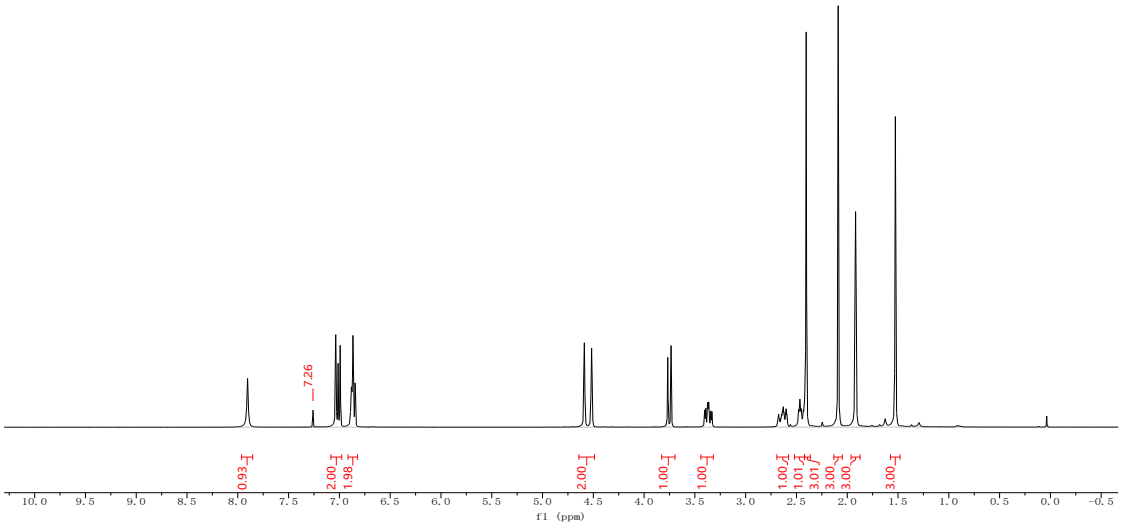

2018-1.3175.fid
LHL1-39-2

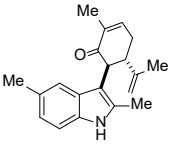

6-3

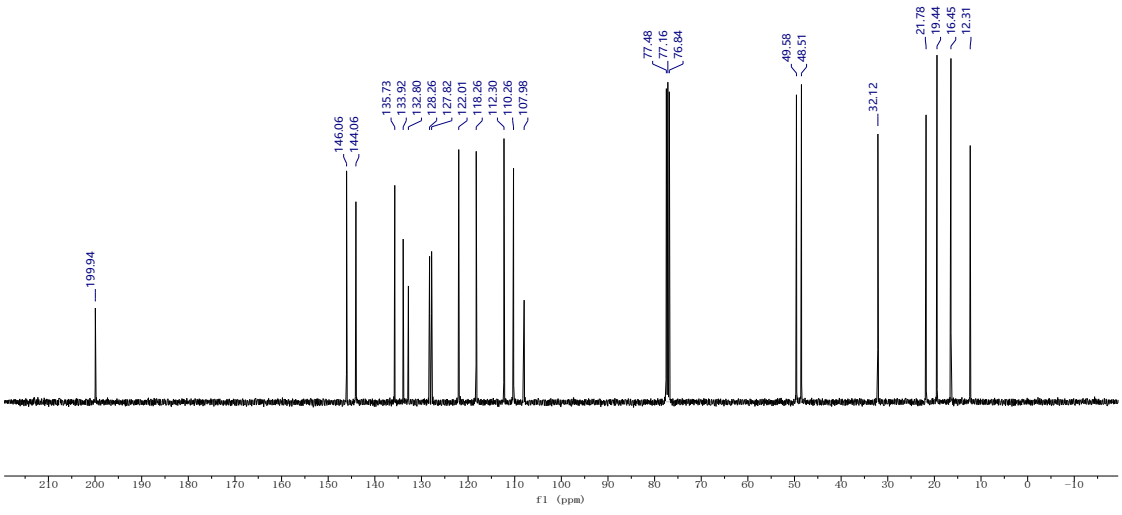

2017-3.17980.fid
LHL1-31-1

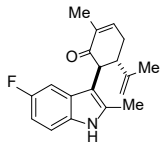

6-4

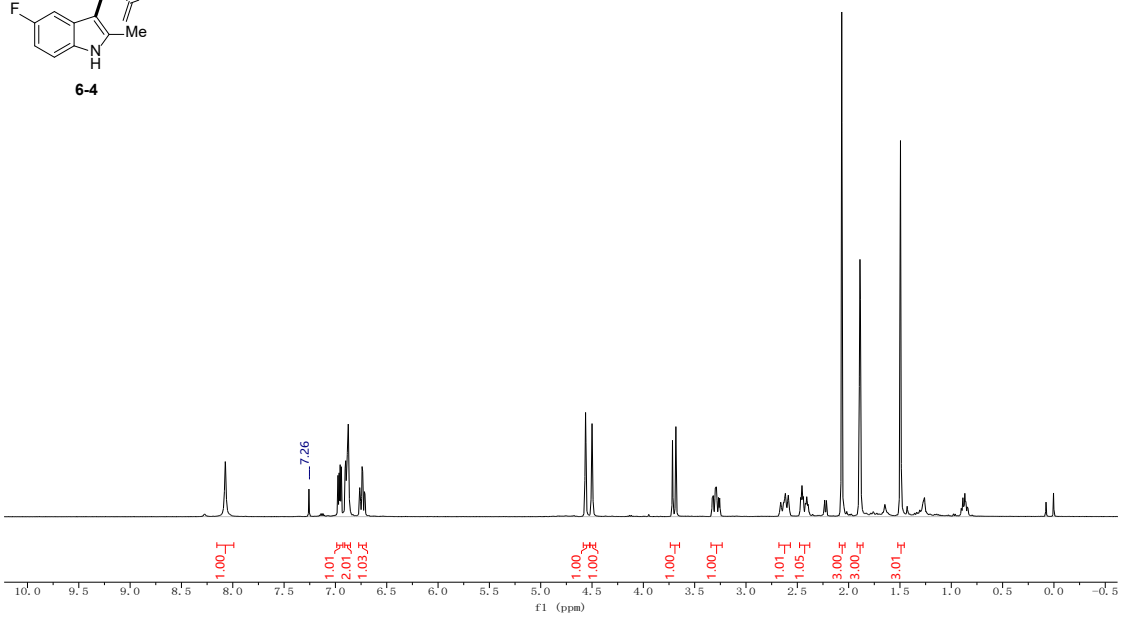

2017-3.18393.fid
LHL1-31-1

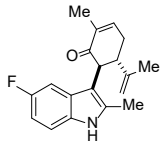

6-4

chenzhilong-20190505-2#.30.fid
LHL-1-31-1

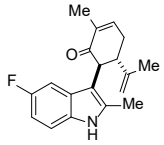

6-4 (F NMR)

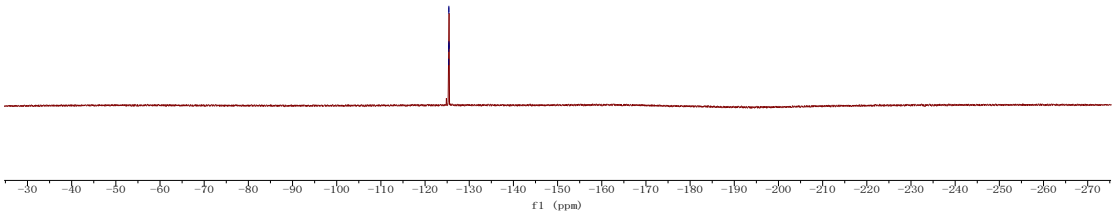

xiangguangya-20180427-37#.1.fid
lhl-1-64-2

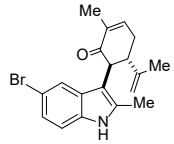

6-5

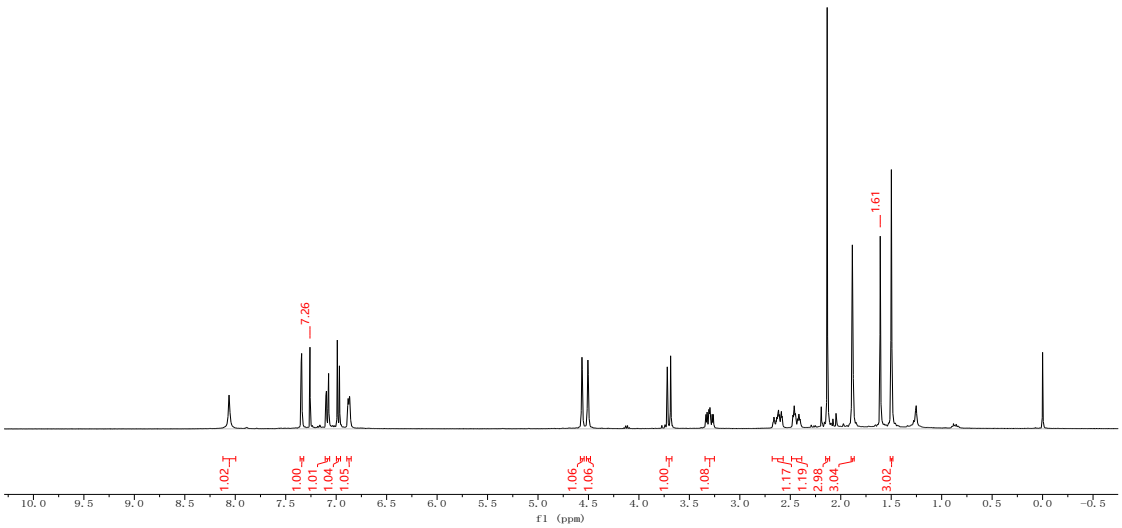

2019-1.2997.fid
LHL-1-64-2

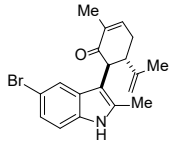

6-5

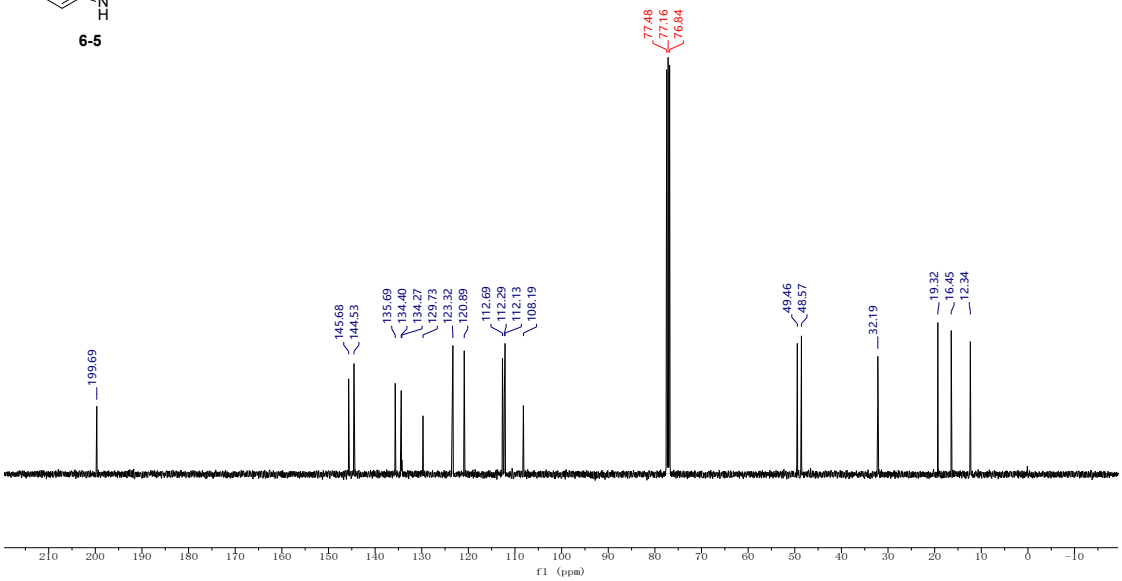

2017-3.17981.fid
LHL1-31-2

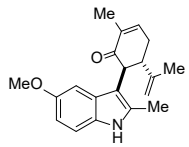

6-6

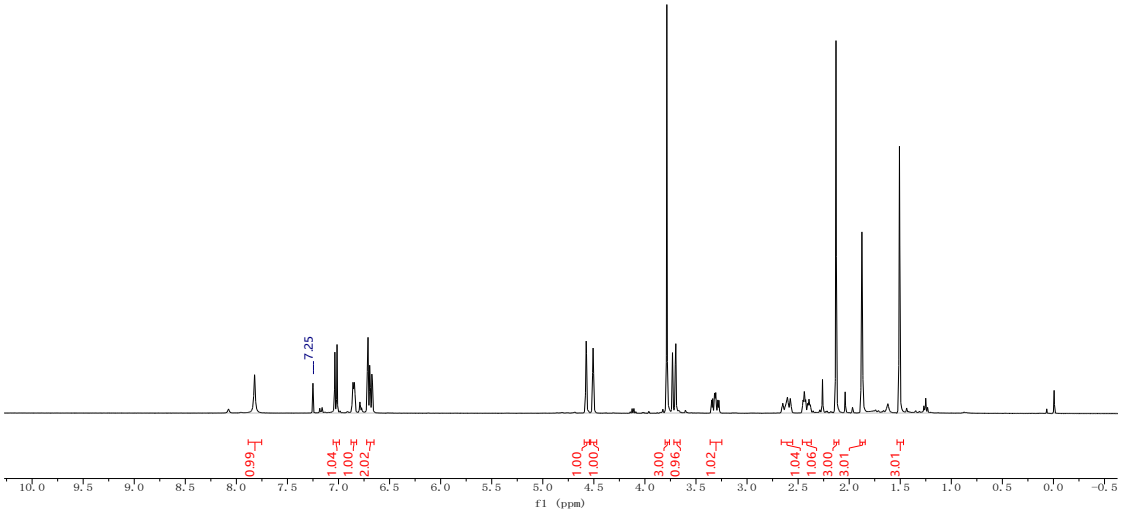

2017-3.18391.fid
LHL1-31-2

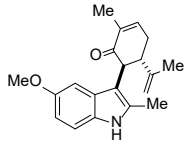

6-6

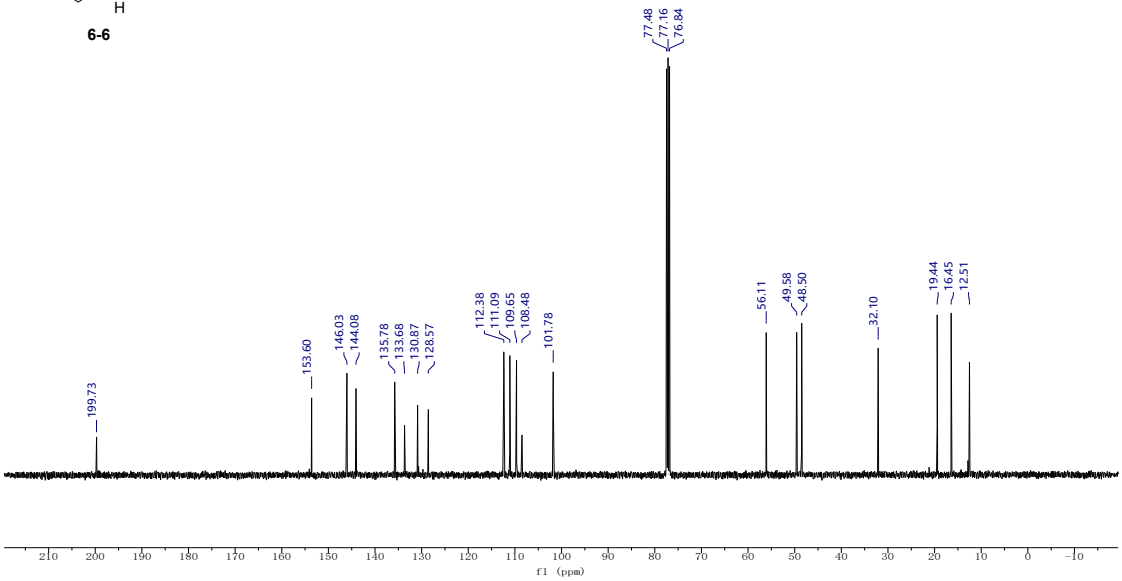

2018-2.8141.fid
LHL-2-32-2

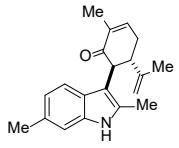

6-7

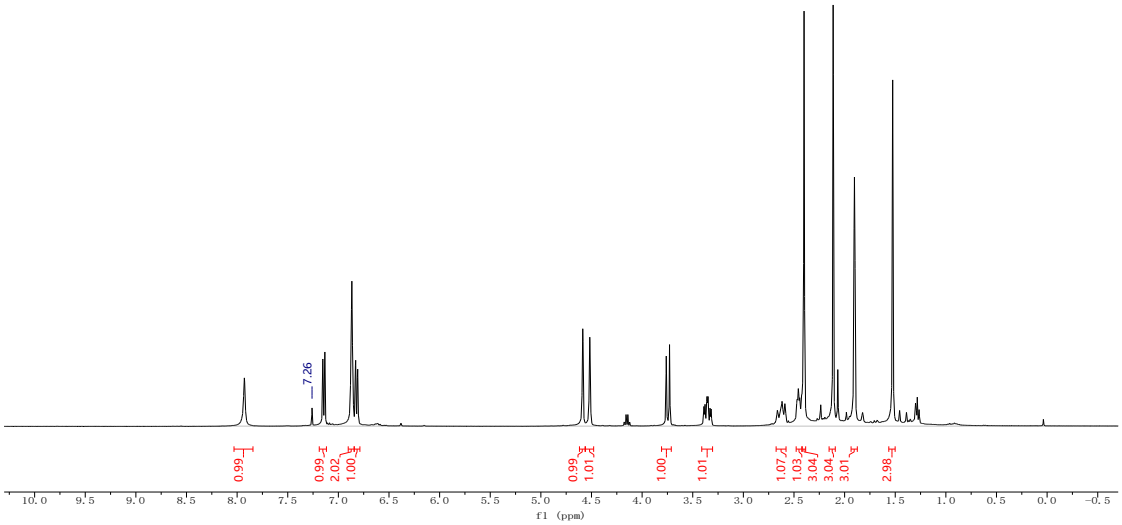

2018-2.8621.fid
LHL-2-32-2

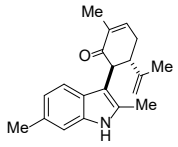

6-7

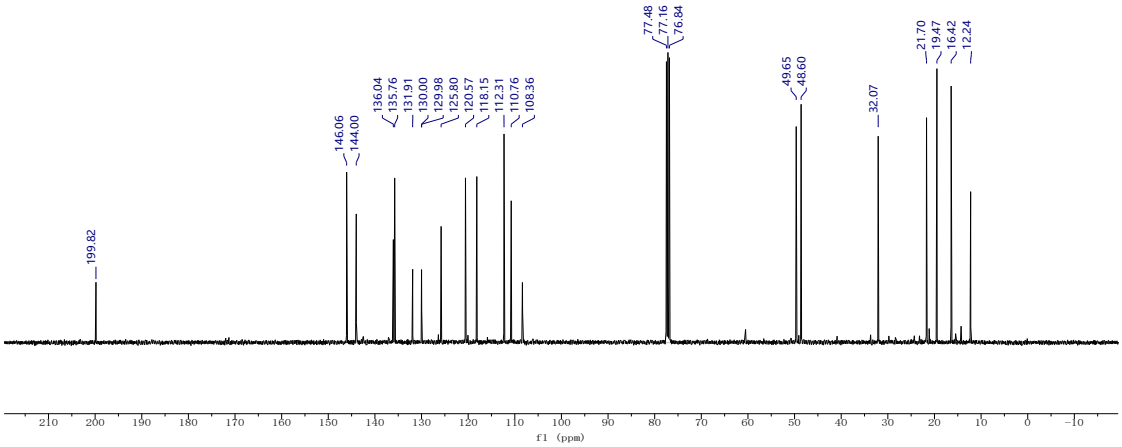

2018-2.8139.fid
LHL-2-33-1.1

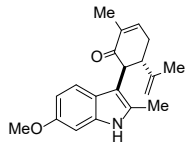

6-8

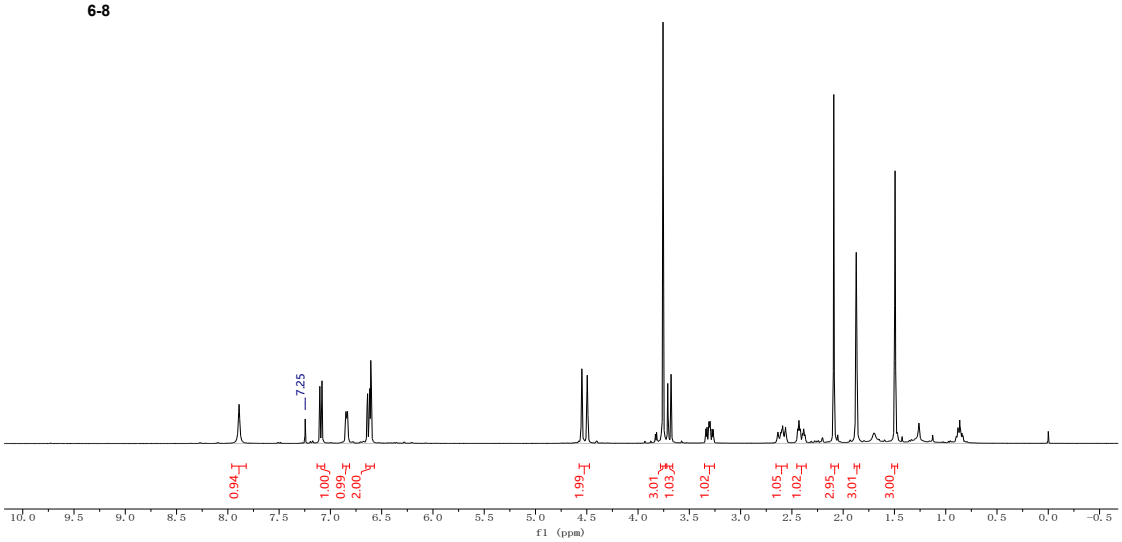

LHL-2-33-1.1

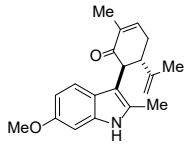

6-8

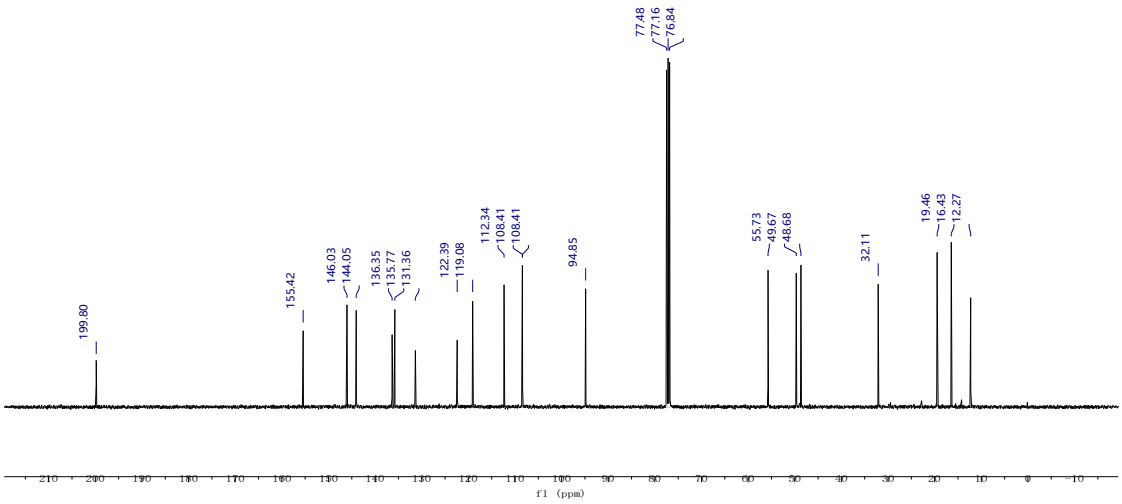

LHL-2-41-2

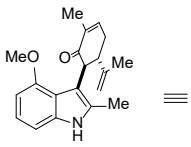

6-9

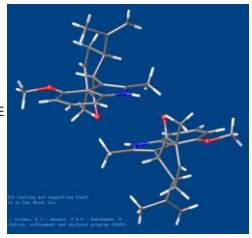

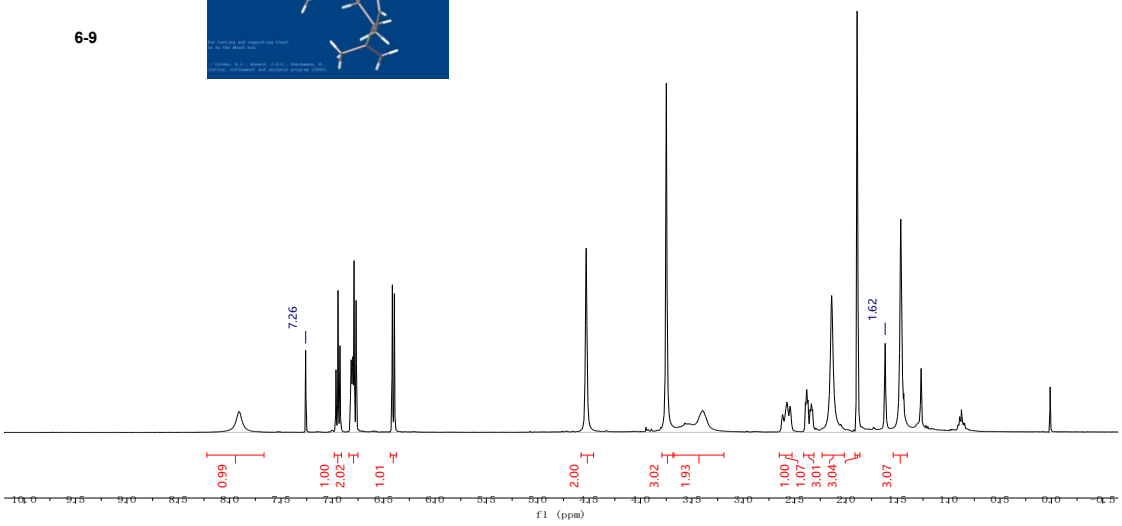

LHL 2-41-2

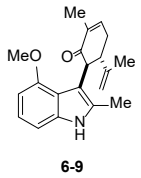

6-9

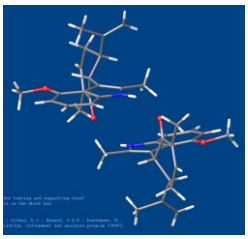

LHL2-25-1

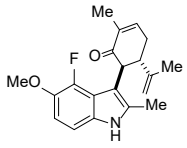

6-10

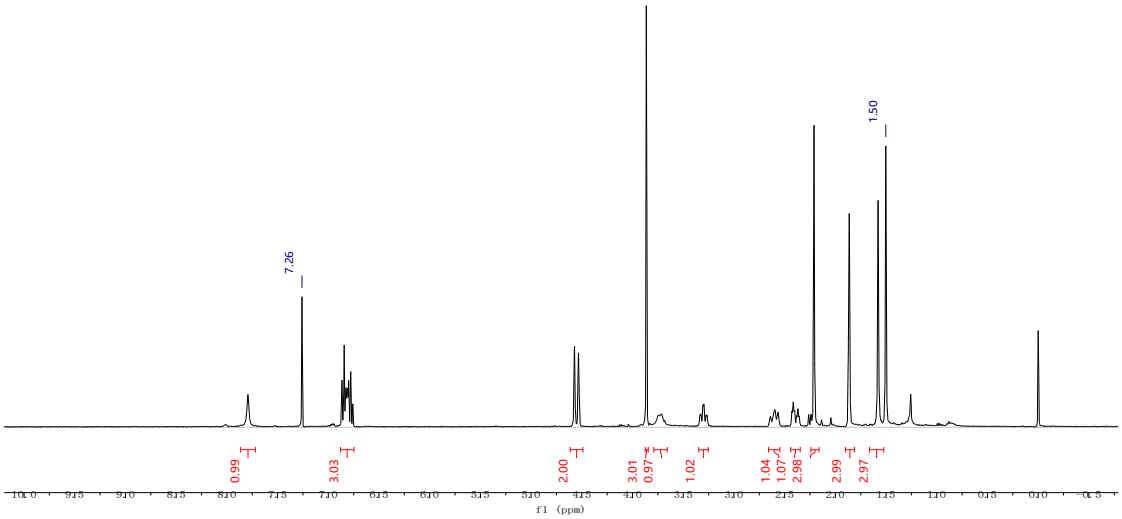

2019-1.4789.fid
LHL 2-25-1

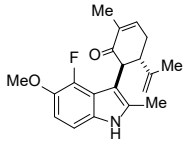

6-10

chenzhilong-20190505-3#.30.fid
LHL-2-25-1

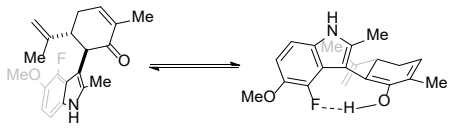

6-10 **6-10'**

2018-2.7054.fid
LHL2-24-1

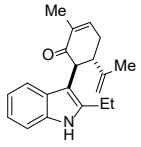

6-11

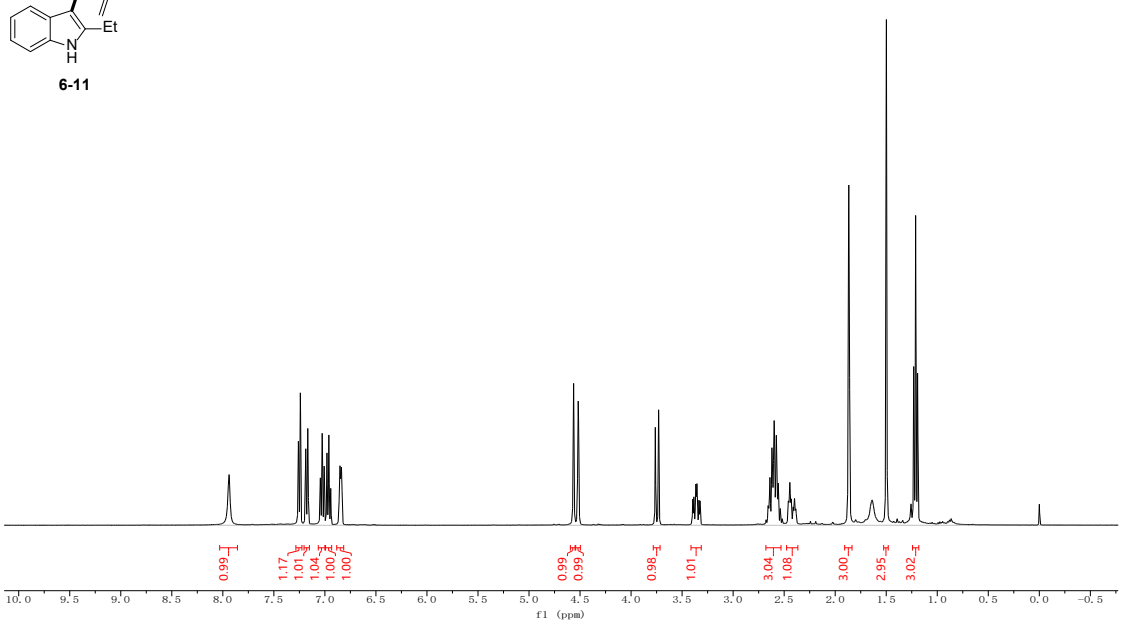

2018-2.7488.fid
LHL-2-24-1

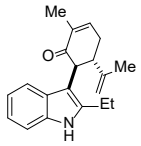

6-11

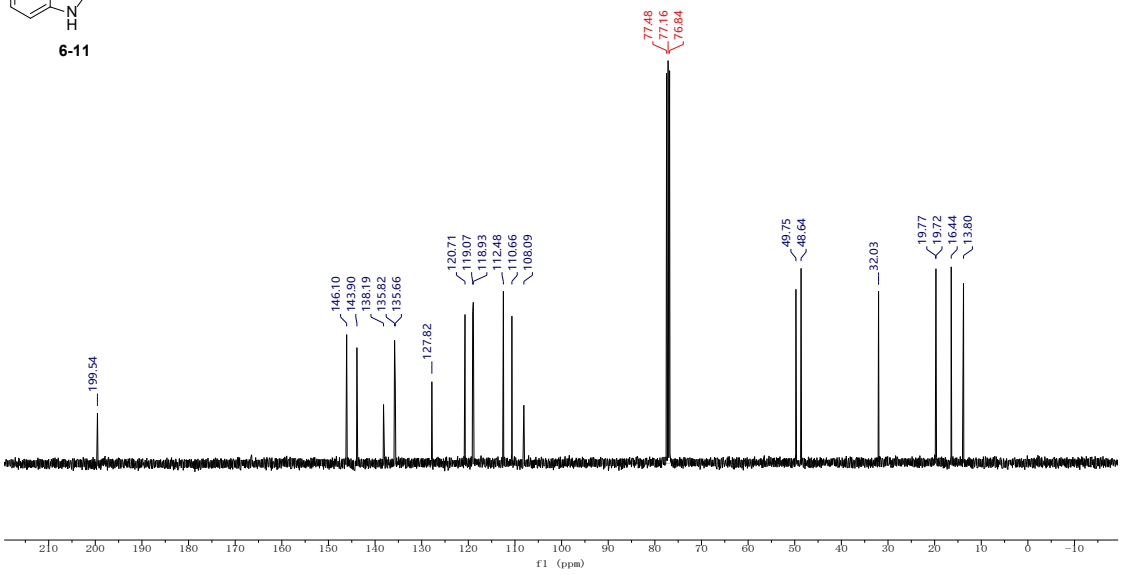

2018-2.13508.fid
LHL-2-78-2

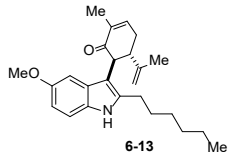

6-13

2018-2.14039.fid
LHL-2-78-2

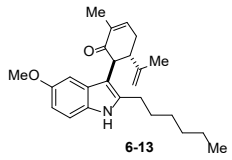

6-13

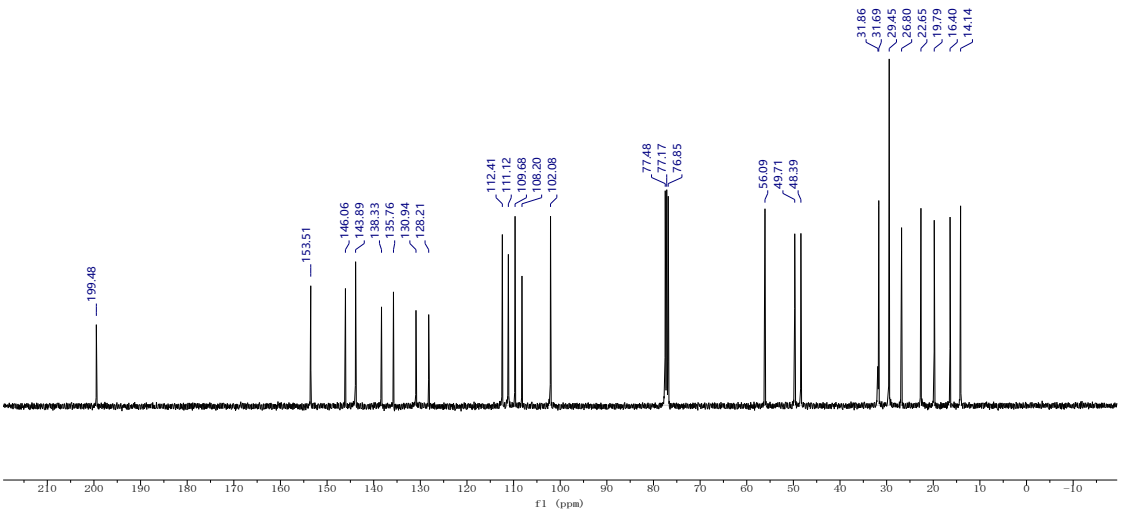

2018-2.13082.fid
LHL-2-74-2.3

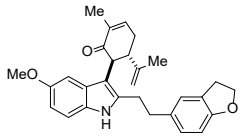

6-14

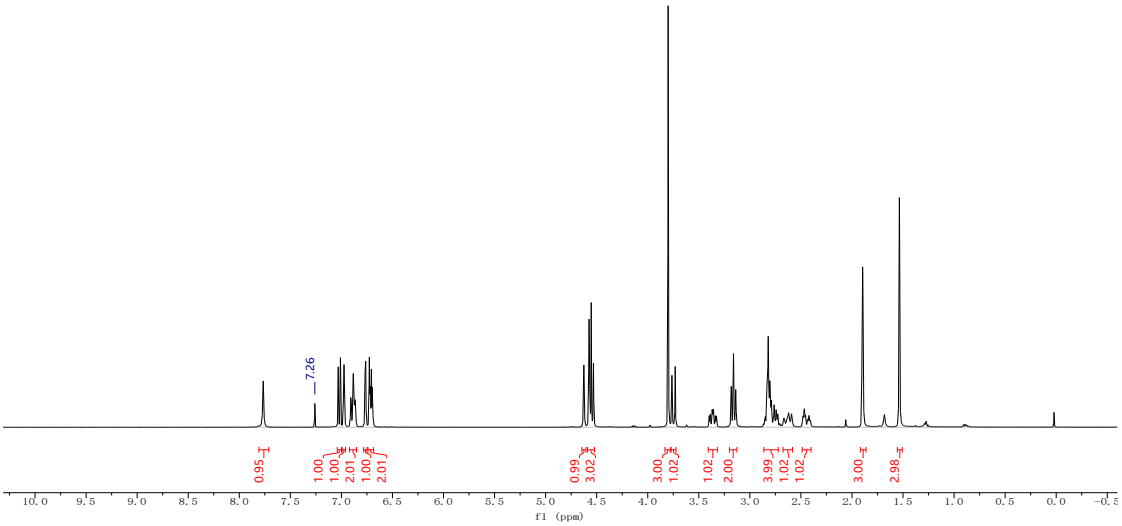

2019-1.2541.fid
LHL-2-74-2.3

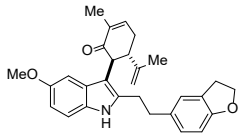

6-14

2019-1.674.fid
LHL-3-7-1

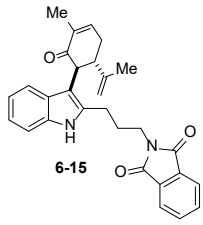

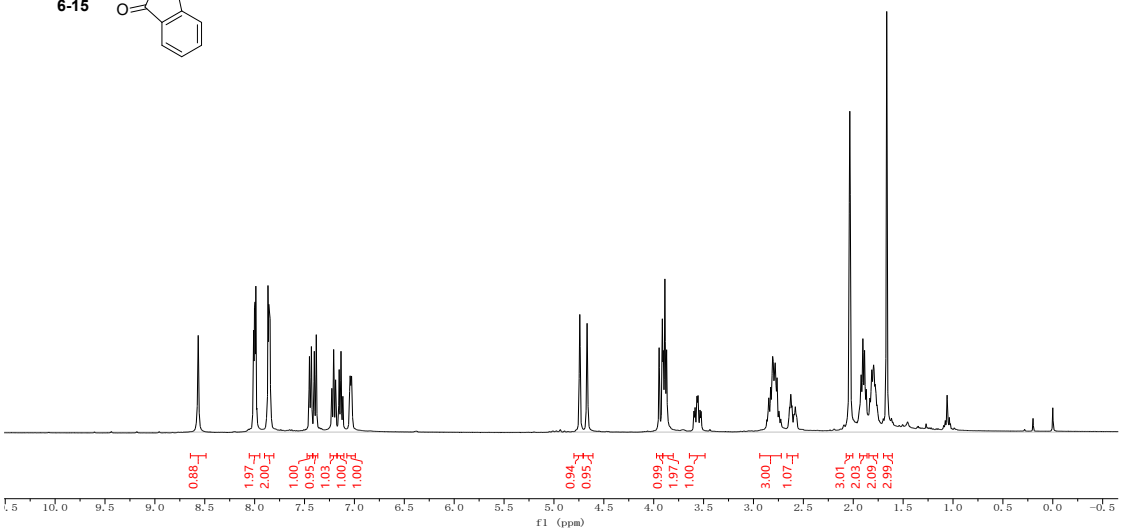

2019-1.861.fid
LHL-3-7-1

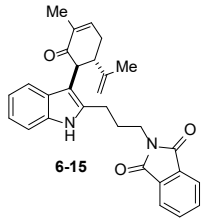

2017-3.18346.fid
LHL1-32-1

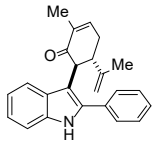

6-16

2018-1.399.fid
LHL-1-32-1

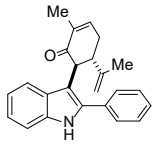

6-16

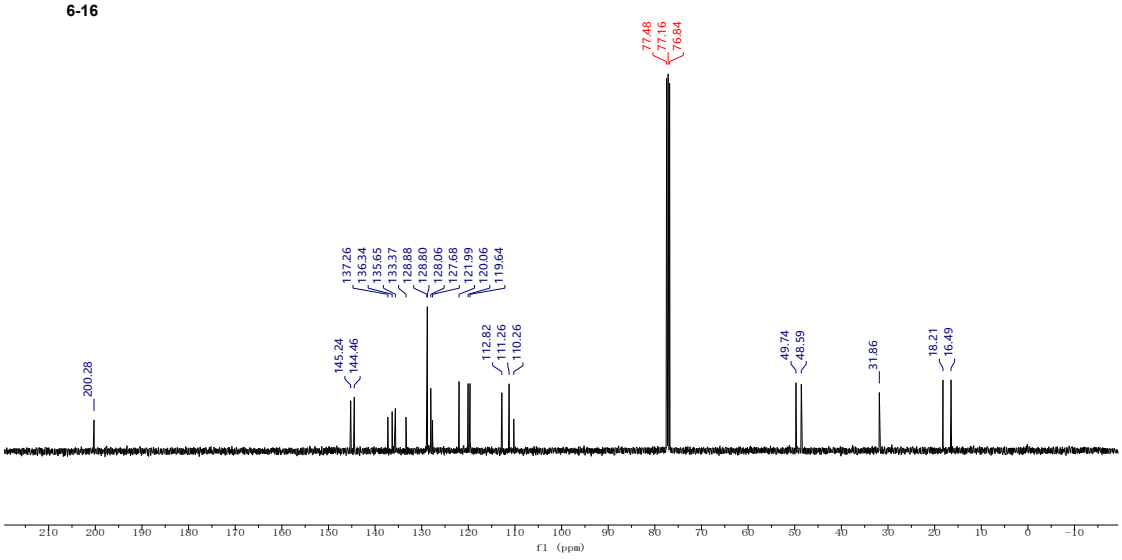

2018-2.5822.fid
LHL1-81-1

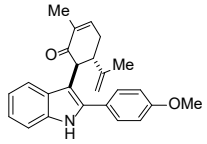

6-17

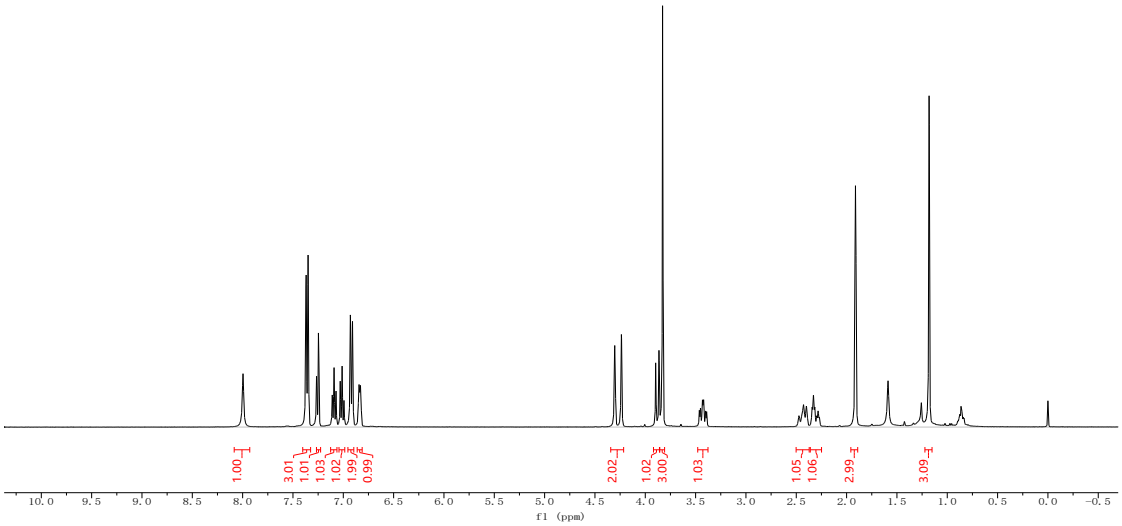

2019-1.2773.fid
LHL -1-81-1

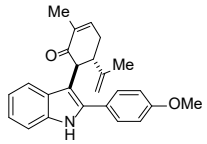

6-17

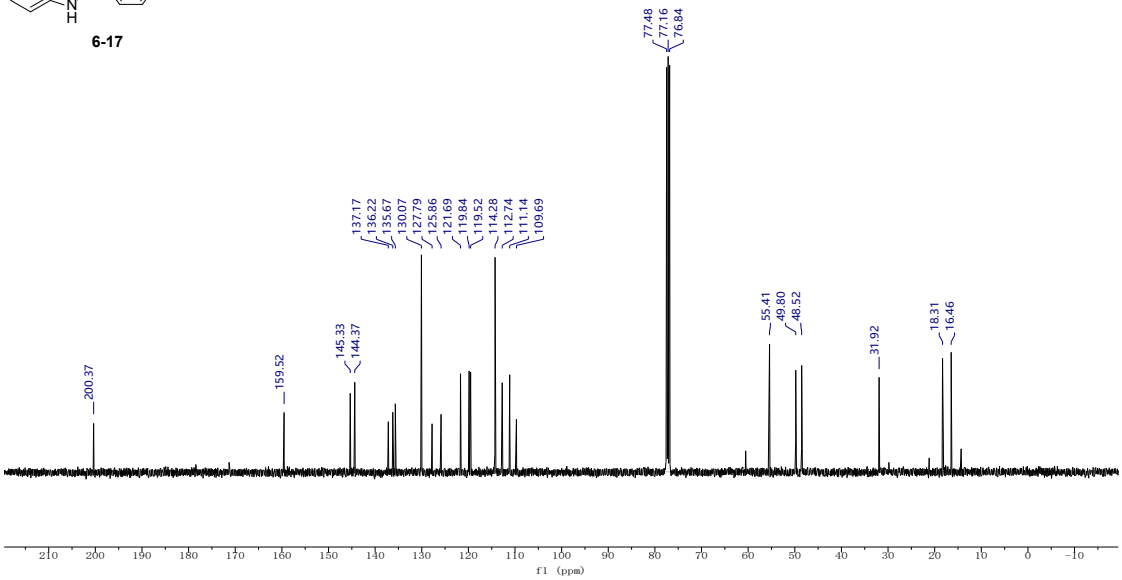

2019-1.3200.fid
LHL-3-15-1

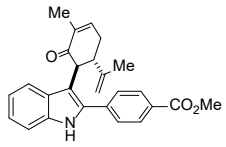

6-18

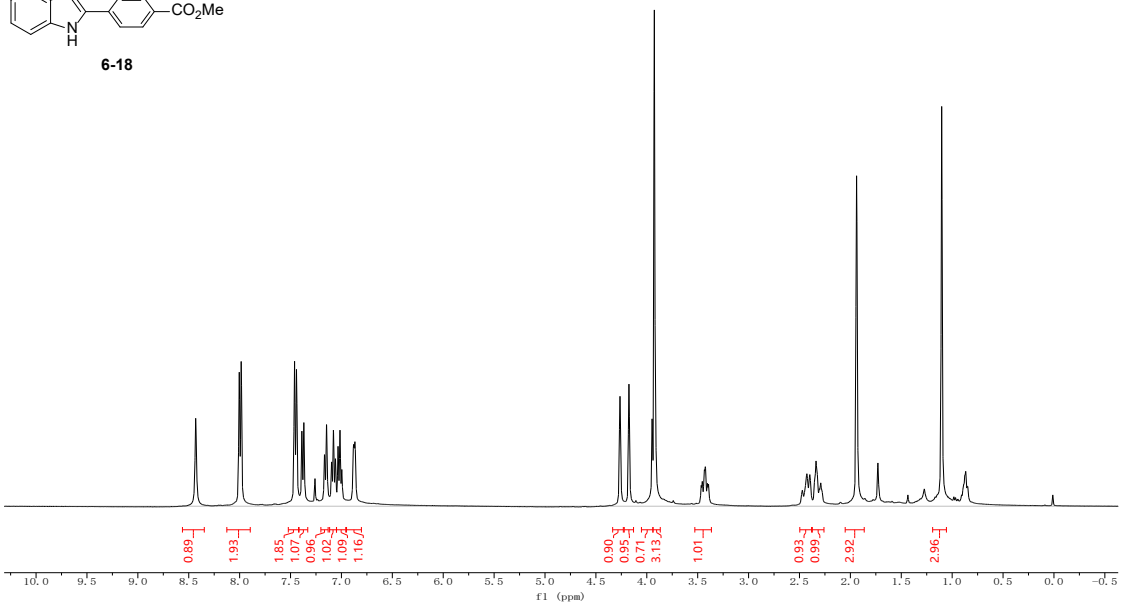

2019-1.3743.fid
LHL 3-15-1

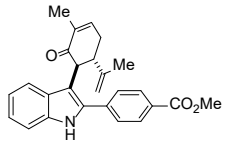

6-18

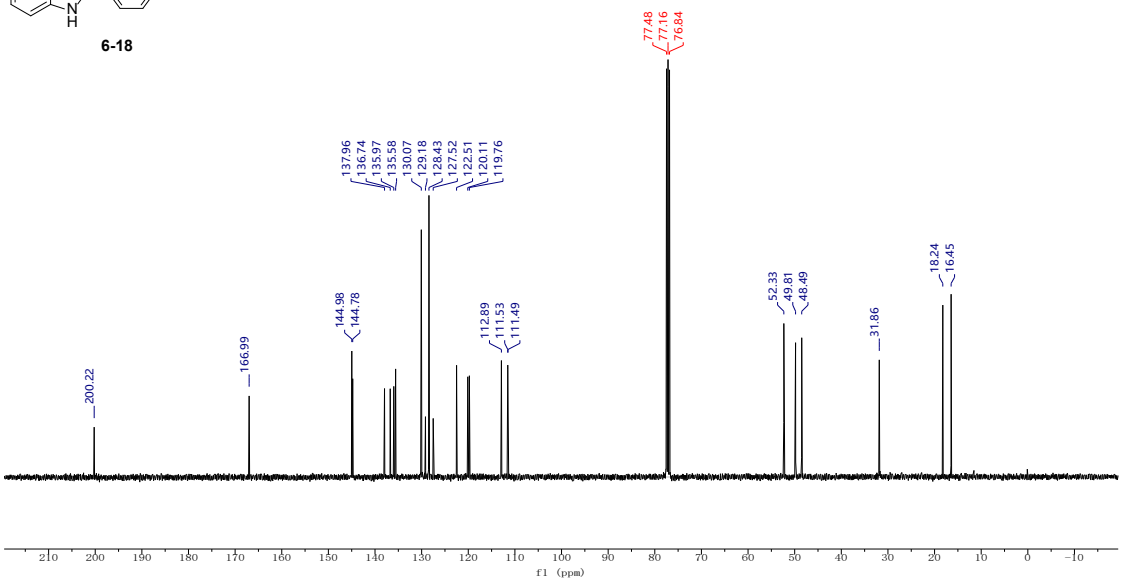

xiangguangya-20180629-003#.10.fid
LHL-1-82-2

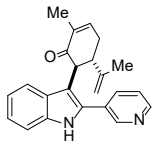

6-19

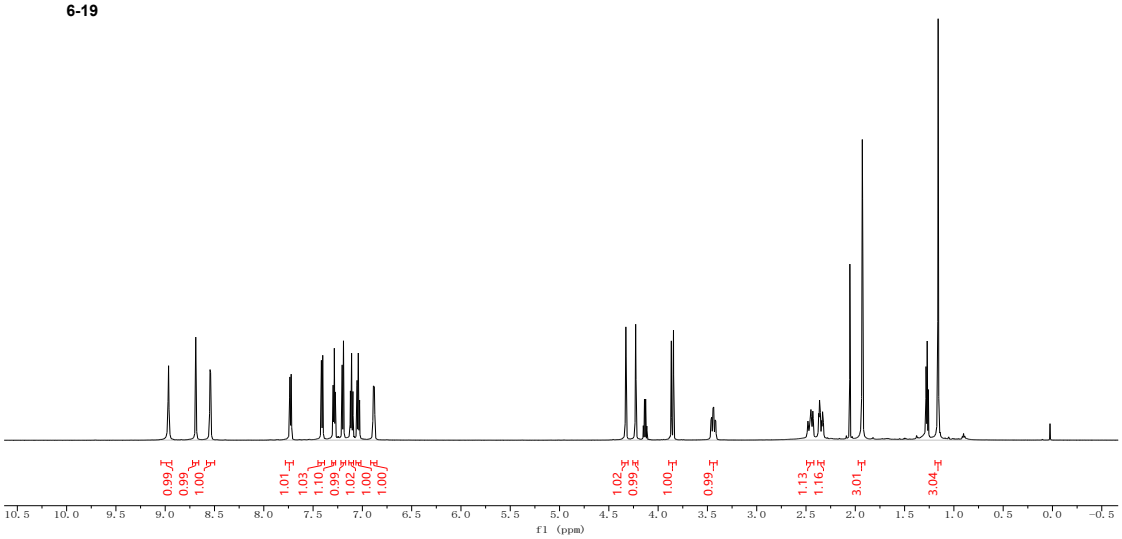

2019-1.3000.fid
LHL-1-82-2

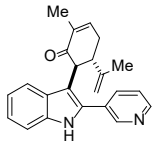

6-19

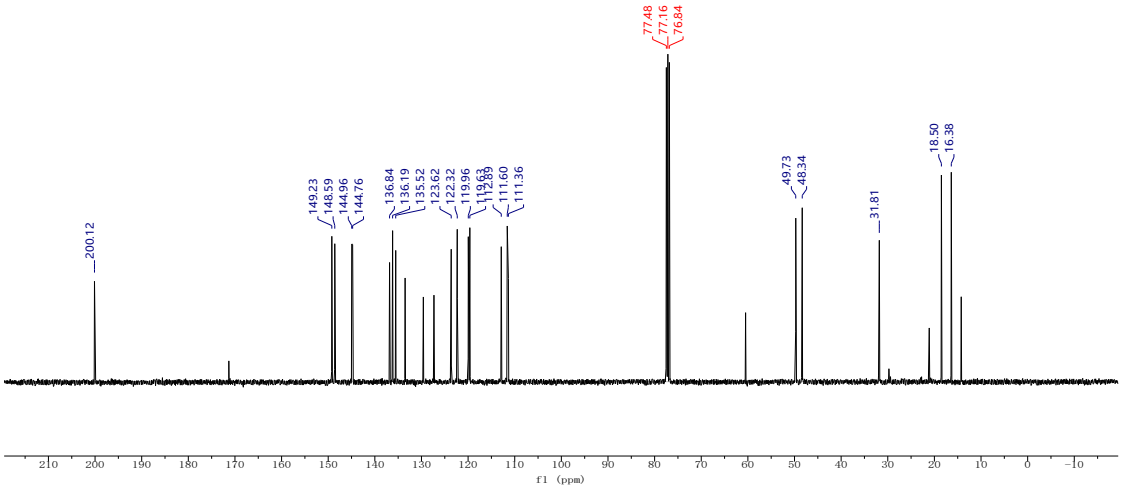

xiangguangya-20180601-18#.1.fid
LHL-1-77-1.2

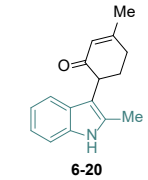

6-20

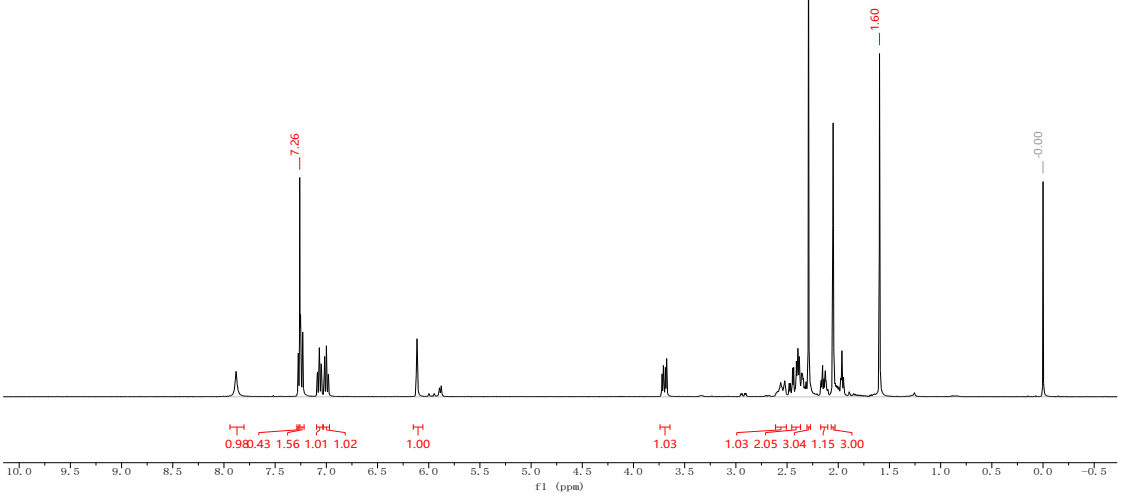

2019-1.2771.fid
LHL -1-71-1.2

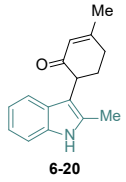

6-20

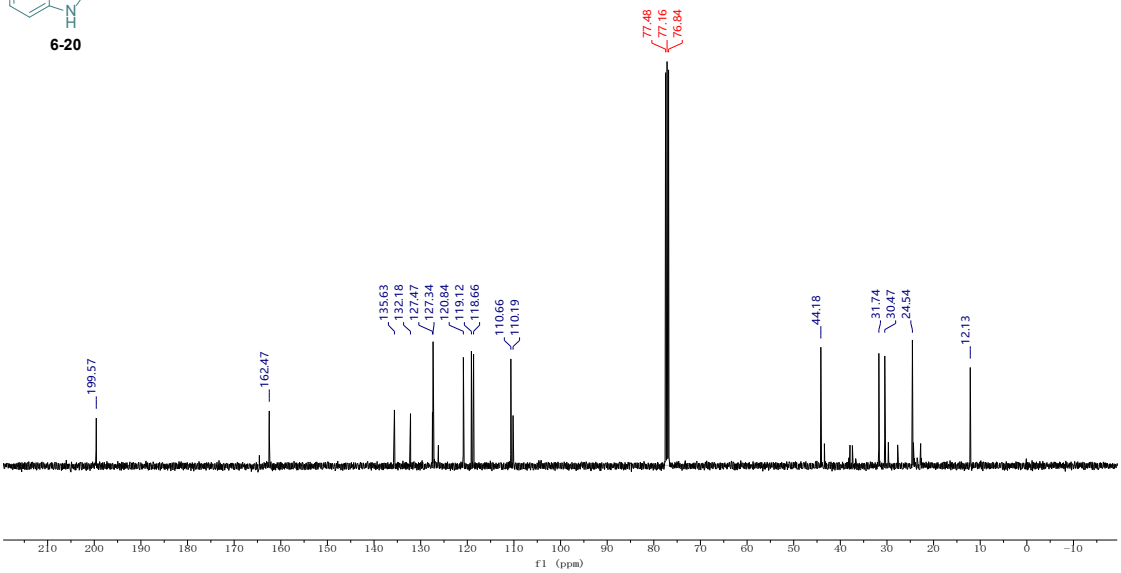

2018-1.55.fid
LHL1-33-1.3

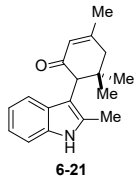

6-21

2019-1.2998.fid
LHL-1-33-1.3

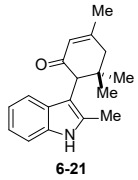

6-21

xiangguangya-20180511-36#.1.fid
LHL-1-66-1

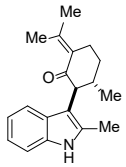

6-22

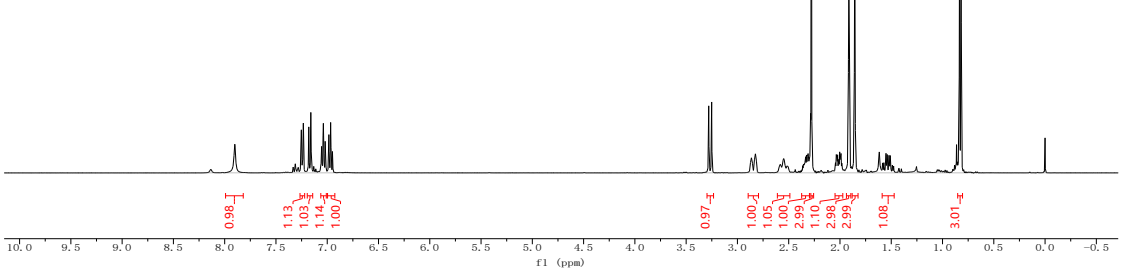

2019-1.2996.fid
LHL-1-66-1

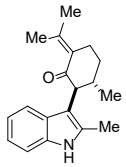

6-22

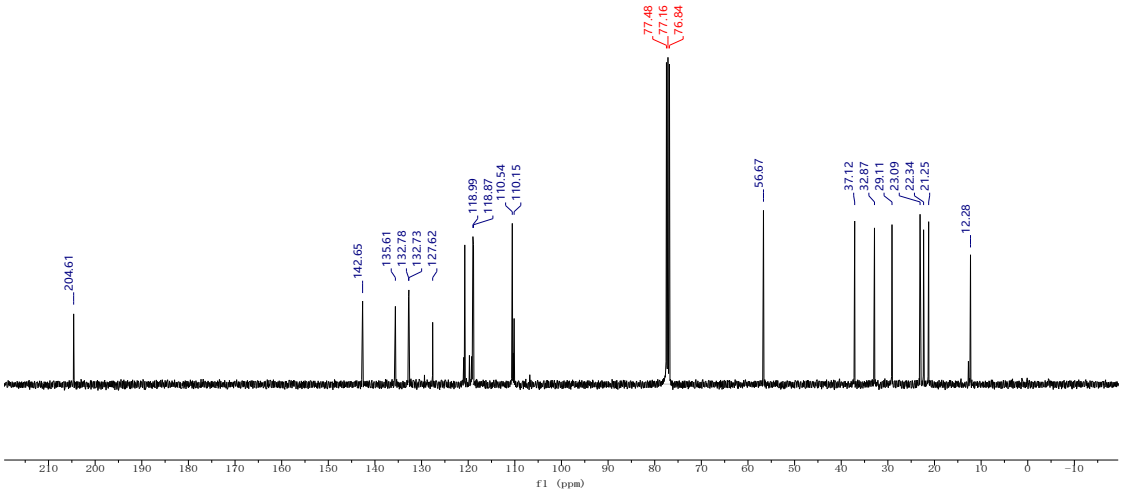

2018-2.3992.fid
LHL-1-74-1.2

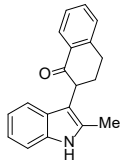

6-23

2018-2.4864.fid
LHL1-74-1.2

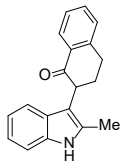

6-23

2018-2.7299.fid
lhl-2-26-2

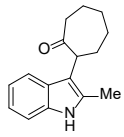

6-24

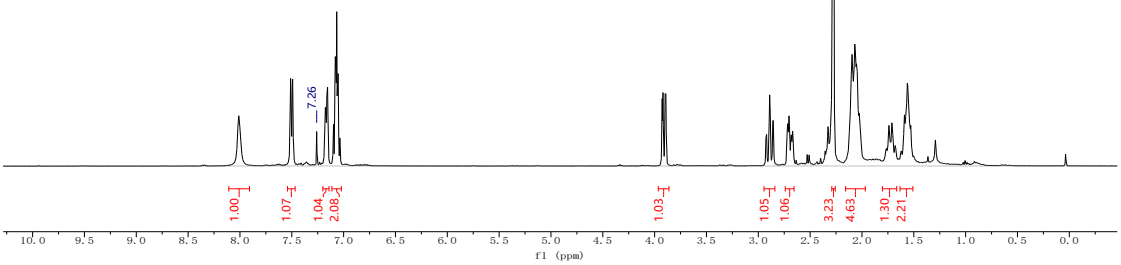

2018-2.8230.fid
LHL-2-26-2

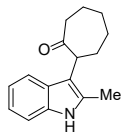

6-24

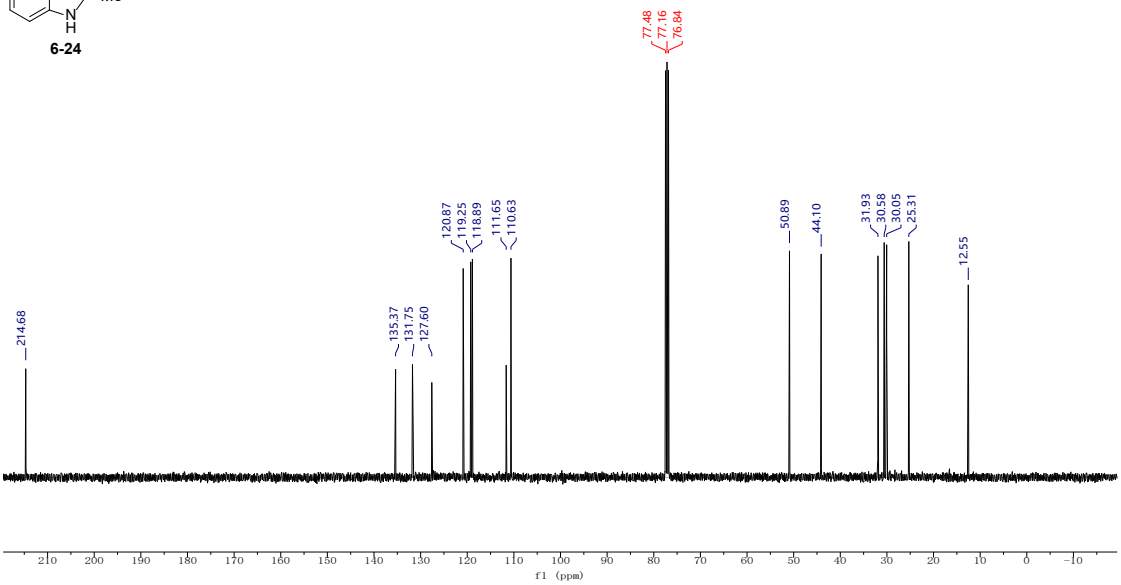

2018-2.13903.fid
LHL-2-80-2

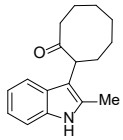

6-25

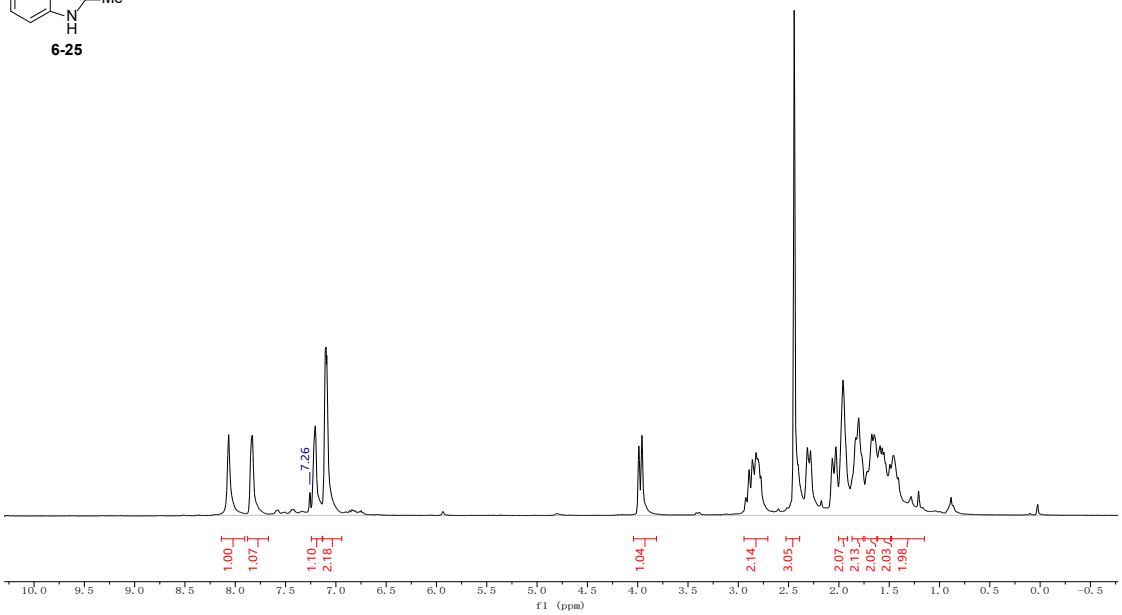

2018-2.14525.fid
LHL-2-80-2

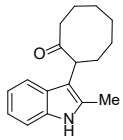

6-25

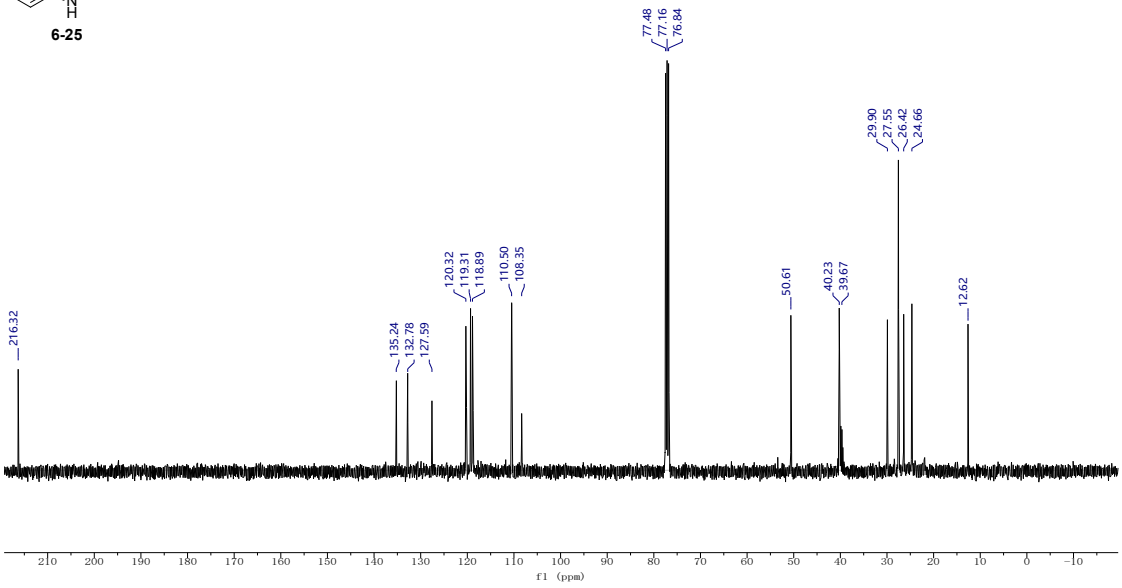

2018-2.7771.fid
LHL2-30-2.2

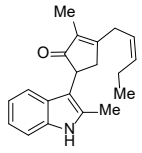

6-26

2019-1.2550.fid
LHL -2-30-2.2

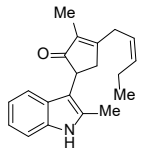

6-26

2018-2.13904.fid
LHL-2-81-1.2

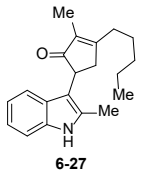

6-27

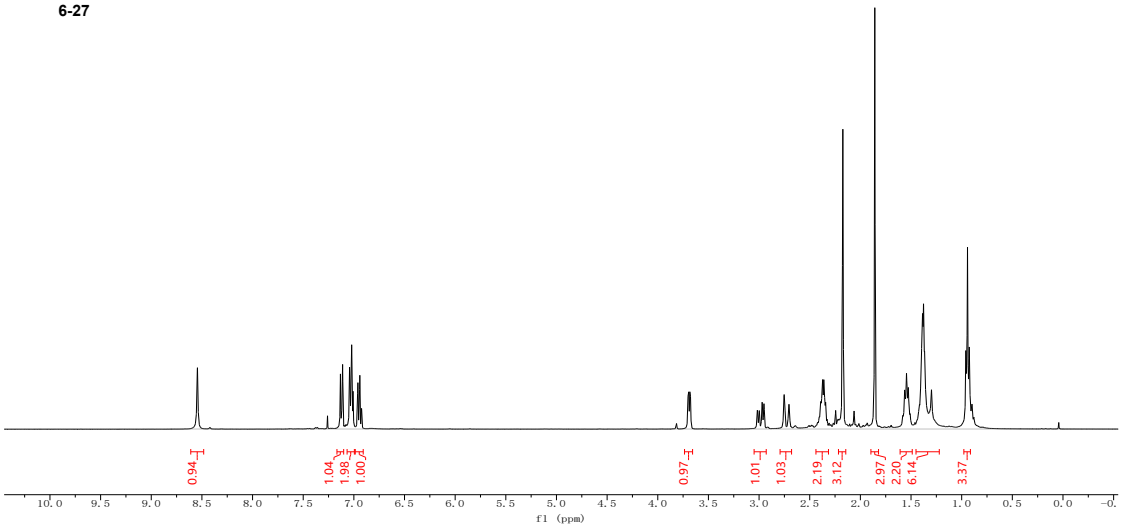

2018-2.14524.fid
LHL-2-81-1.2

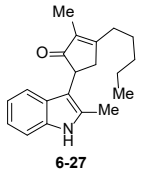

6-27

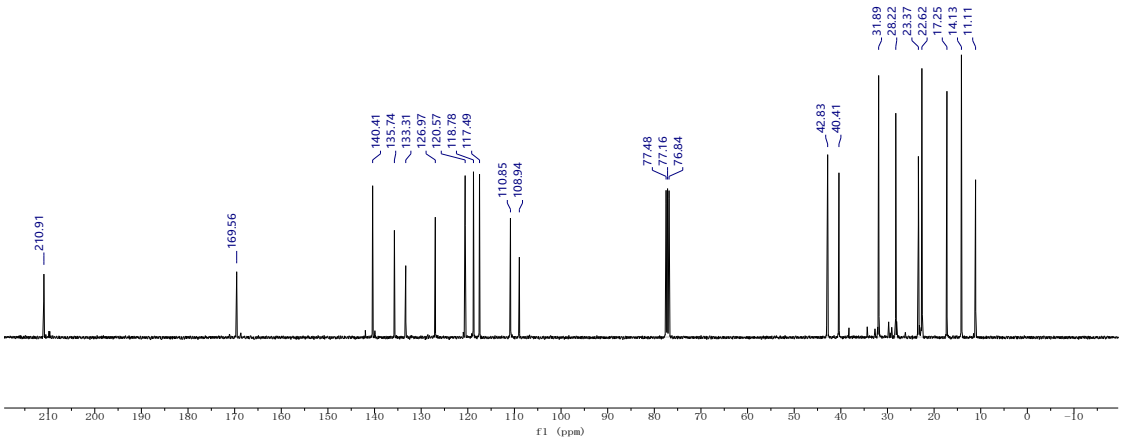

2019-1.3206.fid
LHL-2-35-1.2

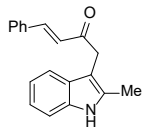

6-28

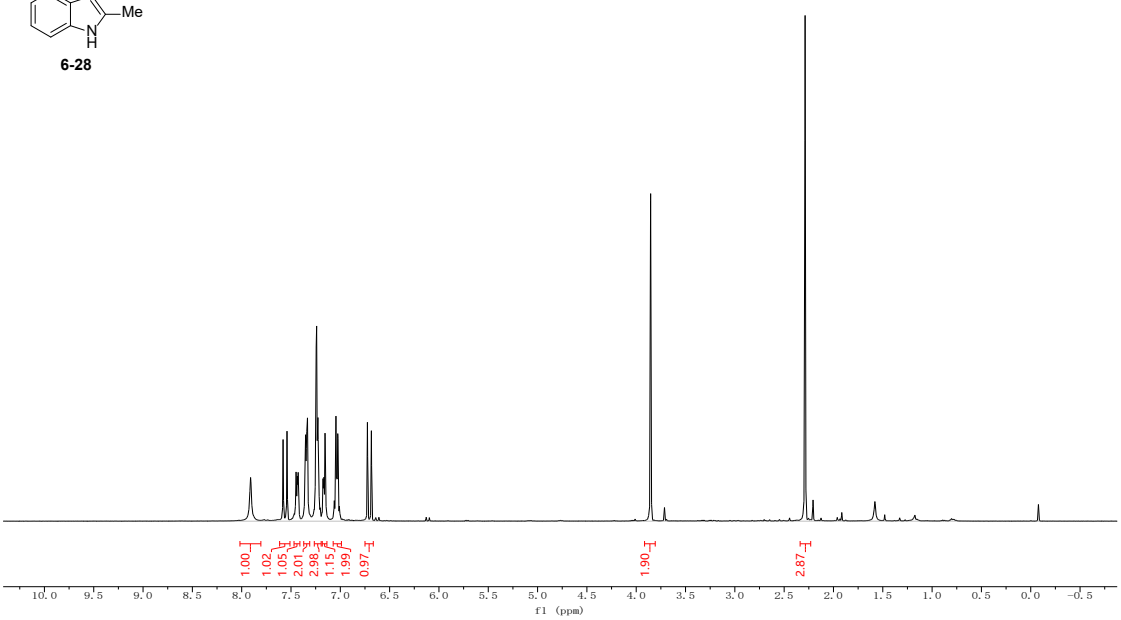

2019-1.3517.fid
LHL 2-35-1.2

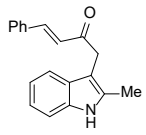

6-28

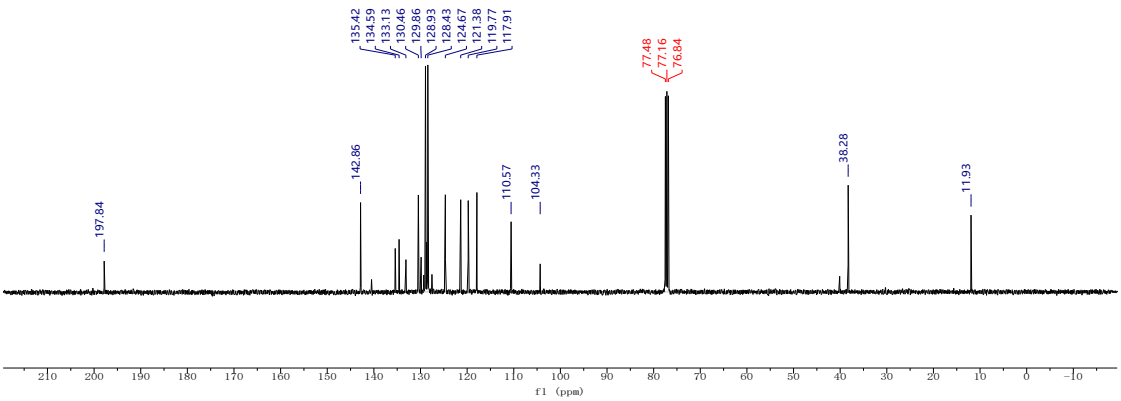

xiangguangya-20180629-002#.10.fid
LHL-1-83-1

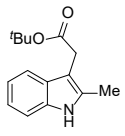

6-29

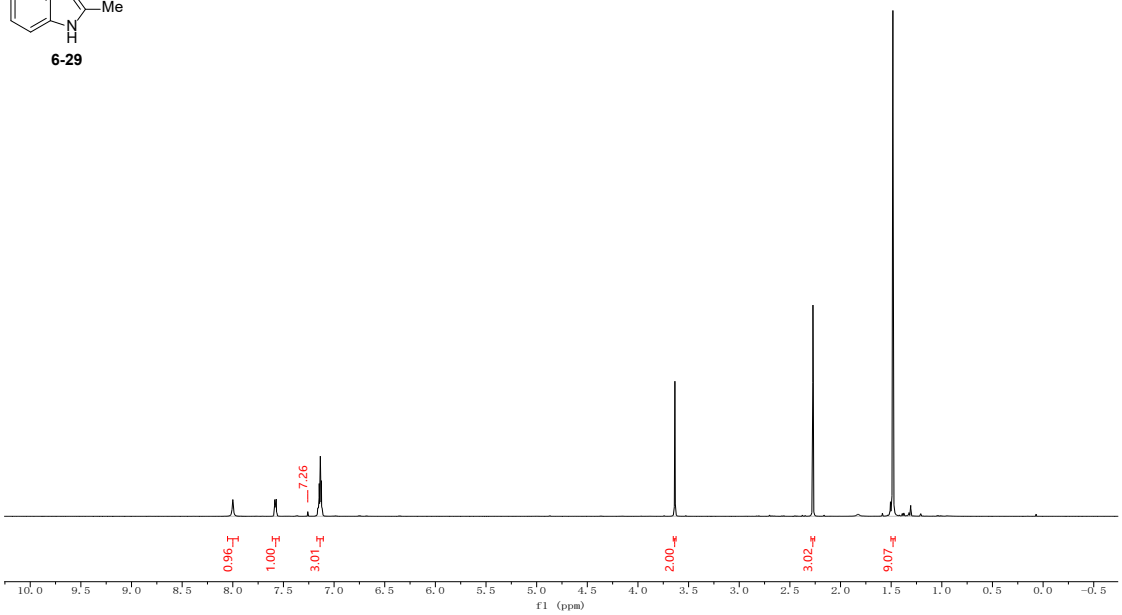

2019-1.7404.fid
LHL-1-83-1

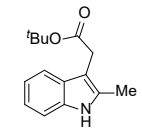

6-29

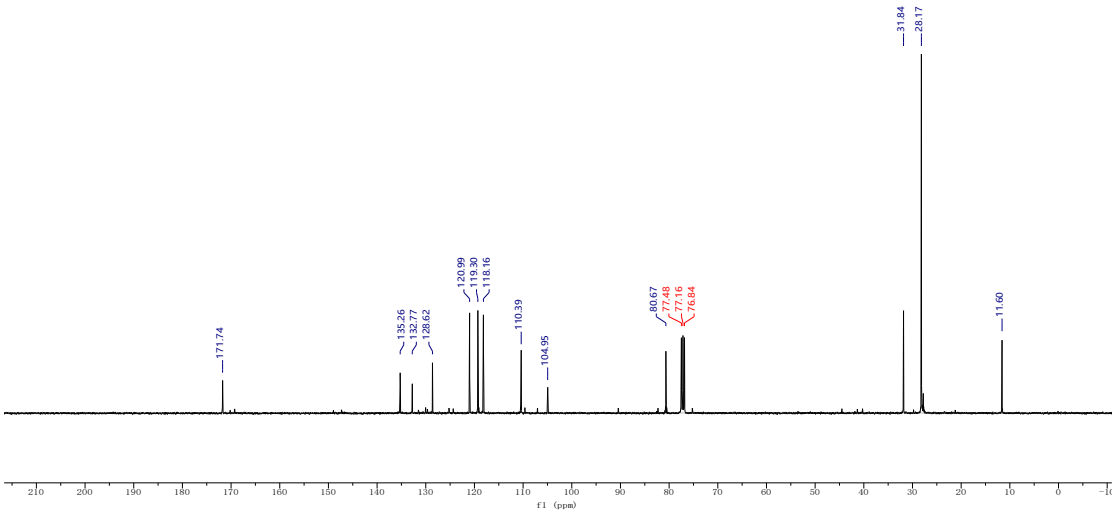

2018-2.11987.fid
LHL -2-64-1.1

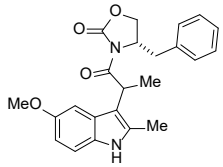

6-30 (1.9:1 dr)

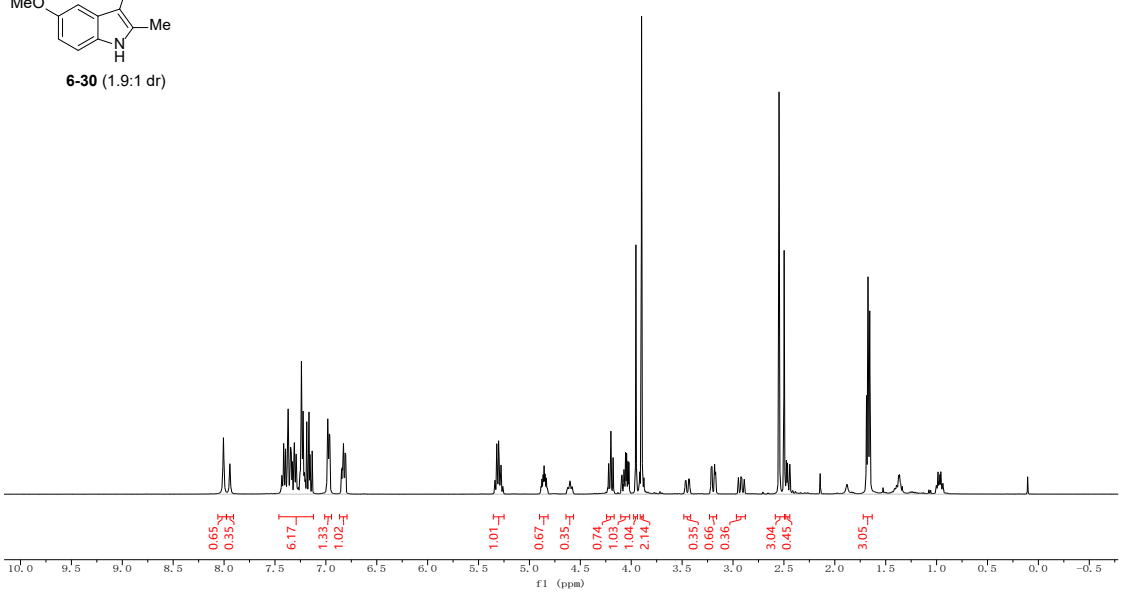

2018-2.12634.fid
LHL-2-64-1.1

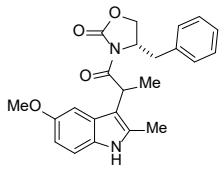

6-30 (1.9:1 dr)

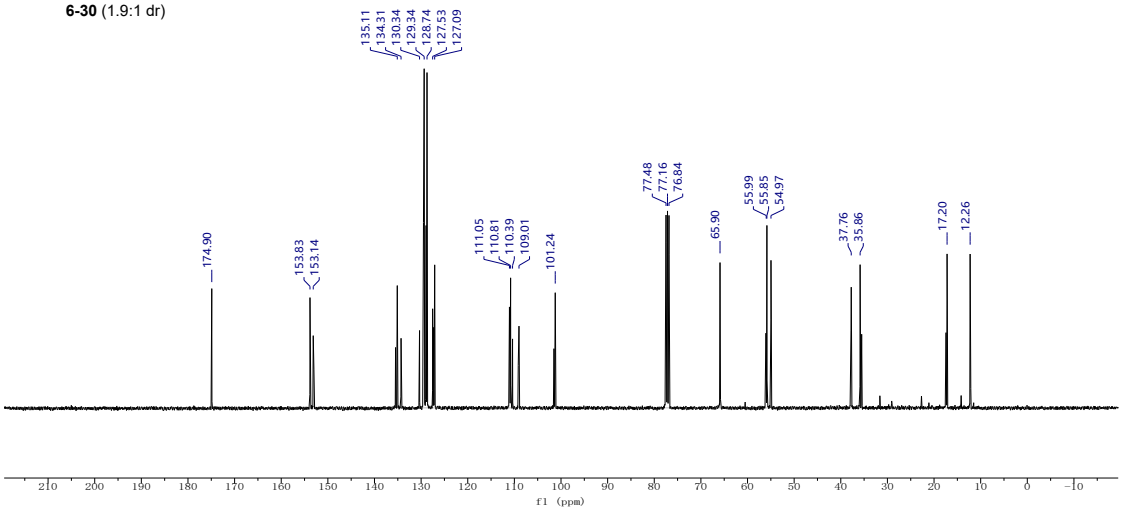

2018-2.14363.fid
LHL -2-83-2

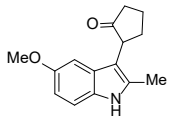

6-31

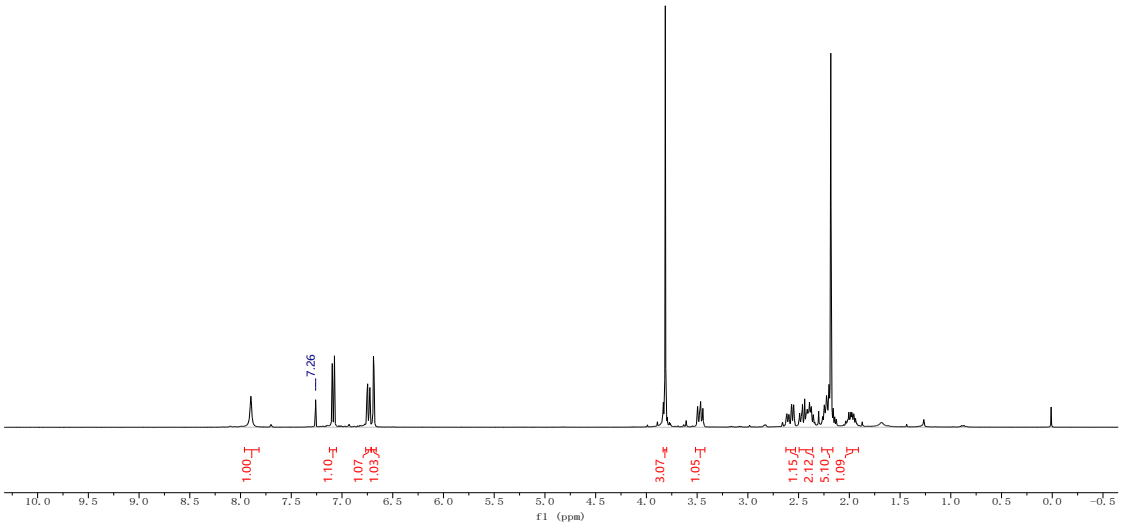

2019-1.6915.fid
LHL -2-83-2.2

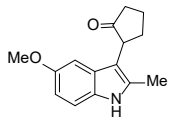

6-31

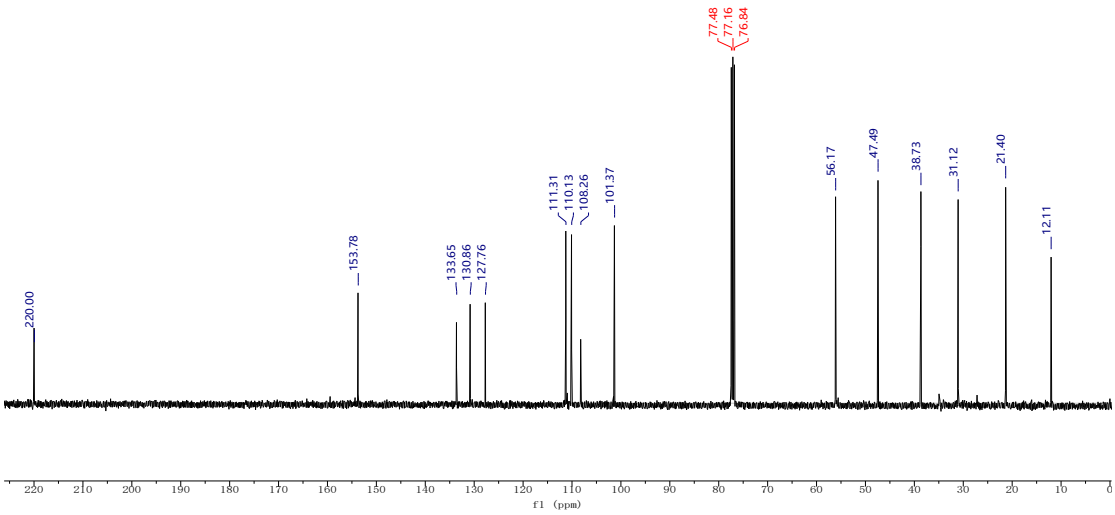

2018-2.14872.fid
LHL-2-84-2.2

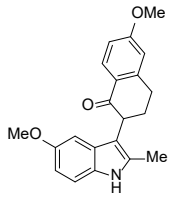

6-32

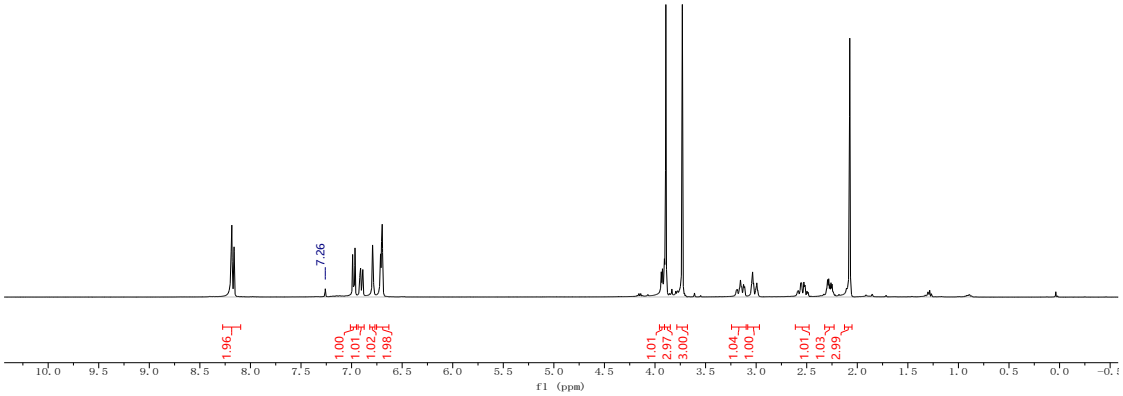

2018-2.15370.fid
LHL -2-84-2.2

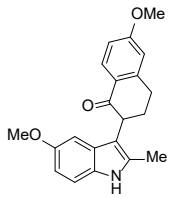

6-32

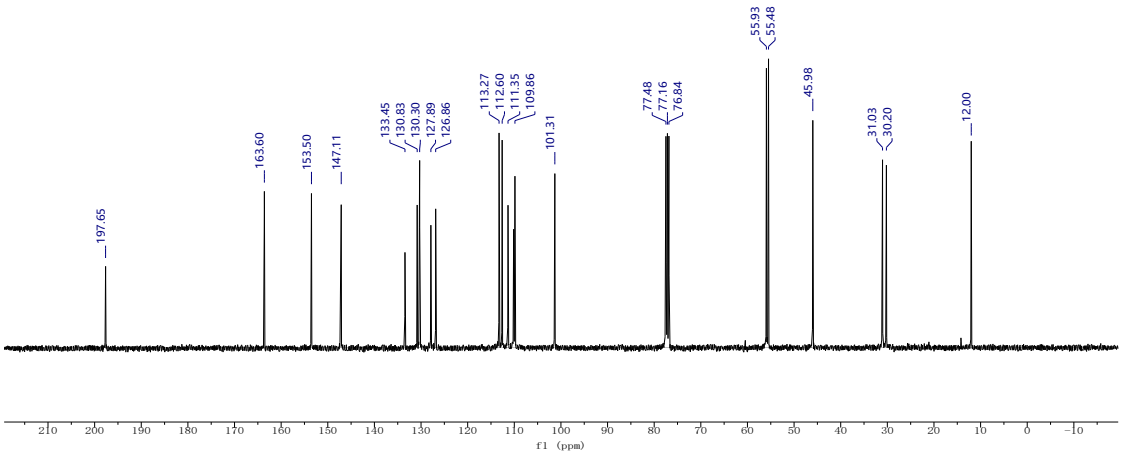

2019-1.2074.fid
LHL-3-14-2.1

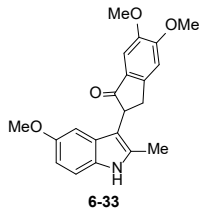

6-33

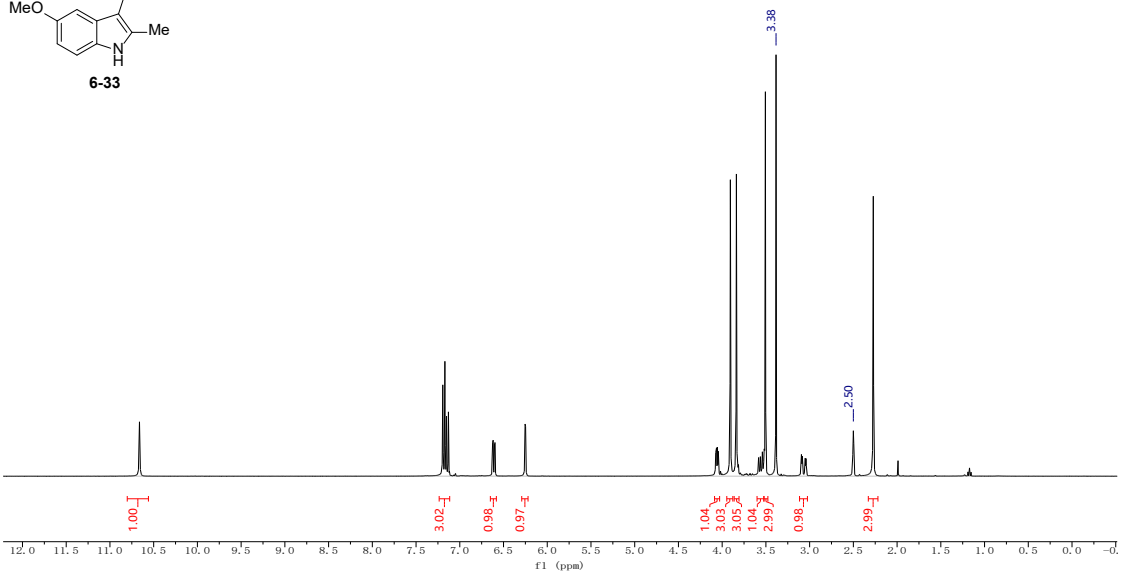

2019-1.2547.fid
LHL -3-14-2.1

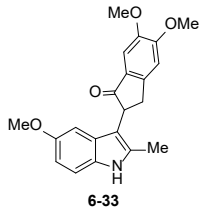

6-33

2019-1.3458.fid
LHL-2-89-2

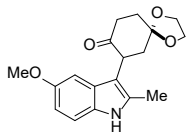

6-34

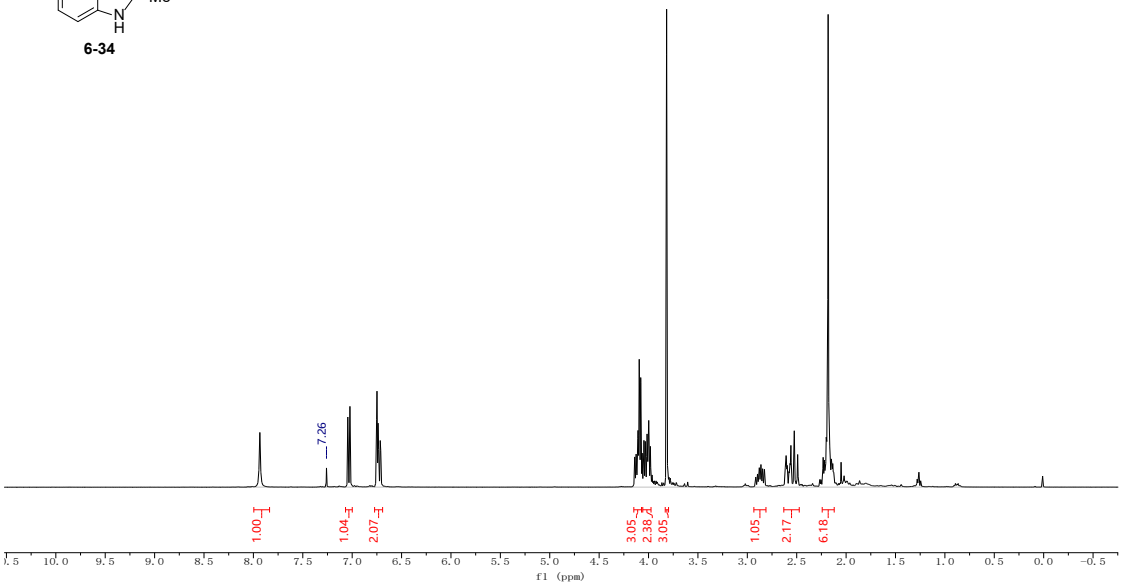

2019-1.3744.fid
LHL 2-89-2

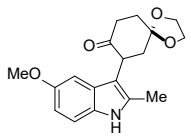

6-34

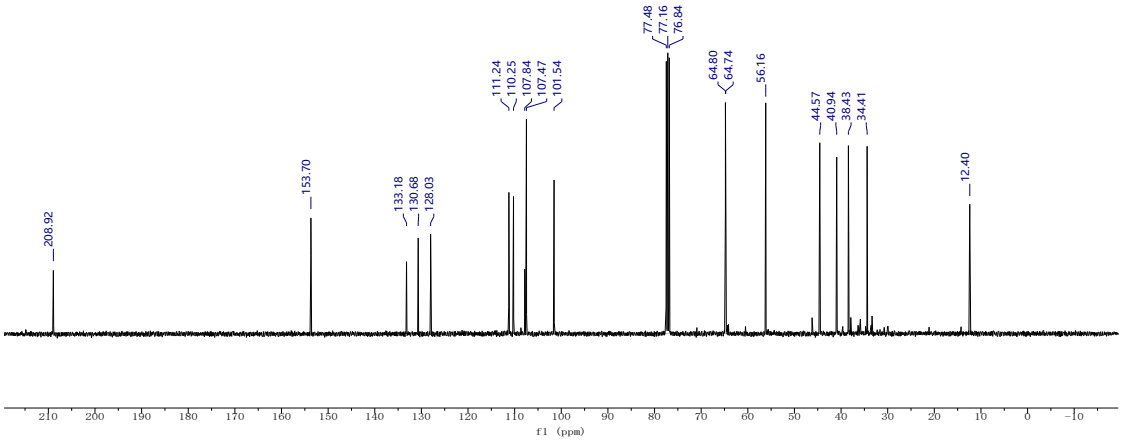

2018-2.13910.fid
LHL-2-82-1.2

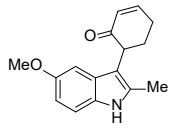

6-35

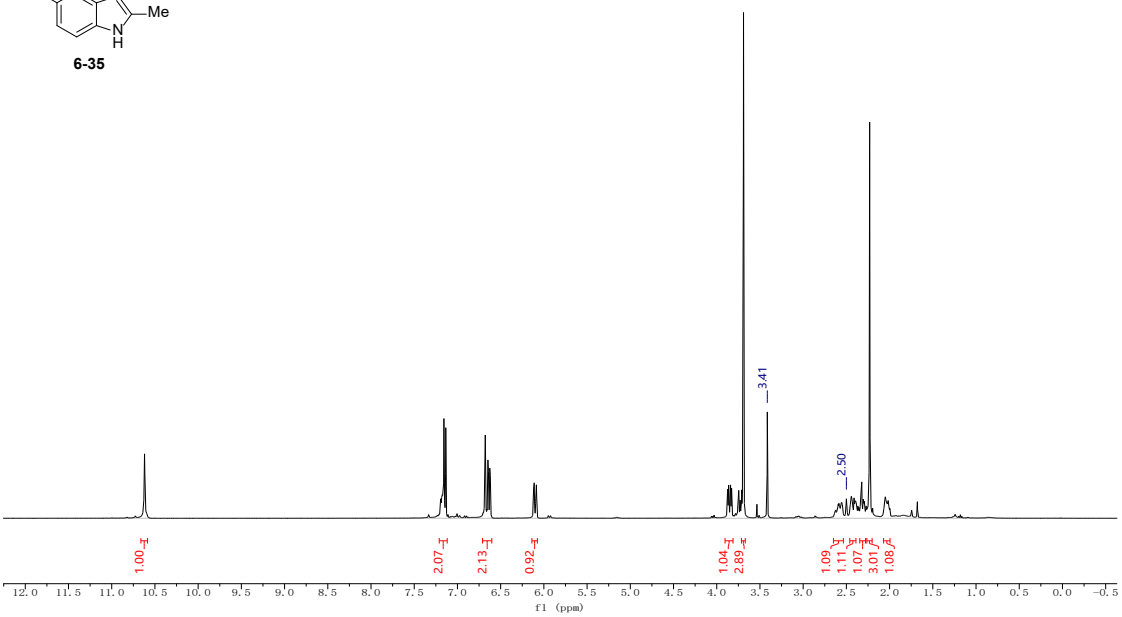

2018-2.14540.fid
LHL-2-82-1.2

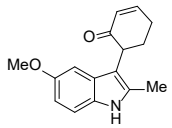

6-35

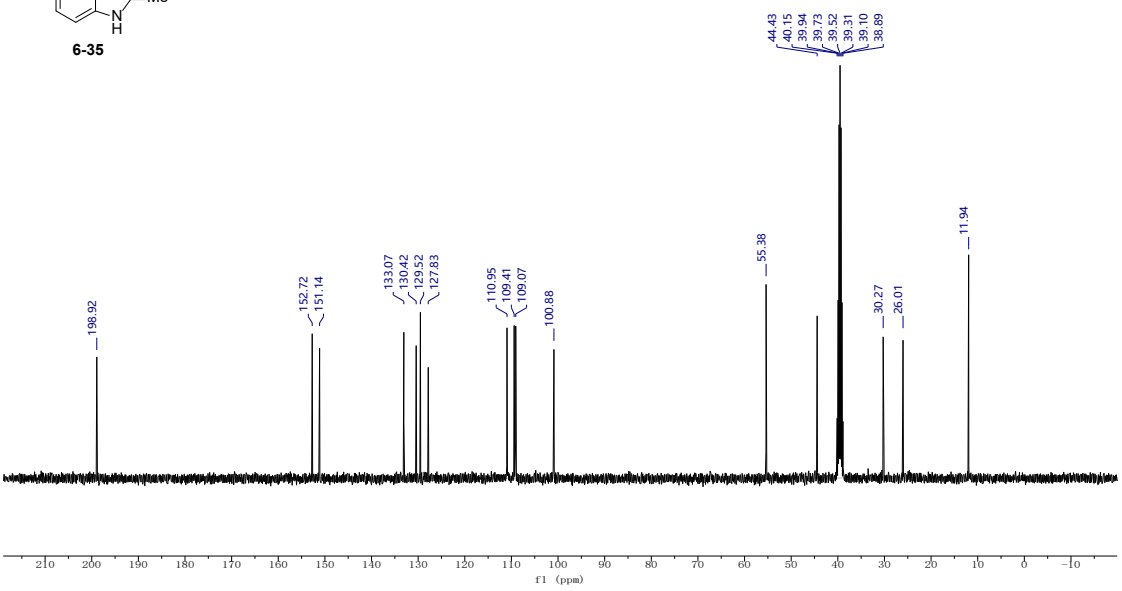

LHL-2-90-1.2

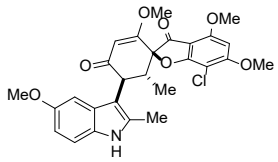

6-36

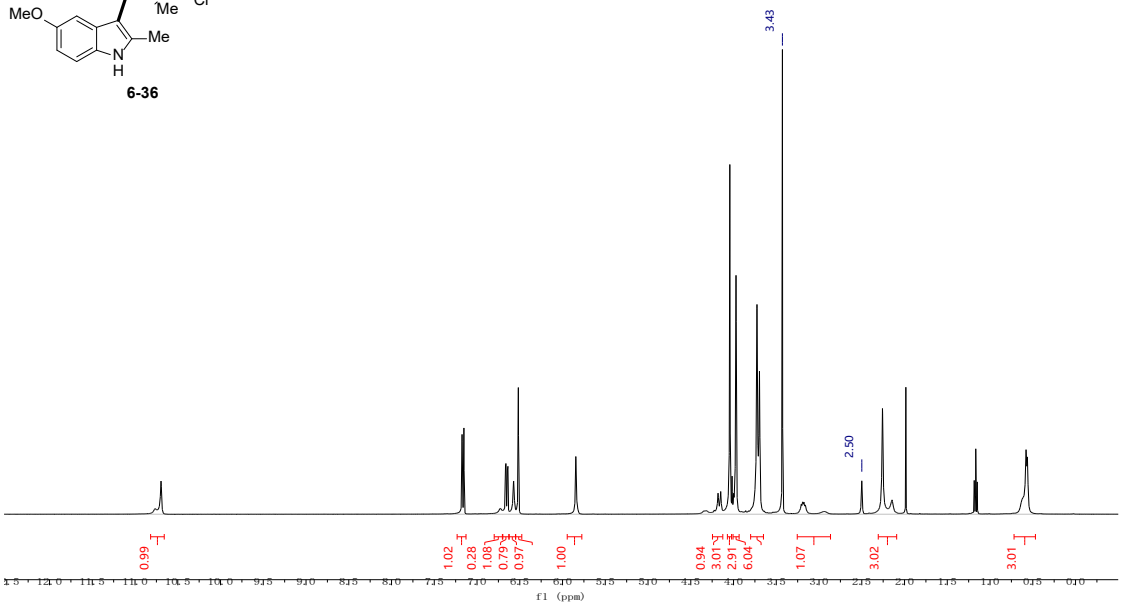

2019-1.717.fid
LHL -2-90-1.2

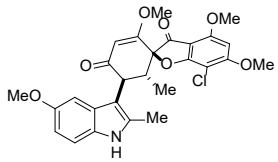

6-36

2018-2.14858.fid
LHL-2-88-1.1

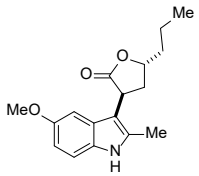

6-37-1 (isomer 1)

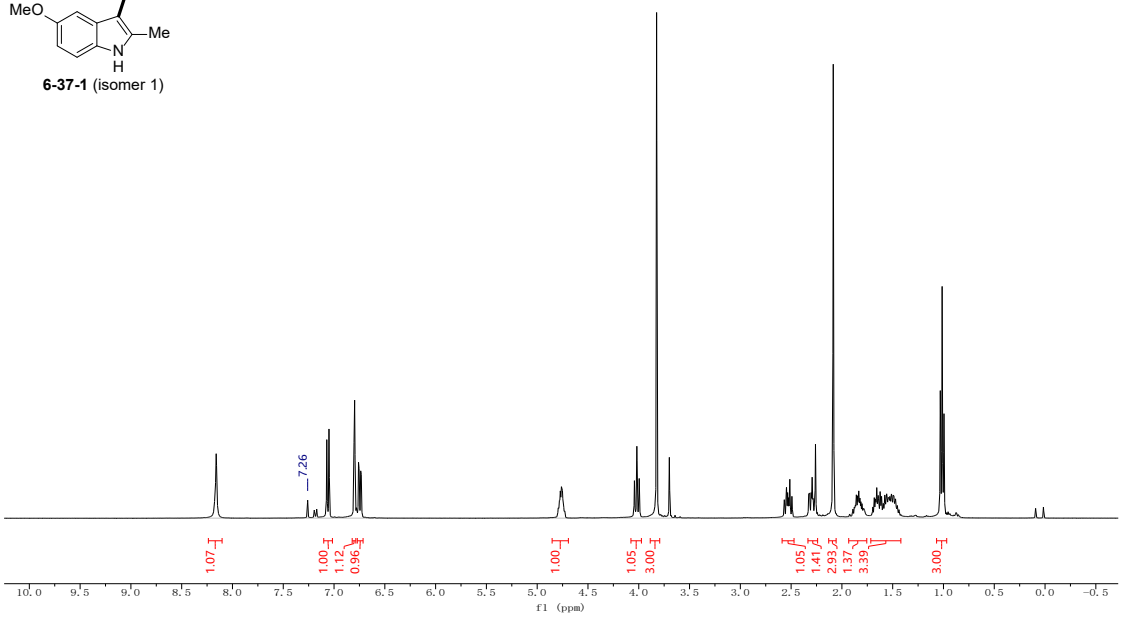

2018-2.15367.fid
LHL 2-88-1.1

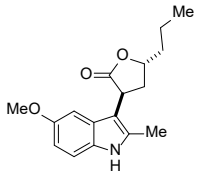

6-37-1 (isomer 1)

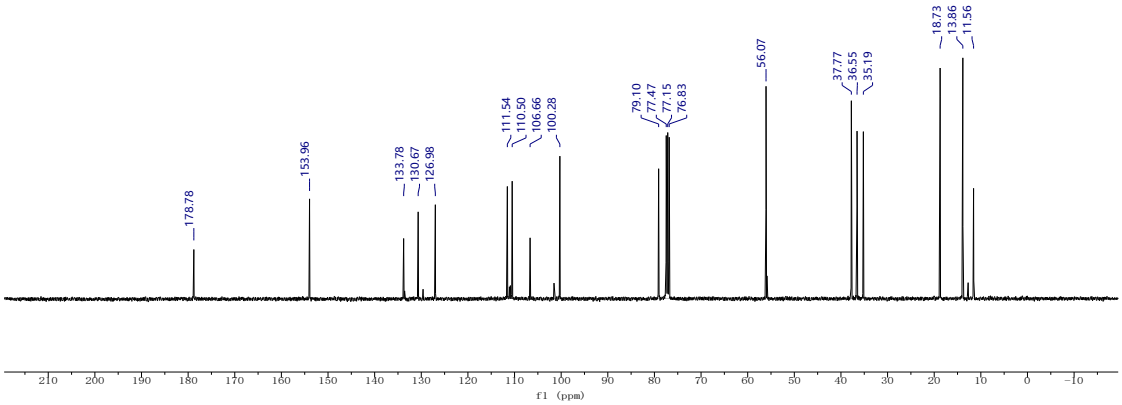

2018-2.14860.fid
LHL-2-88-1.2

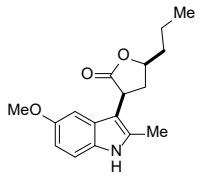

6-37-2 (isomer 2)

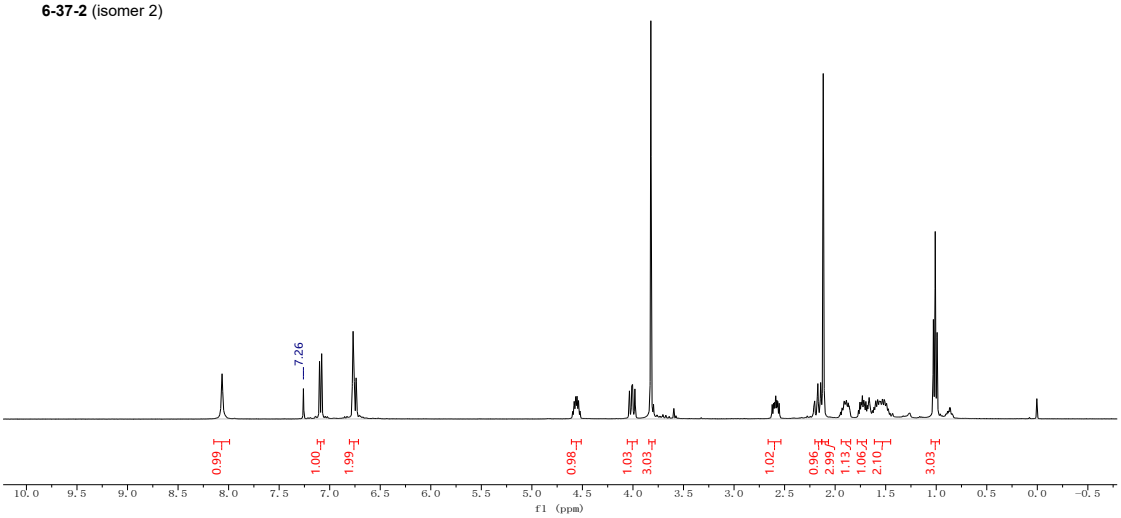

2018-2.15375.fid
LHL-2-88-1.2

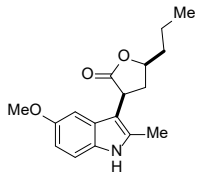

6-37-2 (isomer 2)

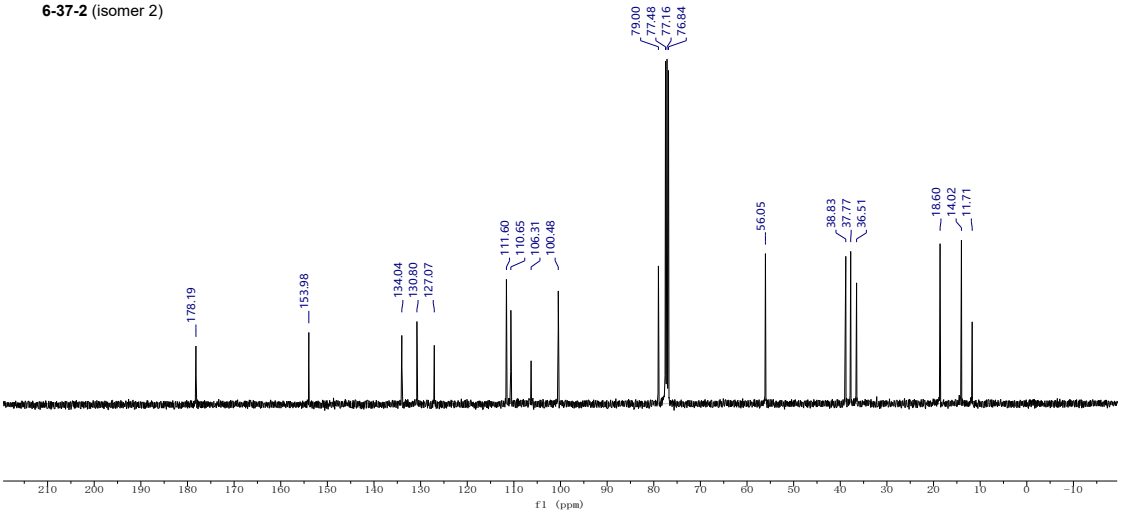

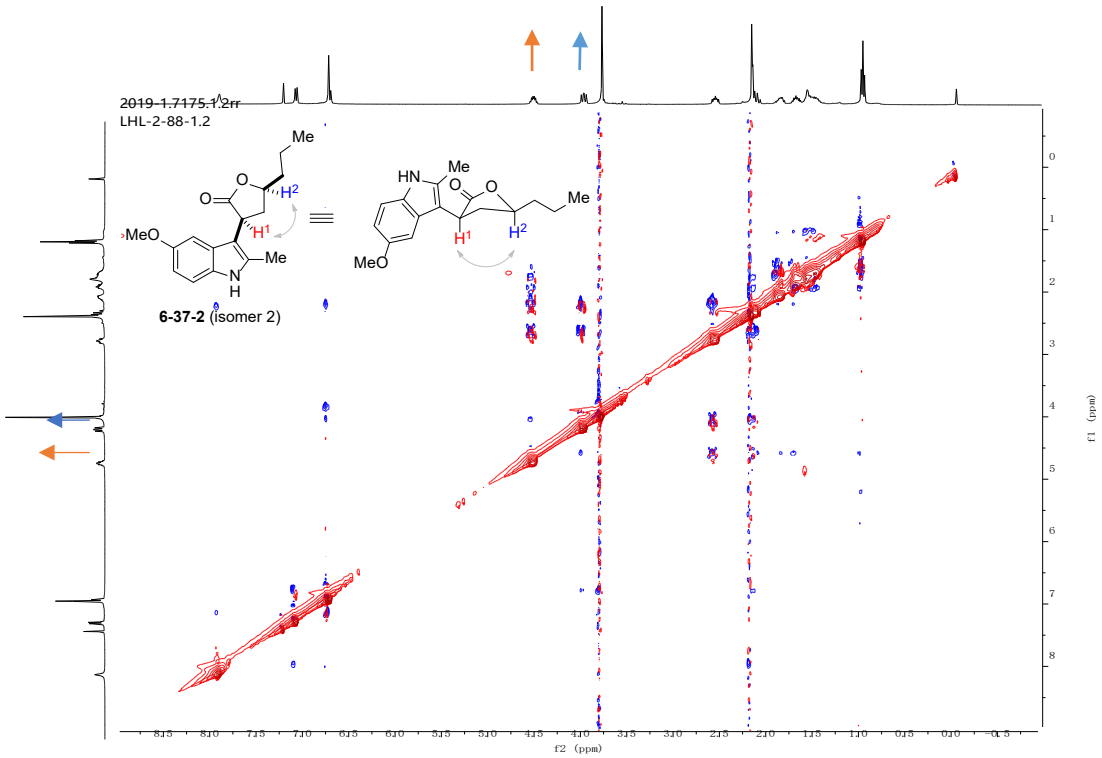

LHL-3-6-2

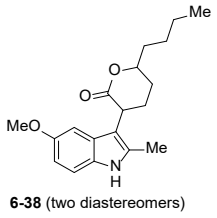

6-38 (two diastereomers)

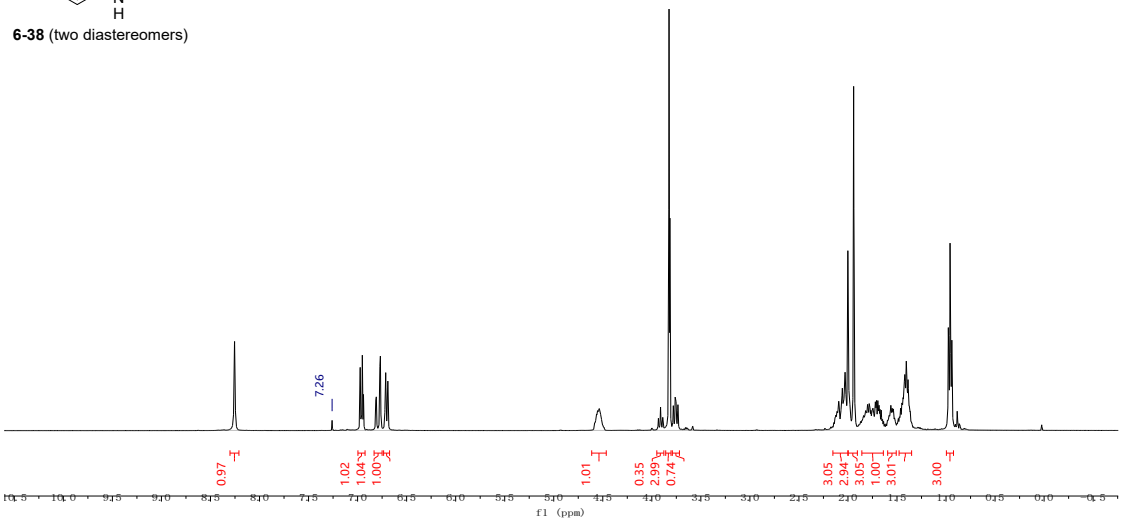

2019-1.859.fid
LHL-3-6-2

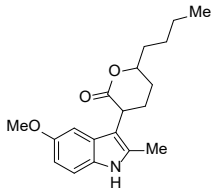

6-38 (two diastereomers)

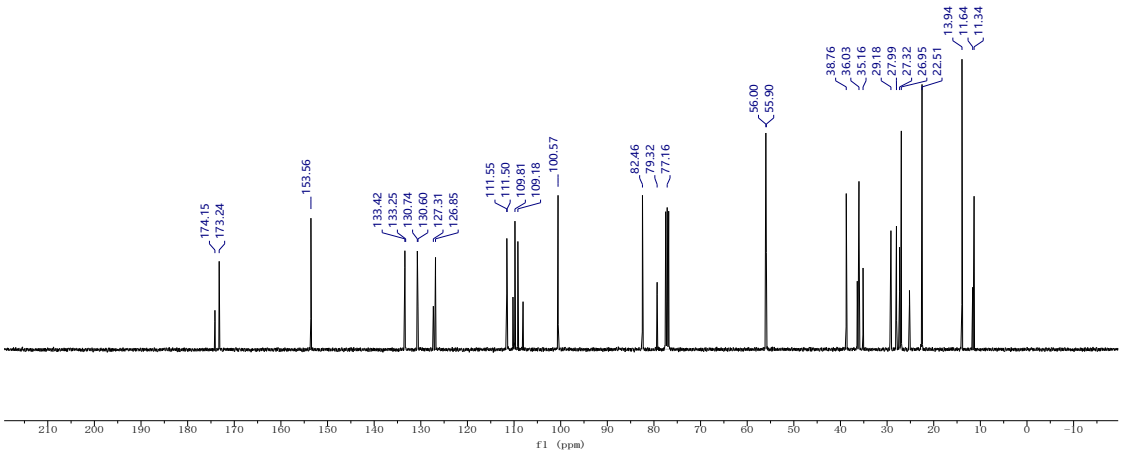

2019-1.675.fid
LHL-3-6-1

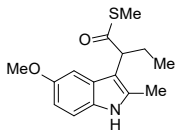

6-39

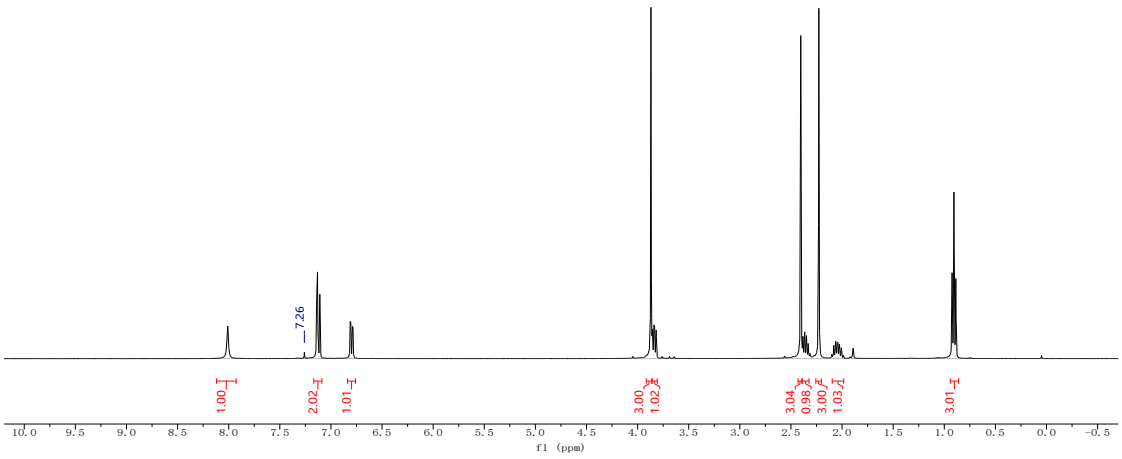

2019-1.860.fid
LHL-3-6-1

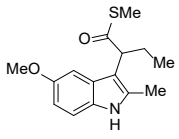

6-39

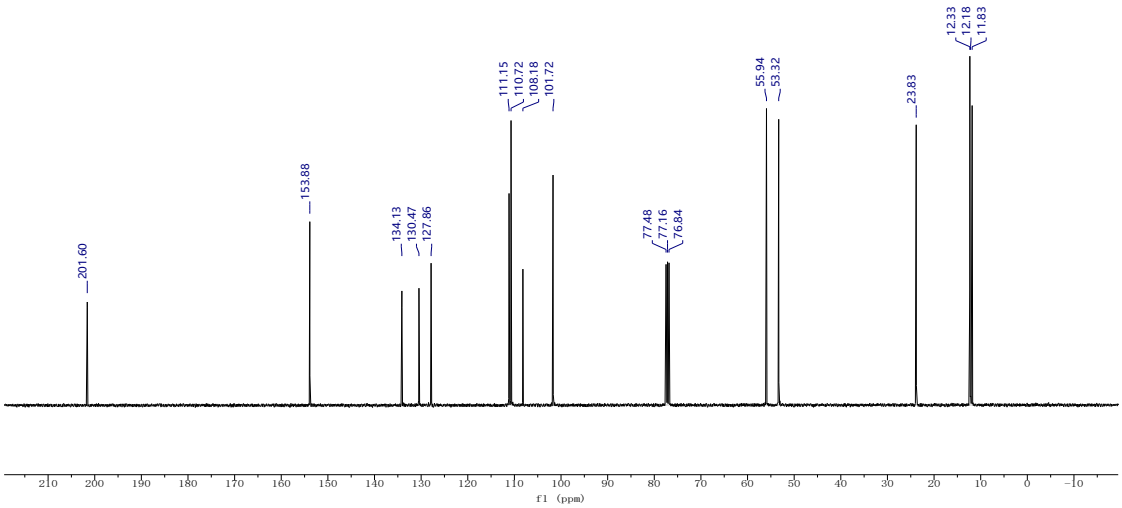

2018-2.14861.fid
LHL-2-89-1

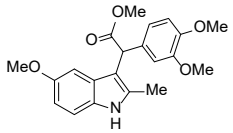

6-40

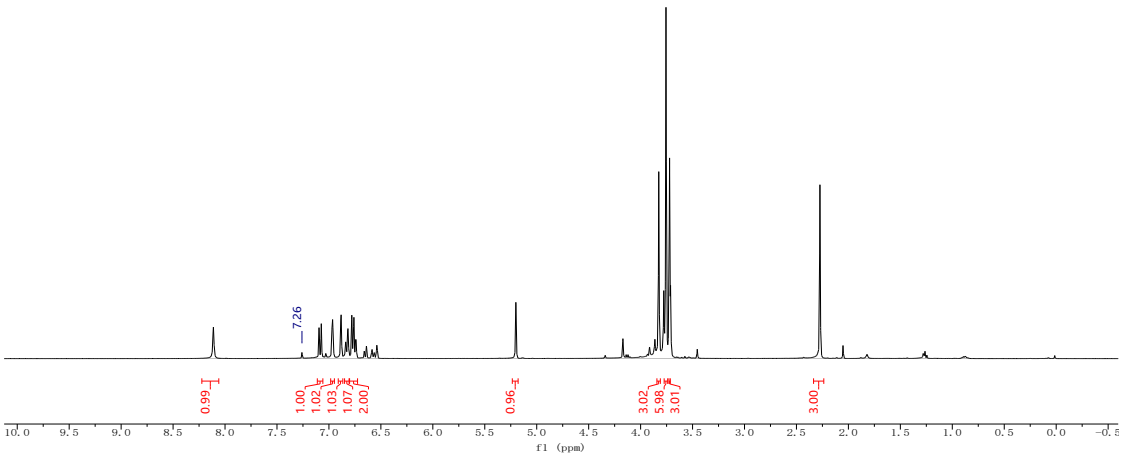

2018-2.15374.fid
LHL -2-89-1

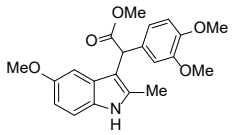

6-40

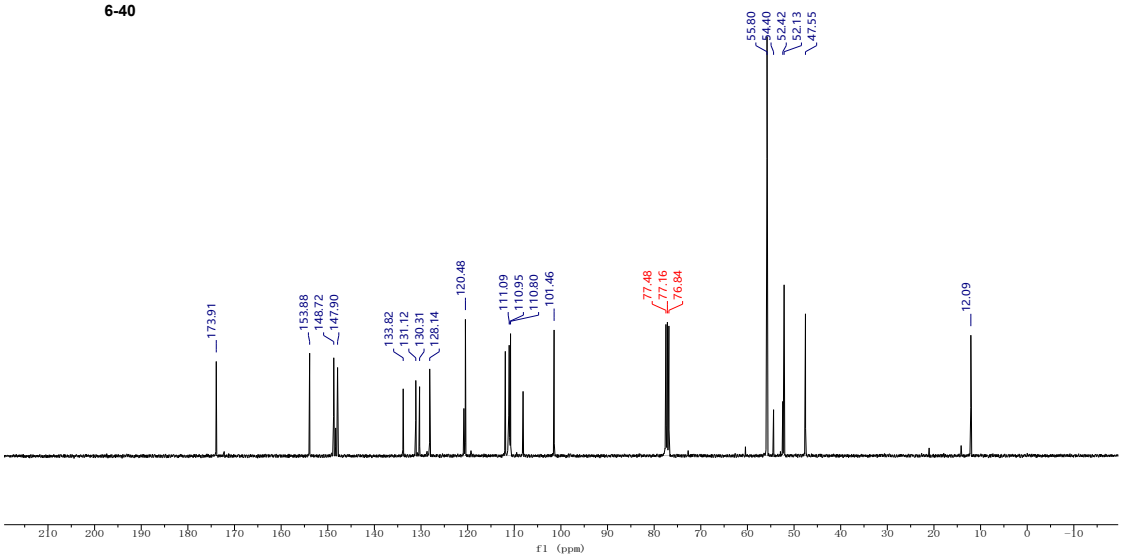

2018-2.14873.fid
LHL-2-86-1.1

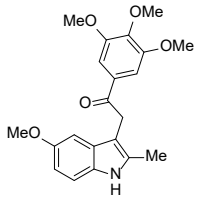

6-41

2018-2.15368.fid
LHL -2-86-1.1

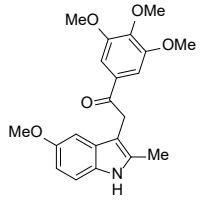

6-41

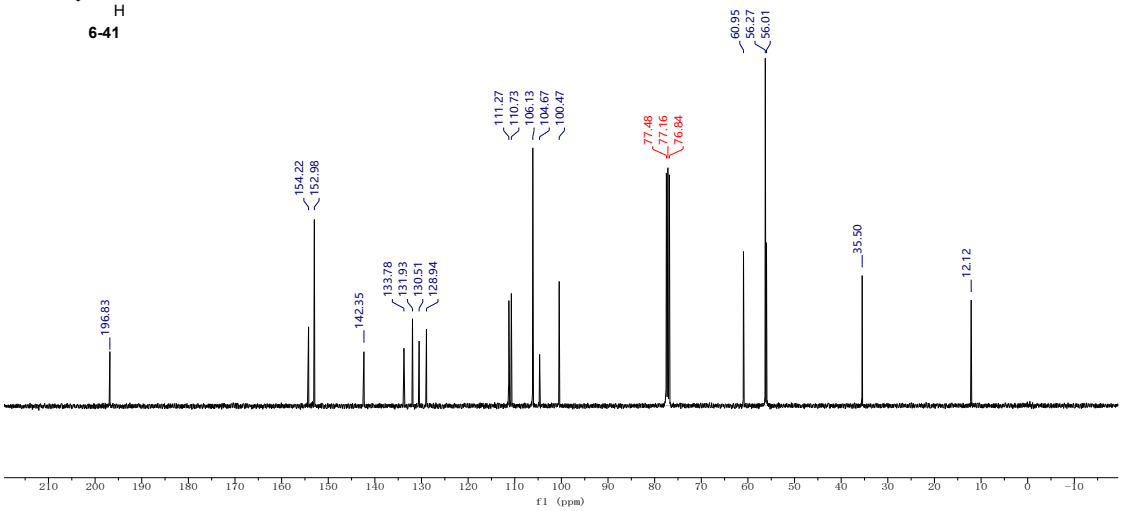

2018-2.14856.fid
LHL-2-85-2.1

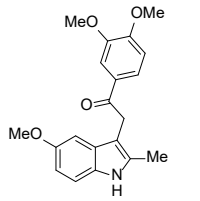

6-42

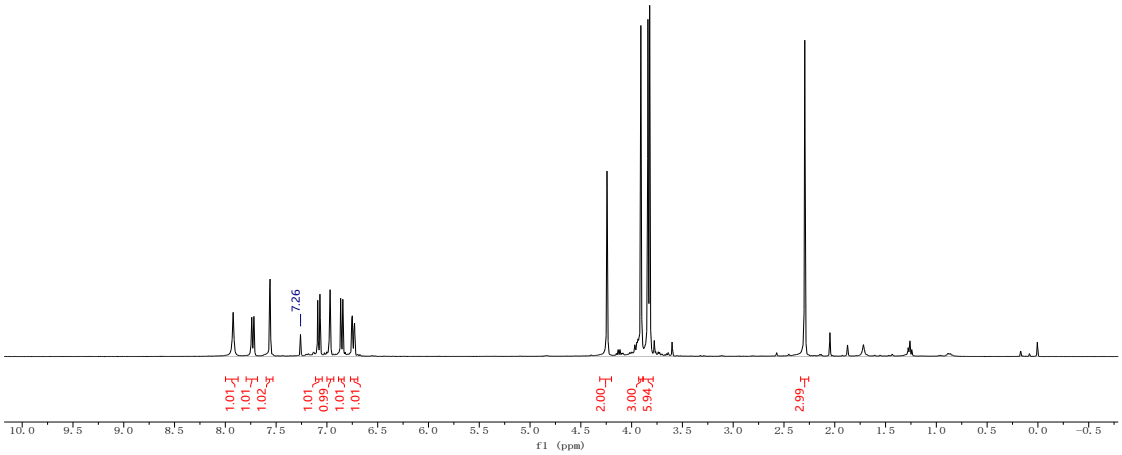

2018-2.15371.fid
LHL -2-85-2.1

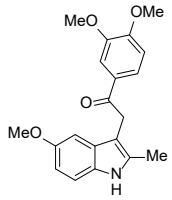

6-42

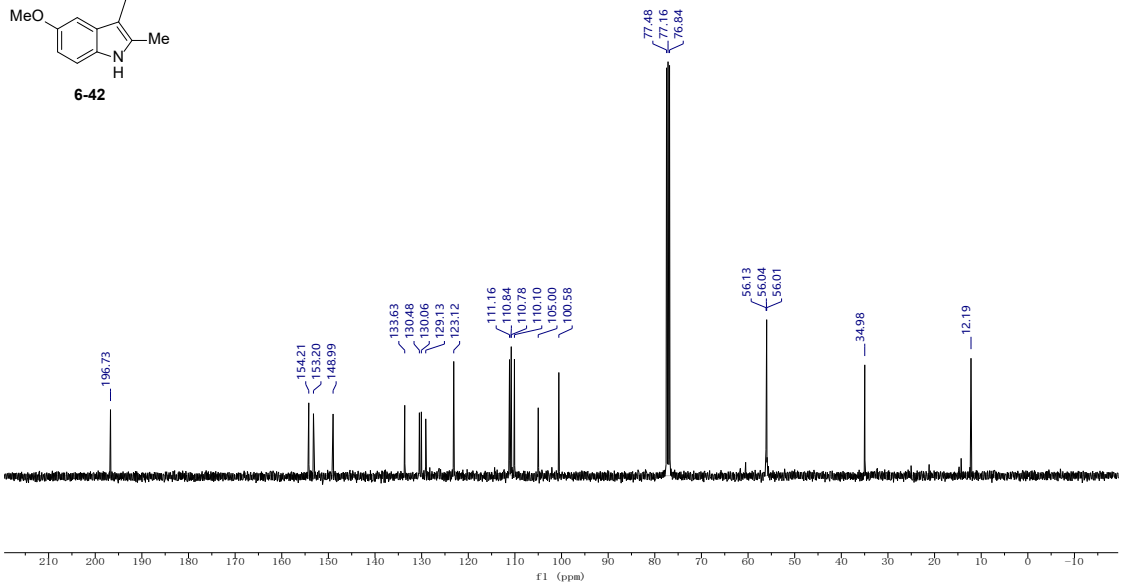

2018-2.3997.fid
LHL-1-73-2.2

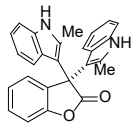

9-1

2019-1.3268.fid
LHL-1-73-2.2

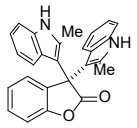

9-1

2018-2.14855.fid
LHL-2-87-1

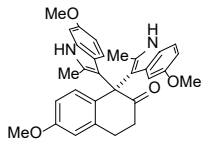

9-2

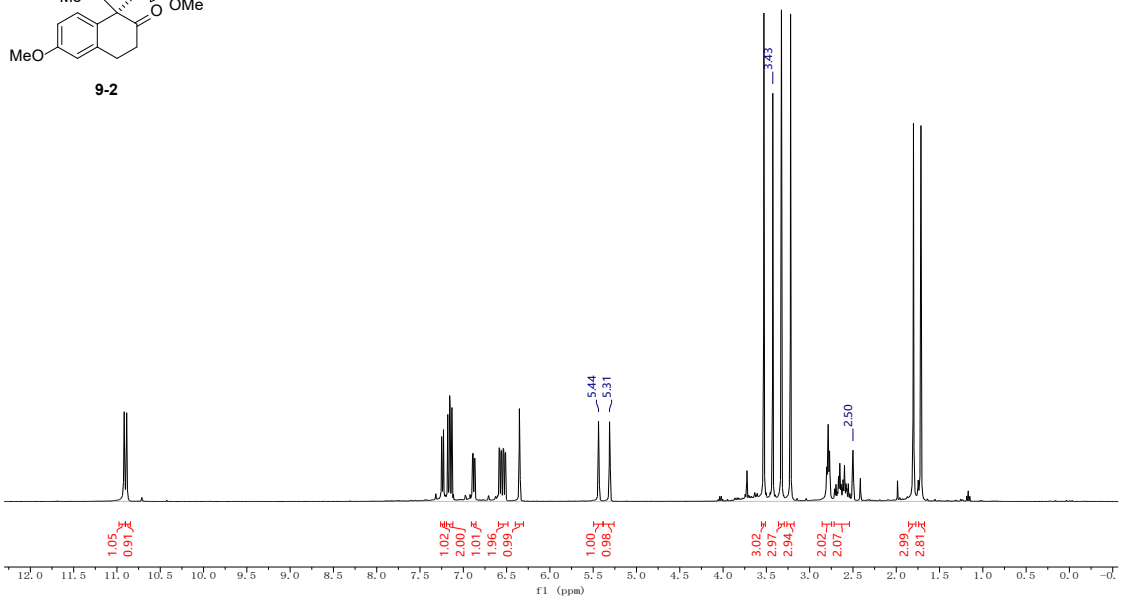

2018-2.15369.fid
LHL -2-87-1

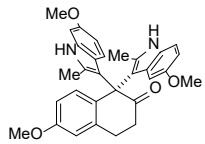

9-2

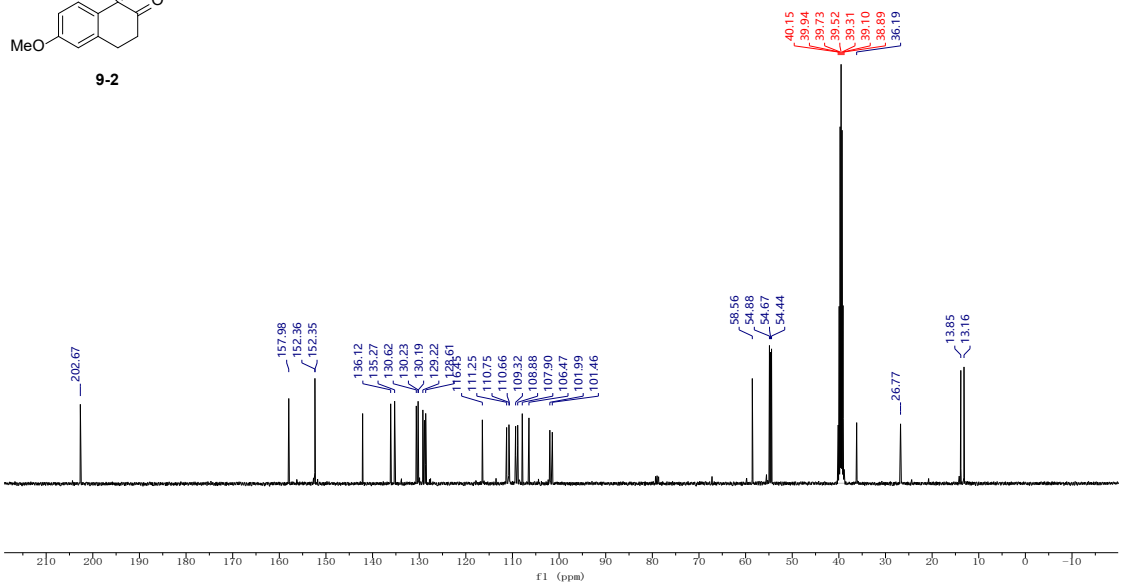

2018-2.9898.fid
LHL-2-46-1

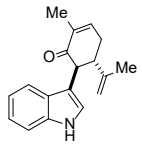

6-43

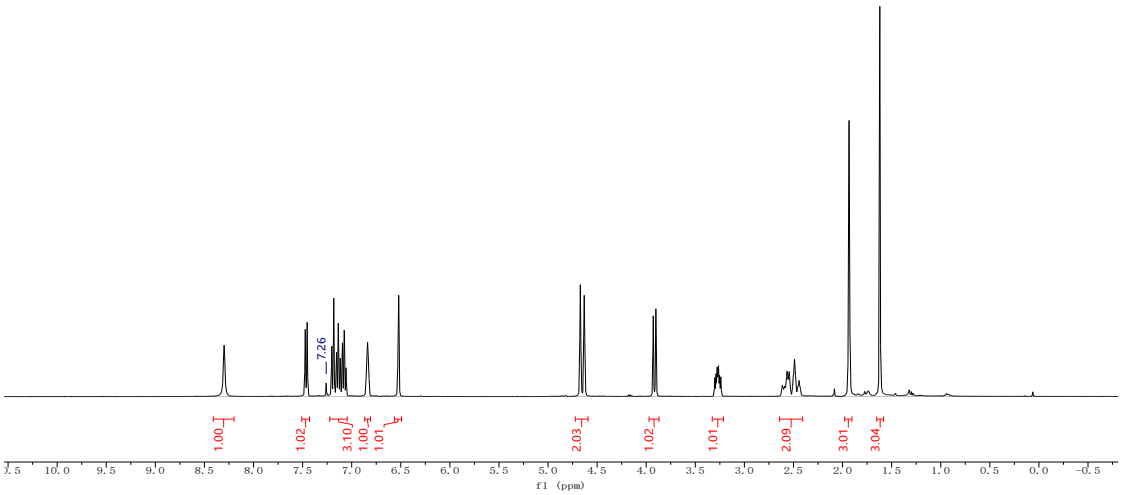

LHL-2-46-2-2

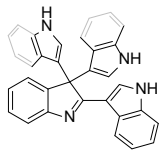

10 (tetramer)

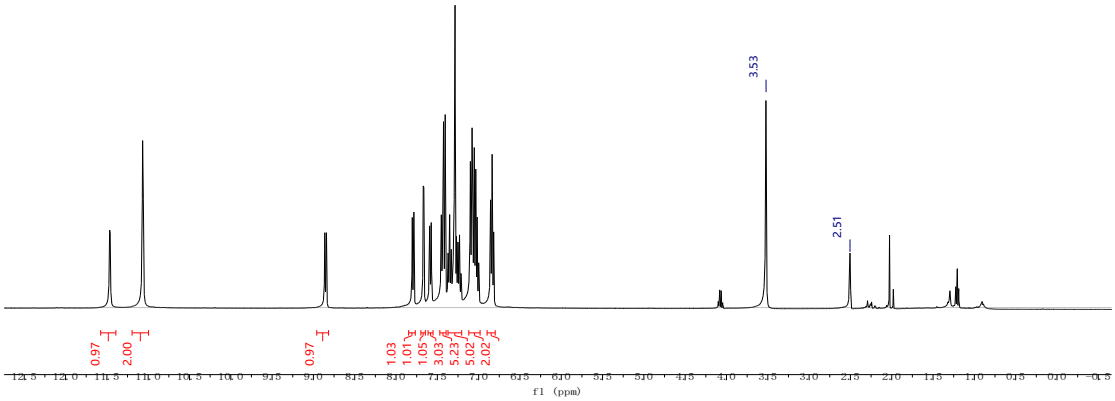

LHL1-75-2-1

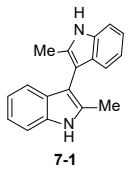

7-1

2018-2.10147.fid
LHL-2-47-2

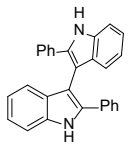

7-2

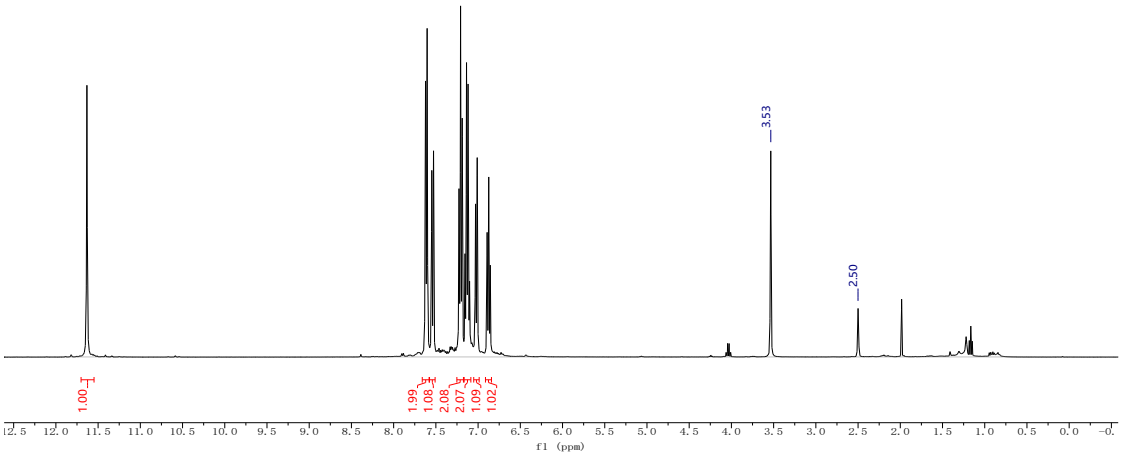

2019-1.46.fid
LHL-3-1-2

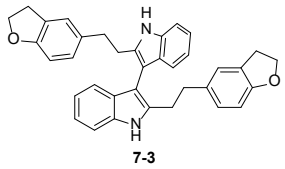

7-3

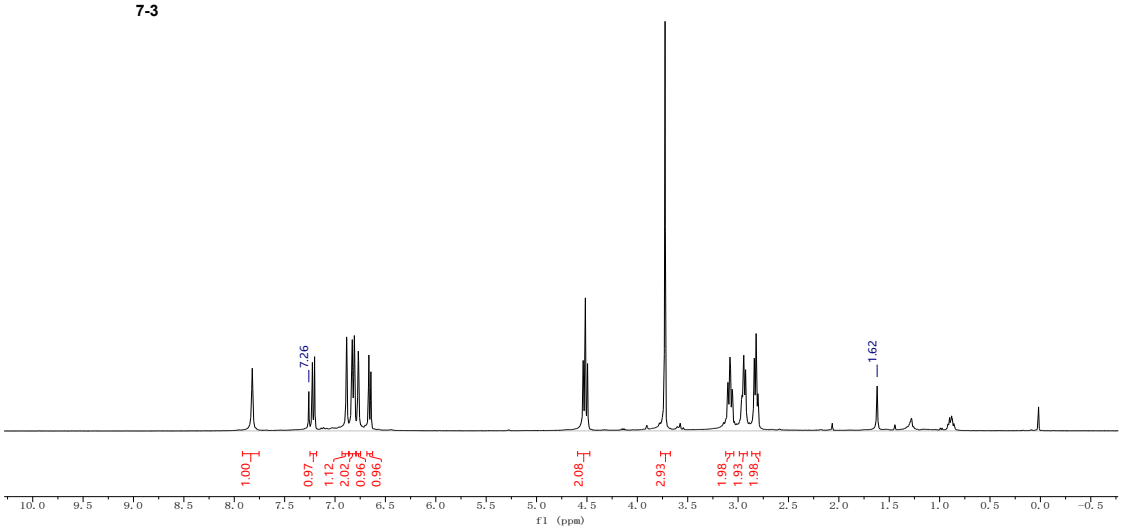

2019-1.718.fid
LHL -3-1-2

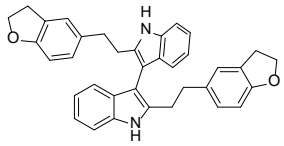

7-3

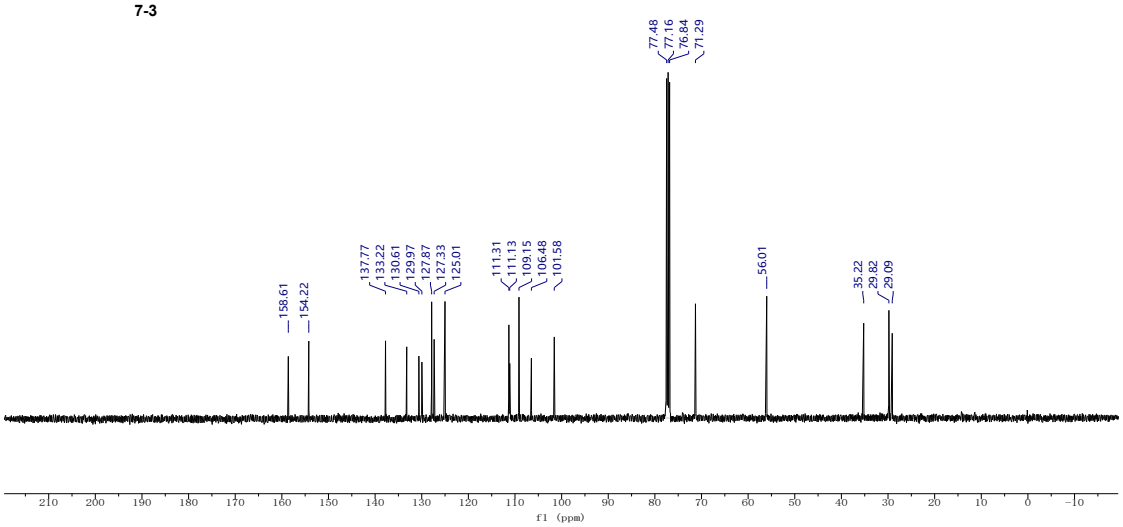

2019-1.15244.fid
lhl 4-30-2.1

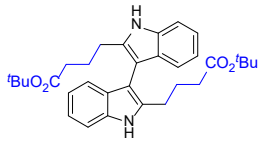

7-4

2019-1.15859.fid
LHL -4-30-2.1

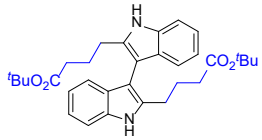

7-4

2018-2.14865.fid
LHL-2-88-2.1

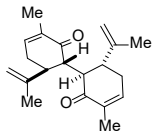

8-1

2018-2.10801.fid
LHL-2-55-2

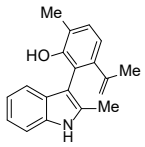

13-1

2019-1.3516.fid
LHL-3-20-1

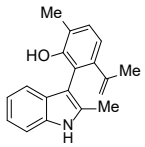

13-1

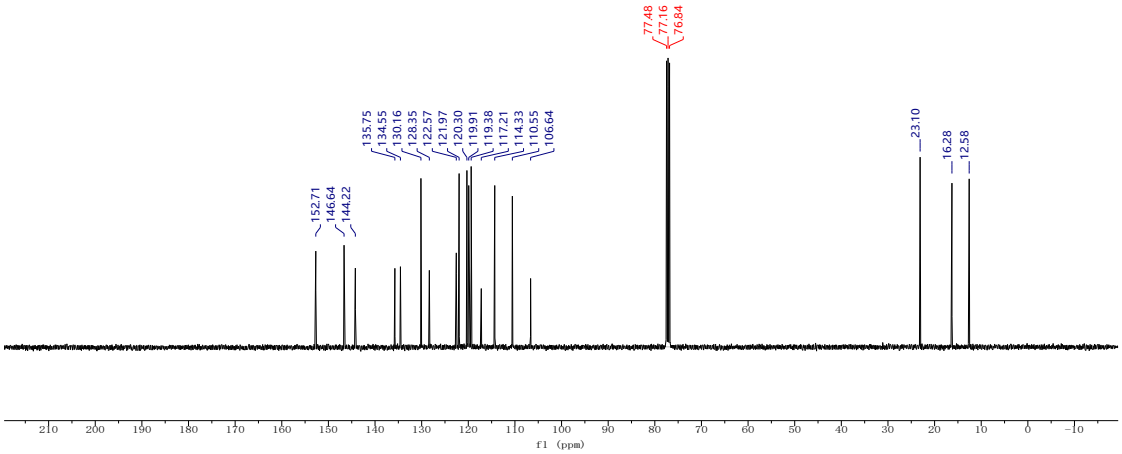

2018-2.13509.fid
LHL -2-79-1

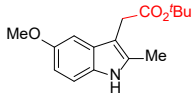

6-46

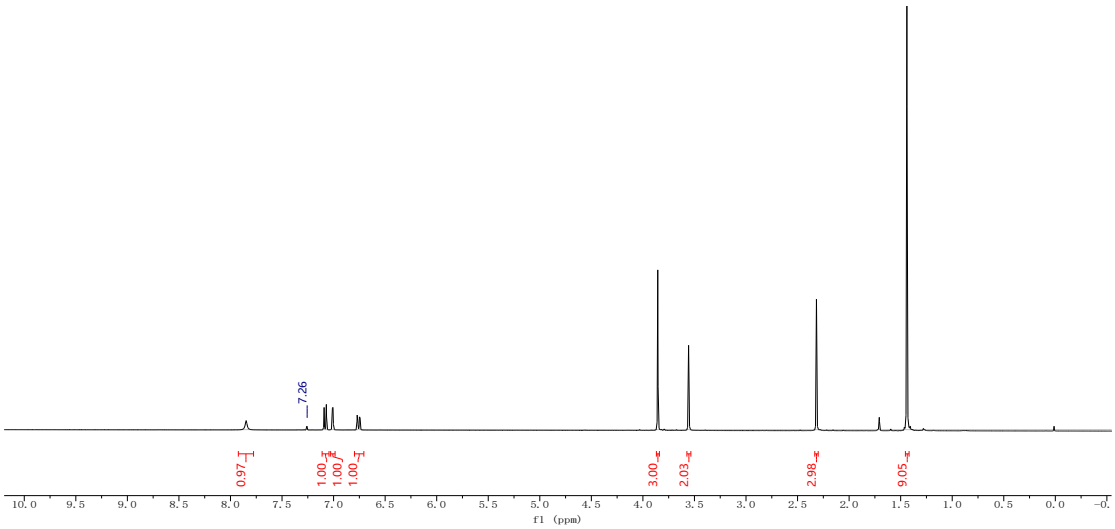

2018-2.14040.fid
LHL-2-79-1

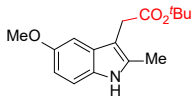

6-46

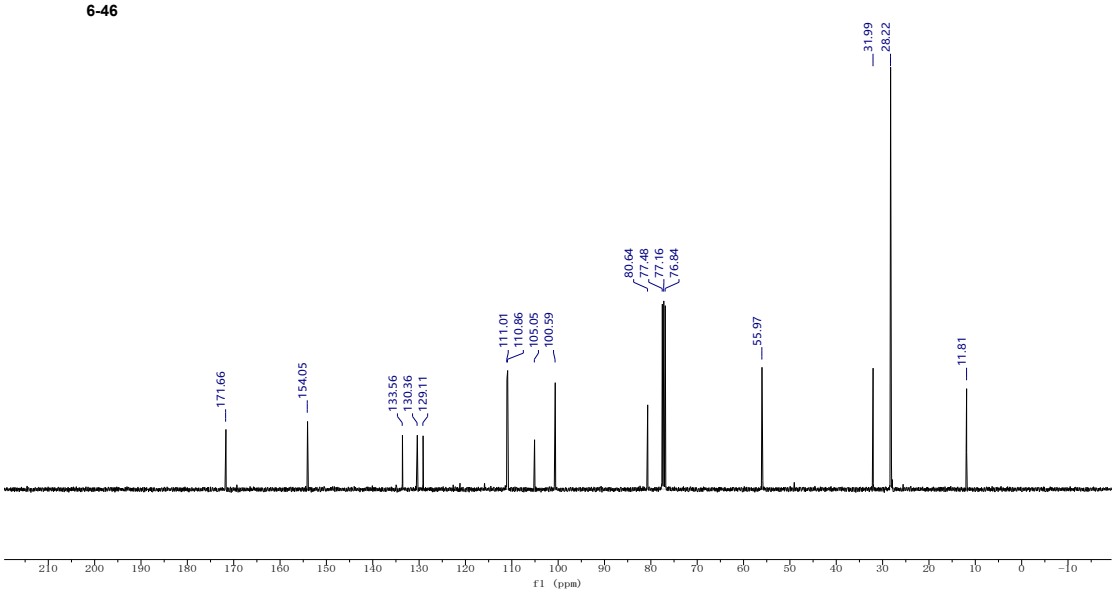

2019-1.2929.fid
LHL-3-19-1

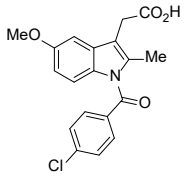

12-2, indomethacin

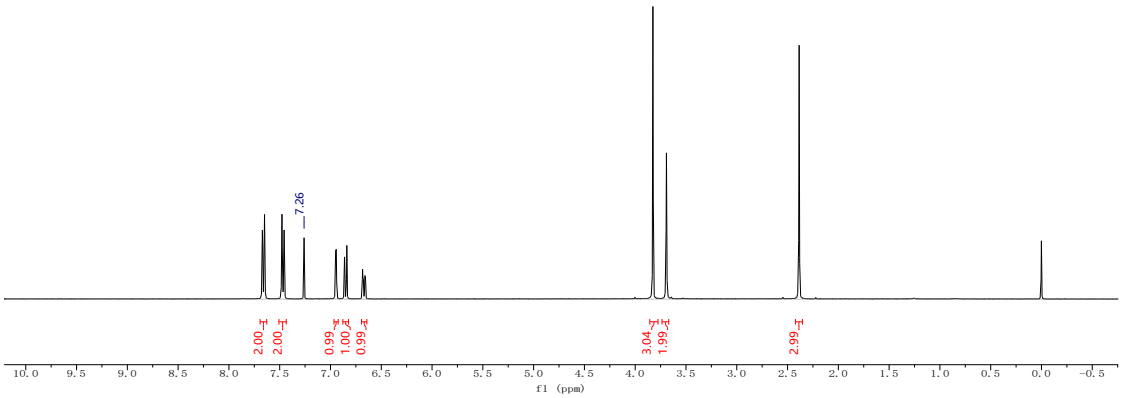

2018-2.12512.fid
LHT-2-68-1.1

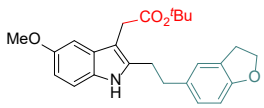

6-47

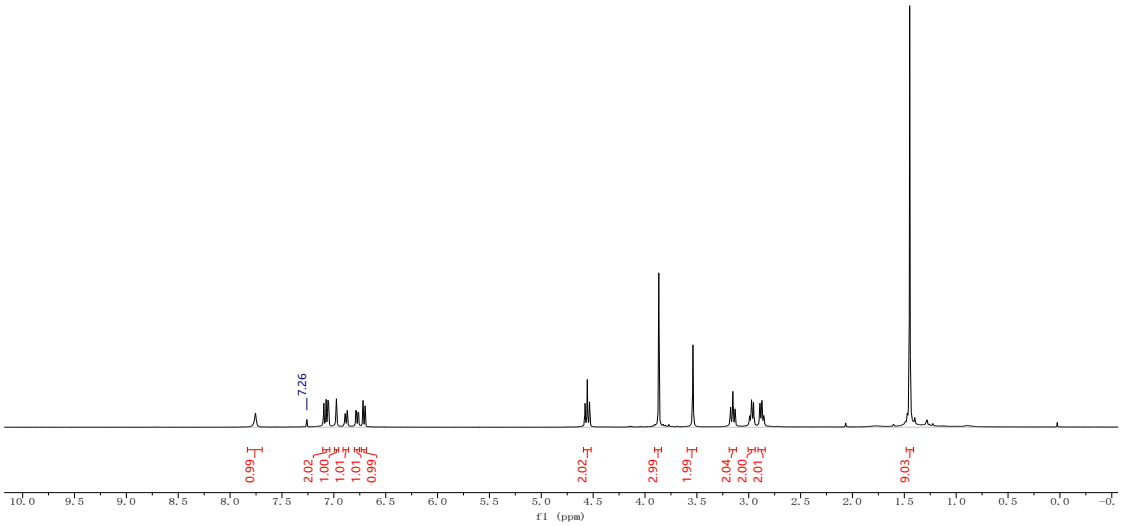

2018-2.13270.fid
LHL -2-68-1.1

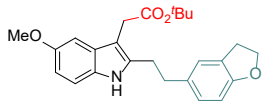

6-47

2019-1.3937.fid
LHL -3-25-1

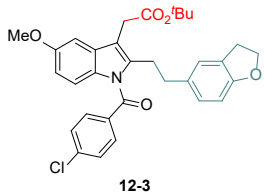

12-3

2019-1.4173.fid
LHL -3-25-1

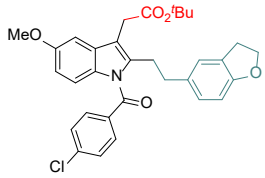

12-3

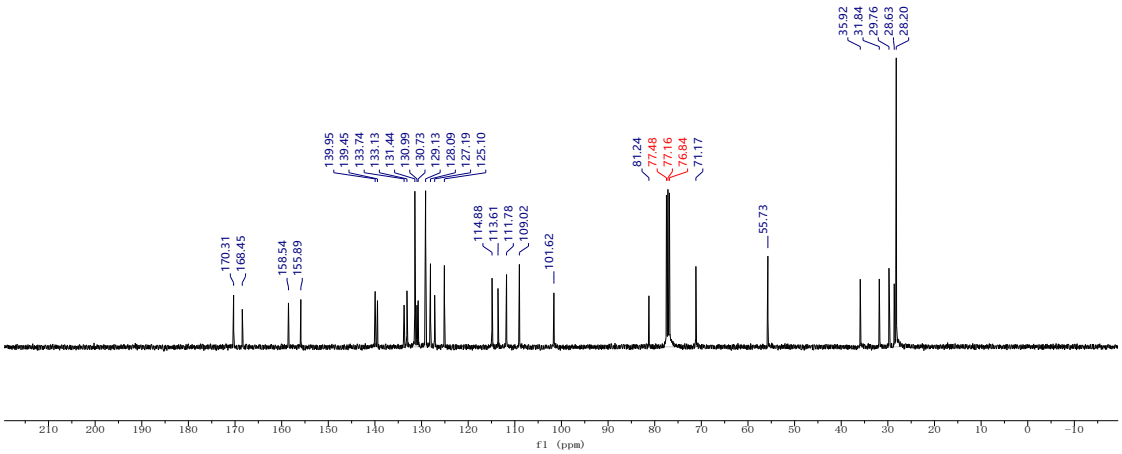

2019-1.5332.fid
LHL-3-39-1

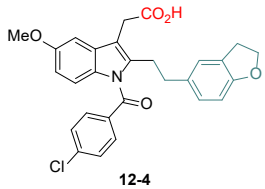

12-4

2019-1.5631.fid
LHL-3-39-1

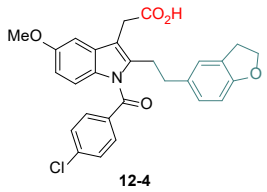

12-4

2018-2.13908.fid
LHL-2-80-1.2

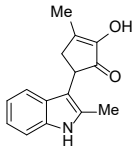

6-48

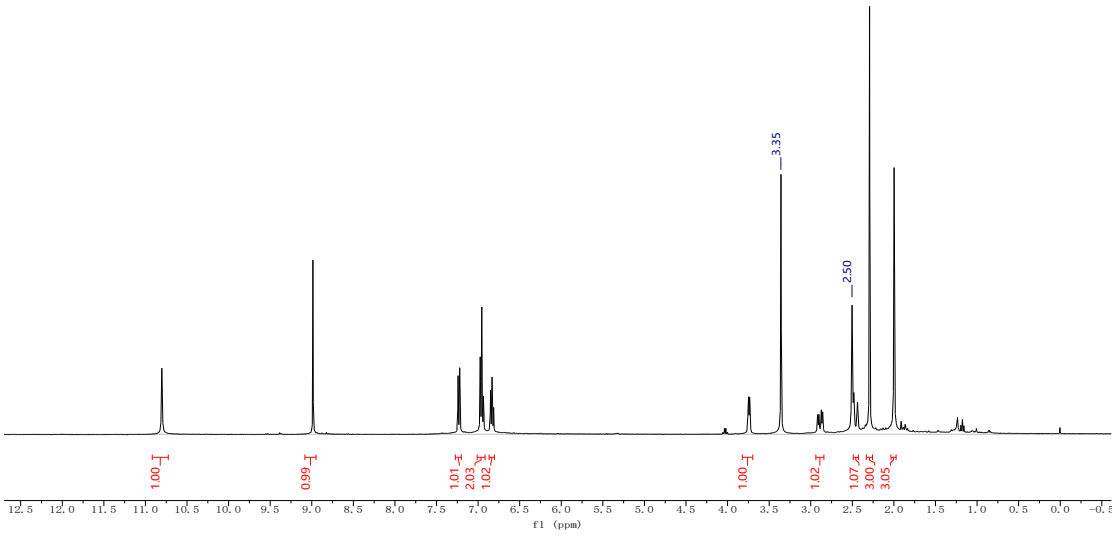

2019-1.2545.fid
LHL -2-80-1.2

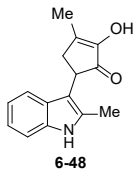

6-48